UTILIZACIÓN DE MEZCLAS DE RESIDUOS PARA LA OBTENCIÓN DE CEMENTOS DE ACTIVACIÓN ALCALINA:

APLICACIÓN EN MORTEROS Y SUELOS ESTABILIZADOS.

Departamento de Ingeniería de la Construcción y de Proyectos de Ingeniería Civil

Tesis Doctoral

Juan Cosa Martínez

Directores

Dr. José María Monzó Balbuena

Dra. Mª Victoria Borrachero Rosado

VALENCIA, MARZO DE 2022

UNIVERSITAT POLITÈCNICA DE VALÈNCIA

Departamento de Ingeniería de la Construcción y Proyectos de Ingeniería Civil

Tesis Doctoral

Utilización de mezclas de residuos para la obtención de cementos de activación alcalina: Aplicación en morteros y suelos estabilizados.

Doctorando: Juan Cosa Martínez

Directores de Tesis:

Dr. José María Monzó Balbuena
Dra. María Victoria Borrachero Rosado

Valencia, Marzo de 2022

Resumen

Esta tesis englobada dentro del programa de doctorado en ingeniería de la construcción sigue la línea de investigación en sostenibilidad y gestión de la construcción.

Las investigaciones se han centrado en el desarrollo de cementos de activación alcalina (CAA) obtenidos a partir de residuos con el fin de reducir tanto el coste económico como medioambiental. Este hecho implicaría la reducción en el uso tanto de materias primas, en el caso de los precursores, como de reactivos químicos en el caso de los activadores. La tesis doctoral que se presenta estudia el uso de diferentes mezclas de residuos como precursores: cerámica sanitaria, catalizador gastado de craqueo catalítico, escoria de alto horno y ceniza volante de central térmica en la preparación de morteros. Así mismo, utiliza también CAA, obtenidos a partir de residuos en la estabilización de suelos. En este último caso también se han usado residuos en la preparación de activadores como son las cenizas obtenidas en la combustión de biomasa.

Los resultados obtenidos ponen de manifiesto la viabilidad en el uso de residuos para la preparación de CAA, y la posibilidad incluso de ser usados en contextos de subdesarrollo.

Resum

Aquesta tesi englobada dins del programa de doctorat en enginyeria de la construcció segueix la línia d'investigació en sostenibilitat i gestió de la construcció.

Les investigacions s'han centrat en el desenvolupament de ciments d'activació alcalina (CAA) obtinguts a partir de residus amb la finalitat de reduir tant el cost econòmic com mediambiental. Aquest fet implicaria la reducció en l'ús tant de matèries primeres, en el cas dels precursors, com de reactius químics en el cas dels activadors. La tesi doctoral que es presenta estudia l'ús de diferents mescles de residus com a precursors: ceràmica sanitària, catalitzador gastat de craqueig catalític, escòria d'alt forn i cendra volant de central tèrmica en la preparació de morters. Així mateix, utilitza també CAA, obtinguts a partir de residus en l'estabilització de sòls. En aquest últim cas també s'han usat residus en la preparació d'activadors com són les cendres obtingudes en la combustió de biomassa.

Els resultats obtinguts posen de manifest la viabilitat en l'ús de residus per a la preparació de CAA, i la possibilitat de ser usats fins i tot en contextos de subdesenvolupament.

Abstract

This doctoral thesis encompassed within the doctoral program in construction engineering follows the research line in sustainability and construction management.

The research has focused on the development of alkaline activated cements (AAC) obtained from waste to reduce the economic and environmental cost. This fact would imply a reduction in the use of raw materials in the case of precursors, and chemical reagents in the case of activators. The doctoral thesis that is presented studies the use of different waste mixtures as precursors: sanitary ceramics, spent fluid cracking catalyst, blast furnace slag and fly ash from thermal power plants in the preparation of mortars. Likewise, also is used CAA obtained from residues in soil stabilization. In the latter case, residues have also been used in the activators preparation, such as the ashes obtained in the combustion of biomass.

The results obtained show the viability in the use of residues for CAA preparation, and the possibility of being used even in underdeveloped contexts.

Contenido

1 Introducción

En las últimas décadas, la producción de cemento ha crecido considerablemente como consecuencia de un desarrollo económico y crecimiento demográfico. Sin embargo, la industria cementera está catalogada como un sector altamente contaminante y de gran impacto ambiental. La producción de una tonelada de cemento requiere la explotación de un elevado volumen de materias primas (principalmente caliza y arcilla) y la emisión de aproximadamente una tonelada de CO_2 y otros gases contaminantes (NO_x y SO_x).

Los geopolímeos y/o cementos activados alcalinamente (CAA) son conglomerantes ampliamente conocidos. Este tipo de compuestos se obtienen generalmente por activación de materiales silicoaluminosos mediante el uso de compuestos de elevada alcalinidad. Los CAA han sido aplicados en una gran variedad de sectores en la ingeniería, incluyendo su utilización como sustituto del cemento portland en la preparación de morteros y hormigones, y también para la estabilización de suelos, aunque en este último caso en menor medida. El uso de estabilizadores para la preparación de suelos deficientes o bloques de construcción está ampliamente establecido. Existen distintos tipos de estabilizadores, el más comúnmente utilizado es el cemento portland. Como alternativa a éste se utilizan diversas soluciones, como puede ser cemento puzolánico (mezclas cal-puzolana), o más recientemente cementos activados alcalinamente o geopolímeros

La exploración de geopolímeros para la estabilización de suelos de última generación tiene importantes implicaciones para la ingeniería civil. Los suelos estabilizados con geopolímeros por regla general necesitan menos tiempo para desarrollar una elevada resistencia inicial frente a los estabilizados con cemento portland. Gracias al aumento de la ductilidad de los suelos estabilizados con geopolímeros, se puede mitigar

eficazmente el agrietamiento durante la construcción de pavimentos, mejorando también el proceso de curado. Adicionalmente, la menor contracción frente al cemento portland puede reducir el daño causado por la fisuración debido a la retracción de los suelos.

En lo que a la investigación en el campo de los CAA se refiere, se pretende reducir tanto el coste económico como medioambiental de estos conglomerantes. Para ello se plantea el uso de materiales residuales tanto en la preparación de precursores como de activadores involucrados en la reacción de activación alcalina. Este hecho implicaría la reducción en el uso tanto de materias primas, en el caso de los precursores, como de reactivos químicos en el caso de los activadores.

La tesis doctoral que se presenta estudia el uso de diferentes mezclas de residuos como precursores: cerámica sanitaria, catalizador gastado de craqueo catalítico, escoria de alto horno y ceniza volante de central térmica. Así mismo, utiliza también CAA, obtenidos a partir de residuos en la estabilización de suelos. En este último caso también utilizan residuos en la preparación de activadores como son las cenizas obtenidas en la combustión de biomasa.

2 Estructura y objetivos

2.1 Estructura

La tesis doctoral que se presenta en la modalidad de tesis doctoral por compendio se sustenta en tres artículos científicos publicados en revistas indexadas en el JCR y cinco congresos (cuatro internacionales y uno nacional), los dos primeros artículos indexados recogen la parte de la investigación correspondiente a morteros que utilizan como conglomerante CAA, que incluyen en su dosificación materiales residuales. El tercer artículo recoge los resultados sobre estabilización de suelos incluyendo el diseño de un molde cúbico de pequeñas dimensiones para la realización de probetas de suelo estabilizado, que presenta mejoras sobre los sistemas habitualmente utilizados. La parte de estabilización de suelos tiene una clara componente de aplicación en construcciones de bajo coste económico y medioambiental en países en desarrollo por lo que se han presentado cinco comunicaciones en congresos de reconocido prestigio en esta área, que han estudiado la posibilidad de implementar estos materiales y tecnologías en los países en desarrollo. Se indica a continuación las referencias de los tres artículos publicados con sus indicios de calidad

Influence of Addition of Fluid Catalytic Cracking Residue (FCC) and the SiO_2 Concentration in Alkali-Activated Ceramic Sanitary-Ware (CSW) Binders

Juan Cosa, Lourdes Soriano, Maria Victoria Borrachero, Lucía Reig, Jordi Payá and José María Monzó *

Received: 7 March 2018; Accepted: 17 March 2018; Published: 21 March 2018

Minerals 2018, 8, 123

DOI:10.3390/min8040123

La revista Minerals en el año 2018, en la Categoría Mineralogy ocupaba la posición 12 de 29 por lo tanto pertenece al segundo cuartil (Q2) y tenía un factor de impacto de 2.250.

La revista Minerals en el año 2018, en la Categoría Mining & Mineral Processing ocupaba la posición 6 de 19 por lo tanto pertence al segundo cuartil (Q2)

Compressive strength and microstructure of alkali-activated binary cements developed by combining ceramic sanitary ware (CSW) with fly ash (FA) or blast furnace slag (BFS)

Juan Cosa, Lourdes Soriano, María Victoria Borrachero, Lucia Reig, Jordi Payá, José María Monzó*

Received: 25 May 2018; Accepted: 2 August 2018; Published: 5 August 2018

Minerals 2018, 8, 337

DOI:10.3390/min8080337

La revista Minerals en el año 2018, en la Categoría Mineralogy ocupaba la posición 12 de 29 por lo tanto pertenece al segundo cuartil (Q2) con un factor de impacto en 2018 de 2.250

La revista Minerals en el año 2018, en la Categoría Mining & Mineral Processing ocupaba la posición 6 de 19 por lo tanto pertence al segundo cuartil (Q2)

Stabilization of soil by means alternative alkali-activated cement prepared with spent FCC catalyst

Juan Cosa, Lourdes Soriano, María Victoria Borrachero, Jordi Payá, José M. Monzó

Received: 12 June 2019; Revised: 26 July 2019; Accepted: 16 August 2019

Int J Appl Ceram Technol. 2019;00:1–7.

DOI: 10.1111/ijac.13377

La revisa International Journal of Applied Ceramic Technology en el año 2019 en la Categoría Materials Science, Ceramics ocupaba la posición 11 de 28 por lo tanto pertence al segundo cuartil (Q2) con un índice de impacto de 1.762

En lo que se refiere a los cinco congresos en los que se han presentado los resultados de la investigación, todos ellos son congresos de referencia en al campo de la cooperación al desarrollo, la construcción con tierra y los materiales residuales. Se indican a continuación las referencias de los mismos.

Comunicación oral presentada en el III congreso internacional de estudios del desarrollo en Zaragoza, con el título: Estabilización de suelos con cementos activados alcalinamente: Una solución más sostenible para la construcción de viviendas en países en desarrollo

Ranking congreso	Nivel C5 Nacionales
Fecha del congreso anual	30/06/2016
Pág. Actas congreso	457-465
ISBN / ISSN	978-84-16723-36-2

Comunicación oral presentada en la 10th International Conference on the Environmental and Technical Implications of Construction with Alternative Materials WASCON en Tampere (Finlandia), con el título: Soil stabilization using geopolymers obtained from wastes

Ranking congreso	Nivel C4 CORE C o internacionales con actas
Fecha del congreso anual	08/06/2018
Pág.	47-52
ISBN / ISSN	978-951-758-631-3 - 0356-9403

Comunicación oral presentada en la 17th International Conference on Non-conventional Materials and Technologies NOCMAT en Mérida (México), con el título: Use of alkaline activated cements from residues for soil stabilization

Ranking congreso	Nivel C4 CORE C o internacionales con actas
Fecha del congreso anual	30/11/2017
Pág.	355-364

Comunicación oral presentada en el 18º Seminario Iberoamericano de Arquitectura y Construcción con Tierra en La Antigua Guatemala (Guatemala), con el título: Uso de geopolímeros obtenidos a partir de residuos en la estabilización de suelos

Ranking congreso	Nivel C4 CORE C o internacionales con actas
Fecha del congreso anual	25/10/2018
Pág.	107-114
ISBN / ISSN	978-9929-778-74-0

Comunicación oral presentada en el 19º Seminario Iberoamericano de Arquitectura y Construcción con Tierra en Oaxaca de Juaárez (México), con el título: Propiedades de suelos estabilizados con Geopolímeros fabricados con residuos

Ranking congreso	Nivel C4 CORE C o internacionales con actas
Fecha del congreso anual	18/10/2019
Pág.	150-161
ISBN / ISSN	978-99923-880-6-8

2.2 Objetivos

Como se ha indicado anteriormente se ha estudiado la posibilidad del uso de residuos en la preparación de cementos activados alcalinamente.

Así, el objetivo de la investigación realizada ha sido la obtención de conglomerantes con un menor coste económico y medioambiental, y su aplicación tanto en la preparación de morteros como en la estabilización de suelos, en este último caso con el interés de utilizarlos en países en desarrollo.

Se han utilizado como precursores, el catalizador usado de craqueo catalítico, residuos cerámicos, cenizas volantes, escorias de alto horno, o mezclas de ellos. En la preparación del activador de la reacción geopolimérica se utilizó ceniza de cascarilla de arroz, así como otras cenizas procedentes de la combustión de biomasa.

Se ha realizado una caracterización físico-química de los materiales utilizados, así como estudios microestructurales de los cementos de activación alcalina obtenidos mediante microscopía electrónica (FESEM), también se han utilizando distintas técnicas analíticas, como termogravimetría (TG) y difracción de rayos x (DRX)

3. Aplicación en morteros

A continuación se recogen dos artículos indexados relacionados con la aplicación en morteros de activación alcalina de mezclas de residuos como precursores.

3.1 Influence of Addition of Fluid Catalytic Cracking Residue (FCC) and the SiO_2 Concentration in Alkali-Activated Ceramic Sanitary-Ware (CSW) Binders

Juan Cosa, Lourdes Soriano , María Victoria Borrachero , Lucía Reig , Jordi Payá and José María Monzó., Minerals, 2018, 8, 123

Abstract: Production of Portland cement requires a large volume of natural raw materials and releases huge amounts of CO_2 to the atmosphere. Lower environmental impact alternatives focus on alkali-activated cements. In this paper, fluid catalytic cracking residue (FCC) was used to partially replace (0 wt %–50 wt %) ceramic sanitaryware (CSW) in alkali-activated systems. Samples were activated with NaOH and sodium silicate solutions and were cured at 65 °C for 7 days and at 20 °C for 28 and 90 days. In order to increase CSW/FCC binders' sustainability, the influence of reducing the silica concentration (from 7.28 $mol \cdot kg^{-1}$ up to 2.91 $mol \cdot kg^{-1}$) was analyzed. The microstructure of the developed binders was investigated in pastes by X-ray diffraction, thermo tests and field emission scanning electron microscopy analyses. Compressive strength evolution was assessed in mortars. The results showed a synergetic effect of the CSW/FCC combinations so that, under the studied conditions, mechanical properties significantly improved when combining both waste materials (up to 70 MPa were achieved in the mortars containing 50 wt % FCC cured at room temperature for 90 days). Addition of FCC allowed CSW to be activated at room temperature, which

significantly broadens the field of applications of alkali-activated CSW binders.

Keywords: sustainable construction materials; waste management; alkali-activated binder; fluid catalytic cracking; ceramic sanitaryware; mechanical strength; microstructure

3.1.1 Introduction

Portland cement is the most widely used construction material, which is attributed mainly to its availability, versatility, familiarity, relatively low cost, and the fact that its properties and durability have been widely investigated. According to the data provided by the U.S. Geological Survey [1], 4.2 billion tonnes of cement were produced worldwide in 2016 and, as reported by Imbabi et al. [2], this production is expected to increase and reach as much as 5.6 billion tonnes by 2050. The cement industry and the scientific community have been seeking alternatives to increase the sustainability of this basic construction material in an attempt to develop less harmful binders to the environment, with lower carbon emissions, that use fewer natural resources, and thus better contribute to a long-term ecologically balanced development. However, approximately 0.9 kg of CO_2 per kg of produced cement is released to the atmosphere [2], which implies that nearly 3.78 billion tonnes of CO_2 are generated yearly (about 6% of global CO2 emissions [2,3]). CO2 emissions come mainly from the decomposition of limestone and clay raw materials, and from the energy used to achieve clinkering temperatures (close to 1450 ◦C).

The cement industry and the scientific community have explored different alternatives to improve Portland cement's sustainability. Some have focused on reducing emissions and the energy used during the production process [2]. Others, such as that by Puertas et al. [4,5], have used waste materials to produce clinker. Several studies have proved the

suitability of different silicoaluminate by-products as pozzolanic admixtures to partially replace Portland cement [6–8]. Further studies have focused on developing new alternative low CO_2 binders, such as calcium sulfoaluminate cements [9] or akali-activated binders [3]. As described in [10], an aluminosilicate material (precursor) is dissolved in alkaline media during the geopolimerization process, and Al and Si ions released as monomers polycondensate to form a new binder with an amorphous to semi-crystalline structure. As previously reported by Mellado et al. [11], the CO2 emissions of the binders developed by the alkali-activation of spent fluid catalytic cracking residue (FCC), a by-product from the petrochemical industry, lowered by 13% when activated with NaOH and commercial waterglass solutions compared with PC mortars, and these emissions dropped by up to 63% when using alternative sources of silica (rice husk ash) in the activating solution. Aluminosilicate materials, such as blast furnace slag, metakaolin or fly ashes, have been widely used as precursors in alkali-activated systems [12–14]. However, in recent decades, different studies have investigated the suitability of other by-products, such as palm oil fuel ash [15], rice husk ash or red mud [16], as silicon and aluminum sources to develop new alkali-activated binders. Among them, the reutilization and valorization of ceramic materials is a very interesting research line to be explored given their prolonged biodegradation period (up to 4000 years) [17].

Ceramic sanitary-ware (CSW) waste (i.e., bidets, lavatories, washbasins, etc.) is a type of ceramic residue with high SiO_2 and Al_2O_3 contents (approximately 90%, some of which are in an amorphous state [17]) that has been successfully used as a precursor in [17,18]. According to Baraldi [19], approximately 349.3 million CSW units were produced worldwide in 2014, and Asia was the main producing region (49.2% of total production), followed by the European Union, where 41.6 million units were manufactured (11.9% of global production). As reported by

Medina et al. [20], 5%–7% of the 7 million CSW pieces produced in Spain in 2008 were rejected for sale due to defects, such as cracks, nicks or glaze damage, or for technical considerations. Additionally, the CSW units deposited in dumps at the end of their life cycle can be easily separated since they are not generally adhered to other construction materials, such as gypsum or cement.

In a previous study, Reig et al. [18] successfully reused ceramic sanitary-ware waste as a precursor to produce alkali-activated binders. These authors observed that applying temperature during the curing process (65 °C) proved essential to activate CSW, and $Ca(OH)_2$ addition played an essential role in the fresh-state behavior of the developed CSW binders. The mix proportions of the activating solution were optimized so that compressive strength values of up to 36 MPa were achieved in the mortars cured at 65 °C for 7 days. Later studies [17] explored the influence of $Ca(OH)_2$, calcium aluminate cement (CAC) and Portland cement (PC) on the microstructure and mechanical properties of alkali-activated CSW. The obtained results decidedly increased the valorization possibilities of CSW as a precursor in alkali-activated binders, since the compressive strength results significantly improved with relatively low cement contents (64.41 and 70.69 MPa were achieved in the mortars blended with 10 wt % PC and 15 wt % CAC, respectively, cured at 65 °C for 7 days). According to the reported results [17], hydration of PC and CAC followed a different pathway from that generally observed in water, and the provided Ca and Al ions were taken up in the new alkali-activated binder to form (N,C)-A-S-H or C-A-S-H gels. Despite the mechanical properties significantly improving with PC or CAC additions, low CSW substitutions were recommended, because these cements use natural resources, release large volumes of CO_2 to the atmosphere and require huge amounts of energy to reach clinkering temperatures (close to 1450 and 1600 °C for PC and CAC, respectively) [17]. Thus, exploring if the partial substitution of CSW for some industrial by-product favors the

activation of CSW at room temperature, providing mechanical properties that allow these binders to be used in conventional construction applications, would contribute significant economic and environmental benefits. In line with this, spent fluid catalytic cracking residue (FCC) is a good candidate to be used. As explained by Trochez et al. [21], FCC is an aluminosilicate material with a zeolitic structure used to transform crude oil into fuel products by breaking long chains in hydrocarbon molecules. FCC is replaced when it loses its catalytic properties and is classified as inert waste. According to Trochez et al. [21], approximately 800,000 tons of this by-product are produced yearly worldwide.

Although FCC has been widely landfilled, in recent years, new alternatives for reusing and valorizing this waste have been explored. Among the uses related with cement and concrete industries, FCC has been successfully used in either Portland cement production [22] as a pozzolanic admixture [6,23–25], or in calcium aluminate systems [26]. The use of FCC as a precursor in alkali-activated binders has also been investigated in the last few years [21,27–29]. In the study by Tashima et al. [27], strength values within the 10–70 MPa range were obtained in mortars cured at 65 °C for 3 days, developed with a water/FCC ratio of 0.60 and activated with SiO_2/Na_2O ratios that ranged from 0 (no silica) to 1.46. Further research [28] analyzed the influence of different SiO_2/Na_2O and H_2O/FCC ratios on the mechanical properties and microstructure of alkali-activated FCC binders. The best results (68.3 MPa) were obtained for the mix prepared with 10 $mol \cdot kg^{-1}$ of Na and SiO_2/Na_2O and H_2O/Na_2O molar ratios of 1.17 and 11.11, respectively, and strength values further improved (up to 83.6 MPa) by reducing the water/FCC ratio from 0.60 to 0.45. The authors attributed the poorer performance of some mortars to a reduced alkalinity in the activating solution, which decreased the dissolution of the precursor and, consequently, the binder formation. Cheng et al. [30,31], who investigated the influence of FCC additions in alkali-activated metakaolin, established 10% as the optimum percentage

of substitution. These authors also concluded that the SiO_2/Na_2O and solid/liquid ratios strongly determined the properties of the blended system.

This research aimed to investigate the influence of different FCC additions (0 wt %–50 wt %) and silica concentrations on the compressive strength and microstructure of alkali-activated ceramic sanitary-ware waste binders.

3.1.2. Materials and Methods

3.1.2.1 Materials

Ceramic sanitary-ware (CSW) units, rejected during the manufacturing process due to production defects, were supplied by the company Ideal Standard (Valencia, Spain). Pieces were produced following the process previously described by Medina et al. [20]: the prepared raw materials were cast into a mold which conferred the piece the desired shape; products were then dried to evaporate water and were finally sintered at temperatures within the 1200–1290 °C range. Units were broken into pieces with a hammer and crushed in a jaw crusher (BB200 Retsch) to reduce particle size to less than 2 mm. Crushed particles were then dry-milled in a Roller 1 jars turner roller by Gabrielli. Grinding was achieved by turning two cylindrical alumina 5 L volume jars for 6 h (190 rpm for the first 10 min and 140 rpm for the remaining time). Each jar was filled with 1500 g of ceramic waste and 6500 g of alumina balls. Fluid catalytic cracking catalyst residue (FCC) was supplied by the company Omya Clariana S.A. (Tarragona, Spain). The material was used as received.

Alkaline solutions were prepared by mixing sodium hydroxide pellets (98% purity, supplied by Panreac), water and waterglass (composed of 28% SiO_2, 8% Na_2O and 64% H_2O, supplied by Merck, Kenilworth, NJ, USA).

3.1.2.2 Experimental Flow Chart, Mix Proportions and Curing Conditions

The experimental process followed herein is summarized in Figure 3.1-1. Designation of samples, together with the mix proportions, concentrations, ratios of the activating solutions and curing conditions, are summarized in Table 3.1-1. In the first step of the study, the influence of different FCC additions (0 wt %–50 wt %) on the CSW systems alkali-activated with a constant SiO_2/Na_2O molar ratio (1.94, obtained with constant Na_2O and SiO_2 concentrations of 3.75 and 7.28 $mol \cdot kg^{-1}$, respectively) was investigated. The 100 wt % FCC binders were also prepared for comparison purposes. After establishing the optimum FCC percentage (30 wt %), the influence of different SiO_2 concentrations (2.91 to 7.28 $mol \cdot kg^{-1}$ of water) on the mechanical properties of the developed systems was analyzed. As the sodium concentration remained constant throughout the study (Table 3.1-1), the SiO_2/Na_2O molar ratios varied from 0.78 to 1.94. Given that, as explained by Mellado et al. [11], the vast majority of the CO_2 emissions in alkali-activated systems are attributed to commercial waterglass, the objective of this part of the study was to minimize the emissions of the newly developed binders, which contributes to improve their sustainability. After establishing the optimum silica concentration (4.37 $mol \cdot kg^{-1}$, which gave good compressive strength results with the lowest silica content), the influence of FCC additions on the alkali-activated CSW systems was explored again. This provided information on the mechanical properties and microstructure developed with both silica concentrations (initial and optimized).

Designation of pastes and mortars (Table 3.1-1) was defined according to their FCC content and SiO_2 concentration in such a way that '10/7.28' corresponded to a sample containing 10 wt % FCC, activated with a solution containing 7.28 mols of silica per kg of water (concentrations in molality terms). Mix proportions were adopted from previous studies [18] were compressive strength results higher than 25 MPa were achieved in alkali-activated CSW mortars containing 4.5 wt % $Ca(OH)_2$, activated with

solutions prepared with 3.75 mol·kg^{-1} of Na_2O and 7.28 mol·kg^{-1} of SiO_2. As previously reported in [32], where porcelain stoneware tiles were used as a precursor (material that behaved similarly to CSW when alkali-activated), addition of $Ca(OH)_2$ was essential to successfully activate this ceramic waste, and strongly influenced the workability and setting time of the developed mortars. Based on both previous studies [18,32], 4 wt % $Ca(OH)_2$ was added to the CSW samples (no calcium hydroxide was used in the 100 wt % FCC systems). Pastes and mortars were cured following the conditions summarized in Table 3.1-1: in a temperature- and humidity- controlled chamber at 20 °C with 95% relative humidity (RH) for 28 and 90 days; and in a water bath at 65 °C for 7 days, inside a sealed box, with 100% RH.

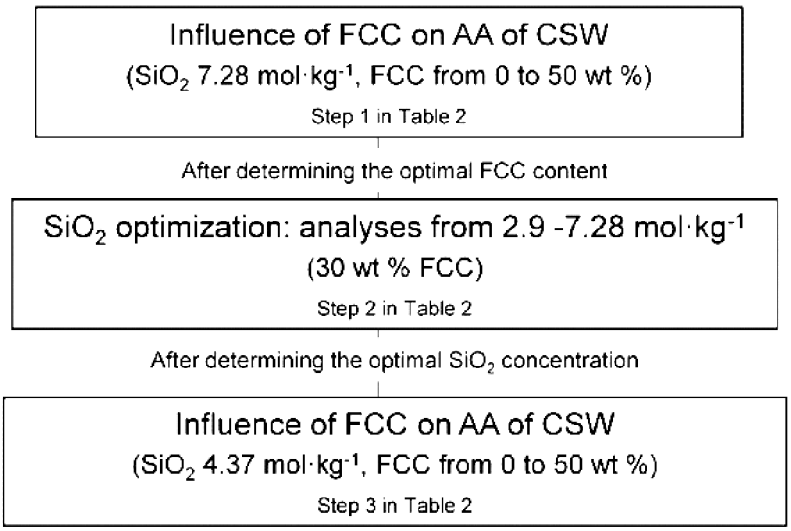

Fig. 3.1-1 Experimental process of the influence of the FCC and SiO2 concentrations on the alkali activation of CSW.

Tab. 3.1-1 Designation, mix proportions, ratios and curing conditions used to develop the CSW/FCC alkali-activated binders.

Step	Designation	FCC wt %	w/b[a]	Activating solution			Na_2O $mol \cdot kg_{binder}^{-1}$	SiO_2 $mol \cdot kg_{binder}^{-1}$	$Ca(OH)_2$[b] wt %	Curing conditions
				Na_2O $mol \cdot kg^{-1}$	SiO_2 $mol \cdot kg^{-1}$	SiO_2/Na_2O Molar ratio				
1	0/7.28	0	0.45	3.75	7.28	1.94	1.69	3.28	4	7 days at 65ºC 28 and 90 days 20ºC
	10/7.28	10								
	20/7.28	20								
	30/7.28	30								
	40/7.28	40								
	50/7.28	50								
	100/7.28	100							0	
2	30/2.91	30			2.91	0.78	1.69	1.31	4	7 days at 65ºC
	30/3.64				3.64	0.97		1.64		
	30/4.37				4.37	1.16		1.97		
	30/5.82				5.82	1.55		2.62		
	30/7.28				7.28	1.94		3.28		
3	0/4.37	0			4.37	1.16	1.69	1.97	4	7 days at 65ºC 28 and 90 days 20ºC
	10/4.37	10								
	20/4.37	20								
	30/4.37	30								
	40/4.37	40								
	50/4.37	50								
	100/4.37	100							0	

[a] Water (w), composed of that provided by the sodium silicate solution plus tap water directly added to the activating solution; binder (b), composed of CSW and the different FCC contents. [b] $Ca(OH)_2$ used as an addition to the binder in the pastes and mortars that contained CSW.

3.1.2.3. Sample Preparation and Characterization

CSW powder and $Ca(OH)_2$ were dry-mixed and having homogenized the mixture, the corresponding amount of FCC was added, and the mixing process continued until a homogeneous blend was obtained. The activating solution (formed by NaOH, waterglass and water) was then mixed with the blended powder until the paste was uniform. Pastes and mortars were prepared with a water/binder ratio (w/b) of 0.45: water was composed of that contained in the sodium silicate solution, plus tap water, and the binder was formed by CSW and its partial substitution with FCC ($Ca(OH)_2$ was used as an addition). Mortar samples of 40 mm × 40 mm × 160 mm were prepared using siliceous aggregates with a fineness modulus of 4.3, and a binder/sand weight ratio of 1:3. The prismatic samples were wrapped with plastic film until they reached the testing age to prevent efflorescence formation and maintain moisture during the curing process.

The particle size distribution of the FCC and CSW milled powder was determined by laser diffraction in a Mastersizer 2000 by Malvern Instruments (Malvern, United Kingdom). Powder was stirred in water at 1200 rpm and ultrasounds were applied for 1 min to disperse possible particle agglomerations. The amorphous content of the CSW and FCC waste was determined according to Standard UNE EN 196-2:2006, and their chemical composition was determined by X-ray fluorescence (XRF) in a Philips Magix Pro spectrometer. Microstructure evolution was investigated in the pastes blended with 0 wt %–50 wt % FCC, activated with SiO_2 concentrations of 4.37 and 7.28 $mol \cdot kg^{-1}$, and cured at 65 °C for 7 days and at 20 °C for 28 days. The 100 wt % FCC pastes were also prepared as a reference. X-ray diffraction (XRD) analyses of raw materials and pastes were run in a Brucker AXS D8 Advance (Billerica, MA, USA) by taking Cu Kα radiation, from 10 to 70 2θ degrees, at 20 mA and 40 kV, using an angle step of 0.02 and a 2-s accumulation time. The

FESEM analyses were run in an FESEM ULTRA 55, by ZEISS (Oberkochen, Germany). The paste samples were coated with carbon and images were taken at 2 kV. The tests were run in a Mettler Toledo TGA 850 thermobalance from 35 to 600 °C, at a heating rate of 10 °C/min, in a nitrogen atmosphere at a flow gas rate of 75 mL·min^{-1}. Aluminum-sealed crucibles (100-µL volume) with a pinholed lid were used. The compressive strength tests were performed in mortars according to Standard UNE EN 196-1.

3.1.3. Results and Discussion

3.1.3.1. Properties of Raw Materials

Figure 3.1-2 shows the morphology of the CSW particles (crushed and milled) and FCC. As observed, the crushed CSW particles are composed of a glaze covering and a ceramic body (Figure 3.1-2a). Both parts homogenized after particle size diminished during the milling process, and the field emission scanning electron microscopy images denote dense irregular particles with a smooth surface (Figure 3.1-2b). The FCC particles (Figure 3.1-2c) exhibited higher porosity and a smaller particle size compared with the milled CSW, which conferred them a larger specific surface.

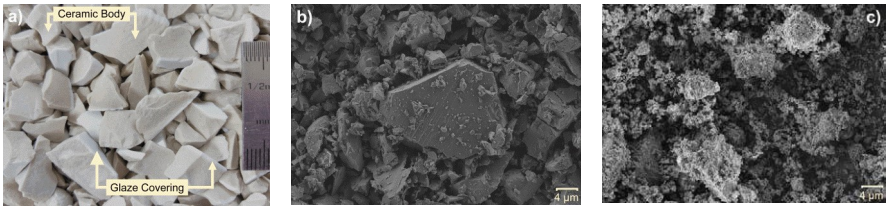

Fig. 3.1-2 Images of the materials used as a precursor: (a) Crushed CSW; (b) Milled CSW; (c) As-received FCC.

The CSW particles presented a mean diameter of 31.24 μm, with 10 vol % of particles under 2.92 μm, 50 vol % under 22.38 μm, and 90 vol % under 73.32 μm (d_{10}, d_{50} and d_{90} values, respectively). In agreement with the FESEM micrographs, the FCC powder had a smaller particle size, with a mean diameter of d_{10}, d_{50} and d_{90} of 17.12, 1.10, 9.61 and 45.12 μm, respectively.

The XRD spectra of the raw materials used as a precursor in the alkali-activated systems are presented in Figure 3.1-3. The main crystalline phases identified in the ceramic material were quartz (Q, SiO_2, PDFcard331161) and mullite (M, $Al_6Si_2O_{13}$, PDFcard150776), and small amounts of calcium feldspar anorthite (A, $CaAl_2Si_2O_8$, PDFcard411486) were also distinguished. The signals attributed to quartz and mullite also arose in the FCC spectra, together with those assigned to sodium feldspar Albite (B, $NaAlSi_3O_8$, PDFcard200554) and sodium-faujasite (F, $Na_2Al_2Si_4O_{12}{\cdot}8H_2O$, PDFcard391380). Both materials exhibited a deviation from the baseline (from 17 to 32 2θ degrees), which denotes the presence of amorphous phases in the waste materials. According to Rodriguez et al. [29], the amorphous phases in FCC are formed by the partial destruction of zeolites during the catalytic cracking process. Zeolitic phases have also been distinguished by Trochez et al. [21], Rodriguez et al. [29] and Tashima et al. [28], who used FCC as a precursor to produce alkali-activated binders. As described by Rodríguez et al. [29], FCC may be considered to be zeolitic phases bound by an aluminosilicate matrix.

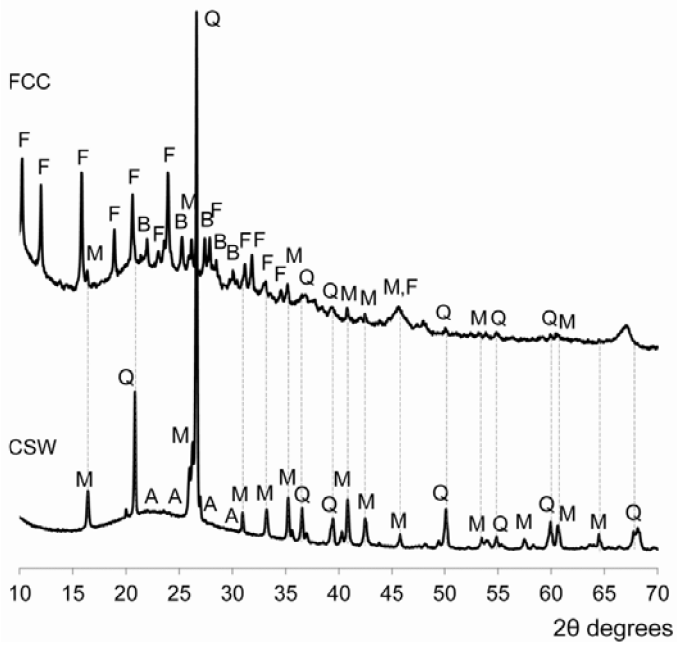

Fig. 3.1-3 Mineralogical composition of the FCC and CSW raw materials. Quartz (Q, SiO2); Mullite (M, $Al_6Si_2O_{13}$); Anorthite (A, $CaAl_2Si_2O_8$); Albite (B, $NaAlSi_3O_8$); sodium-faujasite (F, $Na_2Al_2Si_4O_{12}{\cdot}8H_2O$).

Table 3.1-2 shows the chemical composition of FCC and CSW. As observed, both materials contained large amounts of SiO_2 and Al_2O_3 (97.02 wt % and 89.06 wt % the sum for FCC and CSW, respectively), and the percentage of alumina was significantly higher for FCC. CSW exhibited a SiO_2-to-Al_2O_3 mass ratio of 2.79, and this ratio came close to 1 for FCC. Similar Al_2O_3 and SiO_2 contents have been previously reported by Rodriguez et al. [29] for FCC (48.40 wt %, and 46.94 wt %, respectively), while slightly lower Al_2O_3 values (41.57 wt % and 48.09 wt

%, for Al_2O_3 and SiO_2, respectively) have been recorded by Trochez et al. [21] for an FCC obtained from a Colombian petroleum company (both FCC were also alkali-activated to produce binders). In the study by Pacewska et al. [26], the Al_2O_3 and SiO_2 contents of two different FCC varied within the 38%–41% range and the 50%–54% range, respectively, which led to a slightly higher SiO_2/Al_2O_3 mass ratio (1.33).

Oxides other than alumina and silica (CaO, Fe_2O_3, K_2O or Na_2O) in the ceramic material were attributed to their presence on the clay used to manufacture the CSW units since, as observed by Pacheco-Torgal and Jalali [33], the chemical composition of the ceramic products is similar to that of the original clays. The amorphous content of the CSW and FCC wastes was respectively 45.6% and 88.3%.

Tab. 3.1-2 Chemical composition of the FCC and CSW wastes (wt %).

	Al2O3	SiO_2	CaO	Fe2O3	K_2O	Na_2O	P2O5	Other	LOI *
FCC	49.26	47.76	0.11	0.60	0.02	0.31	0.01	1.42	0.51
CSW	23.60	66.00	1.20	1.30	2.80	2.40	0.50	2.00	0.20

* Determined at 950 °C.

3.1.3.2. Compressive Strength

Figure 3.1-4 shows the compressive strength results of the alkali-activated CSW/FCC blended mortars, developed with 7.28 mol·kg^{-1} of SiO_2 and increasing amounts of FCC (0 wt %–50 wt %), cured at 65 °C for 7 days, and at 20 °C for 28 and 90 days (Step 1 of the study, according to Figure 3.1-3 and Table 3.1-1). The alkali-activated 100 wt % FCC mortars were prepared for comparison purposes. As observed, the compressive strength values significantly improved with FCC addition as up to 70 MPa were achieved in the mortars containing 50 wt % FCC cured at room temperature for 90 days. Both waste materials exhibited a synergetic effect, so that the mechanical properties given by the blended

systems were higher than those obtained when only one waste was used as a precursor (100 wt % CSW or FCC mortars). These results agree with the previous findings of Fernández-Jiménez et al. [34] who, after exploring the influence of reactive alumina on alkali-activated fly ashes, concluded that the ashes which best performed when activated were those with large amounts of reactive SiO_2 and Al_2O_3 (determined as a mass percentage) and with Si/Al reactive atomic ratios below 2. Since FCC is an Al_2O_3-rich residue with a high percentage of soluble fraction (88.3% amorphous content), the FCC additions in the alkali-activated CSW mortars provided reactive silica and alumina and lowered the SiO_2/Al_2O_3 ratio of the blended system (originally 2.79, and 1 for the CSW and FCC precursors, respectively).

The CSW mortars containing up to 20 wt % FCC obtained better compressive strength results when cured at 65 ºC than at room temperature, and this tendency reversed with further FCC additions. This behavior was attributed to the fact that thermal energy was required to activate the chemical reactions in 100 wt % and 90 wt % CSW mortars. Thus, the beneficial effect produced by FCC in the CSW alkali-activated systems was especially important at room temperature since the strength values of the 100 wt % CSW mortars cured at 20 °C for 28 days increased from 3.6 to 26.6 MPa and to 39.5 MPa with the 20 wt % and 30 wt % FCC additions, respectively. These results confirm the beneficial influence of FCC in the alkali-activated CSW binders and greatly extend their application field. Similar results have been previously reported in [17], where addition of $Ca(OH)_2$, PC or CAC significantly improved the strength of the alkali-activated CSW binders: up to 78.6 MPa and 66.3 MPa were achieved in the mortars blended with 20 wt % CAC and 15 wt % PC, respectively (cured at 65 ºC for 7 days). However, the practical benefit of FCC compared with the PC or CAC additions, which have a

high negative environmental impact, lies in an industrial by-product being reused.

The low strength values exhibited by the 100 wt % FCC mortars (lower than 20 MPa) significantly differed from the optimum ones previously reported by Tashima et al. [28]. These authors obtained up to 68.3 MPa in mortars cured at 65 ºC for 3 days, prepared with a water/FCC ratio of 0.60, and activated with 10 mol·Kg^{-1} of Na and a SiO_2/Na_2O molar ratio of 1.17. Trochez et al. [21] have also reported compressive strength values within the 2.5 to 67 MPa range in alkali-activated FCC pastes cured at room temperature for 7 days. The best results were obtained with a SiO_2/Na_2O molar ratio of 0.72 (activating solution), and overall SiO_2/Al_2O_3 and Na_2O/Si_2O ratios of 2.4 and 0.25, respectively. The differences with the strength values obtained herein for the 100 wt % FCC mortars were attributed to the different mix proportions used (7.5 mol·Kg^{-1} of Na and a SiO_2/Na_2O molar ratio of 1.94 in Step 1 of the study) compared with the optimum solutions reported by Tashima et al. [27,28] and Trochez et al. [21]. The cited works [21,27,28] observed that excess silicates in the system (high SiO_2/Na_2O ratios) resulted in reduced strength. Similarly, as explained by Rodríguez et al. [29] and Trochez et al. [21], highly alkaline solutions are required to dissolve the AlO_4^- species in the FCC precursor since an insufficient presence of alkalis retards the dissolution of zeolites and leads to a larger amount of unreacted FCC which, consequently, reduces binder formation.

FCC 30 wt % was established as the optimum percentage in Stage 1 of the study since the compressive strength exhibited by this mortar (40 MPa after 28 curing days at room temperature) was considered high enough to allow its use in general construction applications. Moreover, the improvement of strength observed with 10 wt % increments of FCC progressively reduced, so that compressive strength results improved 20.1 MPa, 17.4 MPa, 9.2 MPa and 3.6 MPa when increasing the FCC

content 10 wt %–20 wt %, 20 wt %–30 wt %, 30 wt %–40 wt % and 40 wt %–50 wt %, respectively. Since, as previously explained in the Introduction, waterglass is the component with the highest environmental impact on alkali-activated binders [11], the purpose of the second part of this study was to lower the SiO_2 concentration to improve the developed mortars' sustainability. The compressive strength of the mortars blended with 30 wt % FCC, prepared with silica concentrations ranging from 2.91 to 7.28 mol·kg^{-1} and cured at 65 ºC for 7 days, is plotted in Figure 3.1-5. As observed, the strength results progressively increased with the SiO_2 concentration, and similar values were recorded in the mortars prepared with the largest amounts of silica (5.82 and 7.28 mol·kg^{-1}). Tashima et al. [27] have also observed a progressive increase in compressive strength with the silica content in FCC mortars alkali-activated with 10 mol kg^{-1} of sodium. In their study [27], optimum results (≈70 MPa after 3 curing days at 65 ºC) were obtained with 1.58 mols of SiO_2 (equivalent to 3.51 mol·kg$_{binder}^{-1}$ which, as reported in Table 3.1-1, comes close to the 3.28 mol·kg$_{binder}^{-1}$ that corresponds to 7.28 mol·kg^{-1} of silica in the activating solution), and decreased with further additions (≈60 MPa with 1.97 mols of SiO_2, equivalent to 4.38 mol·kg$_{binder}^{-1}$).

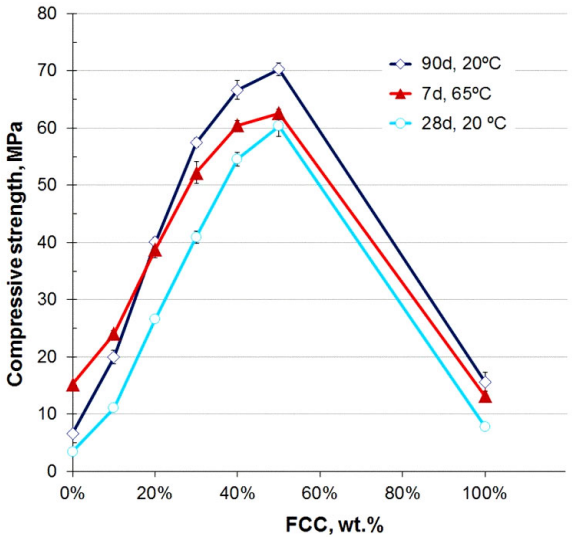

Fig. 3.1-4Evolution of compressive strength with the FCC content in the alkali-activated CSW mortars prepared with 7.28 mol·kg−1 SiO_2 activating solutions, cured at 65 ◦C for 7 days and at 20 ◦C for 28 and 90 days.

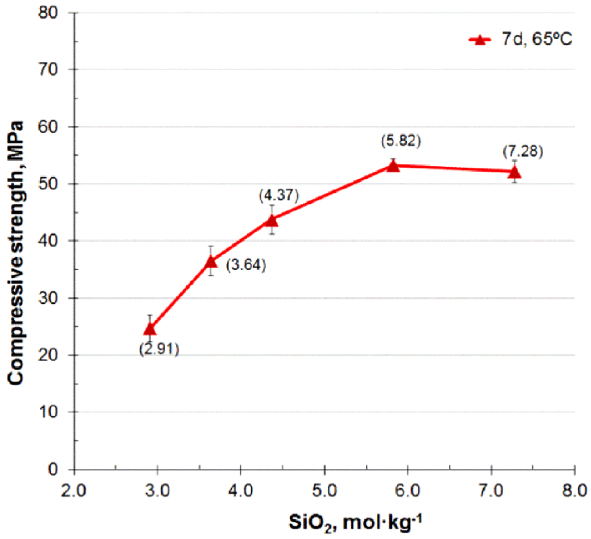

Fig. 3.1-5 Compressive strength evolution with the SiO_2 concentration (indicated in parentheses) in the alkali-activated CSW mortars containing 30 wt % FCC cured at 65 ◦C for 7 days.

A silica concentration of 4.37 mol·kg^{-1} which, as shown in Figure 3.1-5, provided strength results that came close to 44 MPa, was selected for the final study stage. This compressive strength was still significantly higher than that recorded for the 100 wt % CSW mortar activated with 7.28 mol·kg^{-1} of SiO_2, which yielded 15.3 MPa after 7 days at 65 ◦C (Figure 3.1-4). Silica content (added as waterglass) reduced from 3.28 mol·kg$_{binder}^{-1}$ to 1.97 SiO_2 mol·kg$_{binder}^{-1}$ (as reported in Table 3.1-1), which certainly contributed to improve the developed mortars' sustainability. The compressive strength evolution of the CSW mortars blended with 0 wt %–50 wt % FCC, alkali-activated with 4.37 and 7.28 mol·kg^{-1} silica concentrations, cured at 65 ºC for 7 days, and at 20 ◦C for 28 and 90

days, is plotted in Figure 3.1-6. As observed, CSW blended mortars exhibited better mechanical properties with the highest silica concentration, no matter what the FCC content, and these differences were more noticeable at higher temperatures (65 °C) or for longer curing times (90 days). Nevertheless, the strength values recorded after 28 days at room temperature with 4.37 mol·kg^{-1} of SiO_2 and 30 wt % (or higher) FCC contents were high enough to allow the use of these binders in common construction uses. While waterglass content lowered by 40% when using 4.37 mol·kg^{-1} of SiO_2, loss of strength between the high- and low-silica mortars prepared with the same FCC contents reduced by maximum 21.37% and 27.95% after 28 and 90 curing days, respectively (strength loss calculated in the mortars containing 20 wt %–50 wt % FCC). As the better mechanical properties provided by the higher silica concentrations would allow higher strength concrete to be developed, reducing the section of the construction elements or applying loads with shorter curing times, the alkali-activated binders prepared with 7.28 mol·kg^{-1} silica in the activating solution would be recommended for special applications in which higher mechanical properties are required.

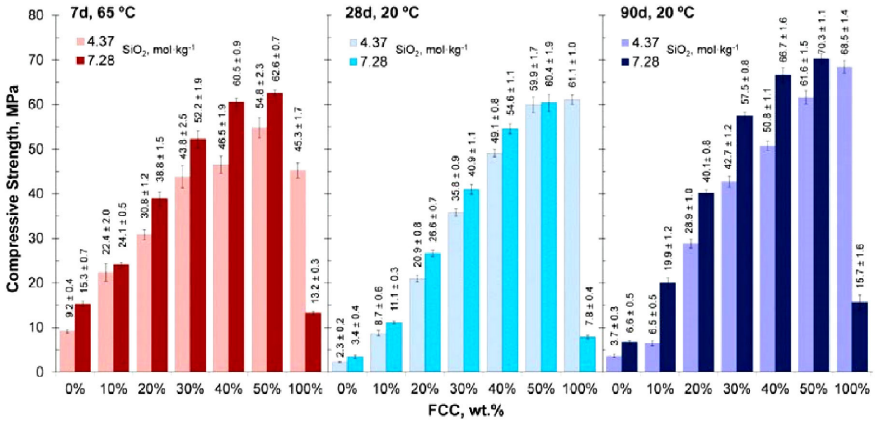

Fig. 3.1-6 Compressive strength of the alkali-activated CSW mortars cured at 65 ◦C for 7 days, and at 20 ◦C for 28 and 90 days. Influence of the FCC contents and SiO_2 concentrations in the activating solution.

2.1.3.3. X-ray Diffraction (XRD)

The XRD spectra for the CSW/FCC blended pastes, alkali-activated with solutions containing 4.37 and 7.28 mol·kg^{-1} of SiO_2, are reported in Figures 3.1-7 and 3.1-8. The spectra of the pastes cured at 20 ºC for 28 days are shown in Figure 3.1-7, while those of the pastes cured at 65 ºC for 7 days are presented in Figure 3.1-8. Quartz and mullite, both previously identified in the raw CSW and FCC materials, were also detected in all the activated pastes. This denotes that these crystalline stable phases did not significantly participate in the alkali-activation process. Signals attributed to the calcium feldspar anorthite were easily distinguished in the 100 wt % CSW activated paste and that blended with 10 wt % FCC, while the intensity of the peaks assigned to albite progressively increased with FCC content. Signals due to sodium-faujasite, which arose in the FCC spectra (Figure 3.1-3), were not distinguished in the activated pastes. This suggests that this zeolite was

dissolved by the activating solution to provide Al and Si, which promoted the formation of an aluminosilicate-type binding gel. These results well agree with those previously reported by Rodríguez et al. [29], who also identified crystalline mullite and quartz, but neither observed the faujasite-type zeolite after the activation of FCC, no matter what activating conditions were used.

A displacement of the baseline toward higher 2θ angles (from 17 to 32 2θ degrees in the raw materials to 25–35 2θ degrees in the activated pastes) was observed with increasing FCC additions. Trochez et al. [21] and Tashima et al. [28] have also reported a deviation from the baseline in FCC activated pastes, which was attributed to the formation of a new amorphous aluminosilicate-type gel during the alkali-activation process. No signals due to $Ca(OH)_2$, which was added to all the CSW pastes, were distinguished in the XRD patterns of the activated pastes, which suggests that calcium hydroxide is consumed during the activation process. These results fall in line with the previous findings reported by Reig et al. [17,32], who did not distinguish $Ca(OH)_2$ after the activation of either porcelain stoneware tiles [32] or CSW [17].

No significant amounts of new crystalline phases were identified by the XRD analyses. Sodium carbonate Natron (N, $Na_2CO_3{\cdot}10H_2O$, PDFcard150800) formed in some of the activated pastes, mainly those prepared using a single raw material as a precursor (100% CSW or 100% FCC). This sodium carbonate has been previously identified in CSW alkali-activated pastes containing up to 8 wt % $Ca(OH)_2$ [17], and in similar alkali-activated ceramic materials, such as porcelain stoneware tiles (blended with 2 wt %–5 wt % calcium hydroxide) [32]. Sodium carbonates have also been distinguished by Tashima et al. [28] in alkali-activated FCC pastes, and have been attributed to sample carbonation, or to the presence of unreacted reagents. The zeolite natrolite (T, $Na_2Al_2Si_3O_{10}{\cdot}2H_2O$, PDFcard 200759) formed in the 100 wt % FCC

pastes activated at room temperature with 4.37 mol·kg^{-1} of SiO_2 (Figure 3.1-7a). Peaks attributed to other zeolites were observed only in the pastes cured at 65 °C and developed with 100 wt % or 50 wt % FCC (Figure 3.1-8). More specifically, of the pastes cured at 65 °C, zeolite A (Z, $Na_2Al_2Si_{1.85}O_7{\cdot}7.5H_2O$, PDFcard380241) arose in the 100 wt % FCC pastes (regardless of the silica concentration), and that blended with 50 wt % FCC and activated with 7.28 mol·kg^{-1} of silica. Zeolites Herschelite (H, Na $AlSi_2O_6{\cdot}3H_2O$, PDFcard191178) and Rh0 (R, formed by eight sodalite units, $Al_{12}H_{12}Si_{36}O_{96}$, PDFcard270015) were identified in the 100 wt % FCC pastes activated with 7.28 and 4.37 mol·kg^{-1} SiO_2, respectively. Different zeolite type phases have also been distinguished by Trochez et al. [21] in alkali-activated FCC systems. It is important to highlight that zeolites formation was not favored in the systems with higher CSW contents (0 wt %–30 wt % FCC), which denotes the high metastability of the formed amorphous binding gel.

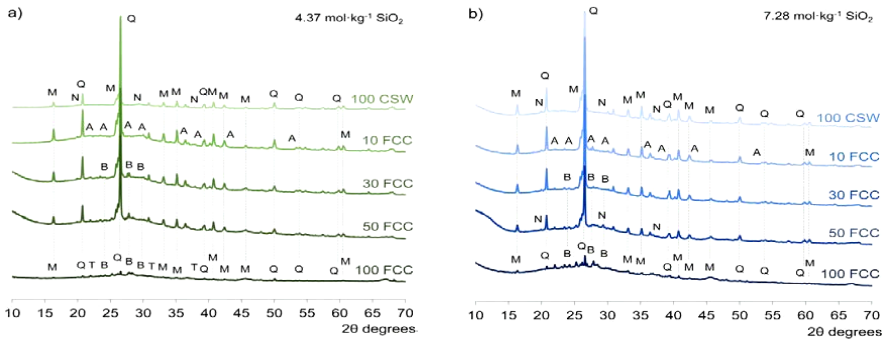

Fig. 3.1-7 XRD spectra for the CSW/FCC blended pastes containing different amounts of FCC, cured at 20 ◦C for 28 days, and alkali-activated with solutions prepared with SiO2 concentrations of: (a) 4.37 mol·kg−1; (b) 7.28 mol·kg−1. Quartz (Q, SiO_2); Mullite (M, $Al_6Si_2O_{13}$); Anorthite (A, $CaAl_2Si_2O_8$); Albite (B, $NaAlSi_3O_8$); Natron (N, $Na_2CO_3{\cdot}10H_2O$); Natrolite (T, $Na_2Al_2Si_3O_{10}{\cdot}2H_2O$).

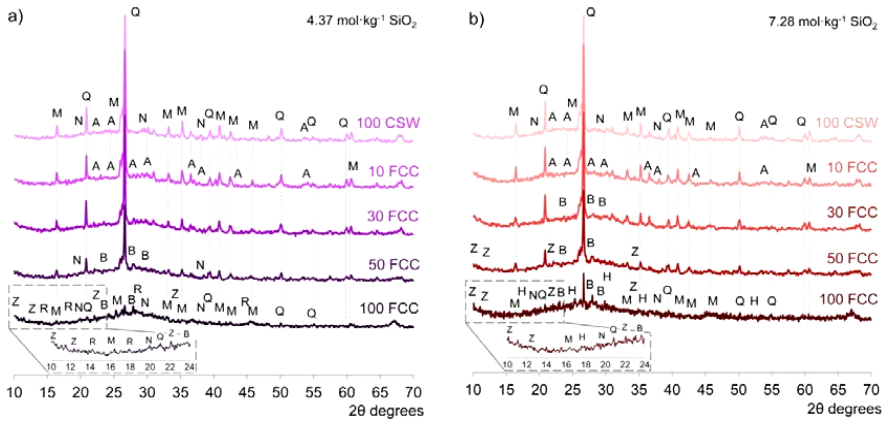

Fig. 3.1-8 XRD spectra for the CSW/FCC blended pastes containing different amounts of FCC, cured at 65 ◦C for 7 days, alkali-activated with solutions prepared with SiO_2 concentrations of: (a) 4.37 mol·kg−1; (b) 7.28 mol·kg−1. Quartz (Q, SiO_2); Mullite (M, $Al_6Si_2O_{13}$); Anorthite (A, $CaAl_2Si_2O_8$); Albite (B, $NaAlSi_3O_8$); Natron (N, $Na_2CO_3{\cdot}10H_2O$); Herschelite (H, Na $AlSi_2O_6{\cdot}3H_2O$); Zeolite A (Z; $Na_2Al_2Si_{1.85}O_7{\cdot}7.5H_2O$); Zeolite Rh0 (R, $Al_{12}H_{12}Si_{36}O_{96}$).

3.1.3.4. Thermal Analysis

Figure 3.1-9 shows the curves for the CSW/FCC blended pastes prepared with 0 wt %, 10 wt %, 30 wt % and 50 wt % FCC, activated with SiO_2 concentrations of 4.37 and 7.28 mol·kg^{-1} and cured at 20 ◦C for 28 days and at 65 ◦C for 7 days. 100 wt % FCC pastes were also prepared for comparison purposes. The total mass loss recorded during the tests is indicated as a percentage.

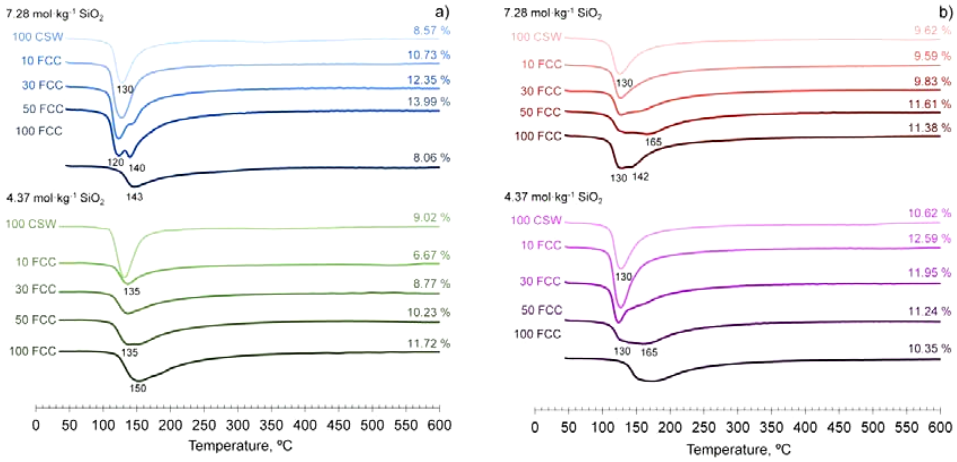

Fig. 3.1-9 Differential curves for the CSW and FCC blends, activated with solutions prepared with SiO_2 concentrations of 4.37 and 7.28 mol·kg−1, cured at: (a) 20 ◦C for 28 days; (b) 65 ◦C for 7 days. Total mass loss indicated as a percentage.

All the DTG curves presented a single band from 100 to 200 ◦C which, according to [35], typically arises due to the dehydration of the newly-formed N-A-S-H or (N,C)-A-S-H gels. The TG analyses were unable to confirm the presence of zeolitic phases, previously identified by XRD, since the signal originated by the dehydration of zeolites also appears within this temperature range (60–160 ◦C) [35]. While the 100 wt % CSW activated pastes exhibited a narrower and defined peak at 130 ◦C, it broadened with increasing FCC contents, which suggests a change in the binding gel structure. Total loss of mass generally increased with FCC addition, and was greater for the blended pastes than for those prepared with a single raw material (100 wt % CSW of 100 wt % FCC). Mass loss results well agree with the compressive strength evolution reported in Figure 3.1-6, and are attributed to greater binding gel formation, whose

dehydration resulted in a greater loss of water and/or OH groups with increasing FCC contents.

No signals attributed to $Ca(OH)_2$ (520–580 °C) [32] were distinguished in any of the CSW activated pastes, which confirms the results previously obtained by XRD, where no peaks assigned to calcium hydroxide arose after the activation process. This indicates that calcium is consumed during the activation process and, as previously described in [32], it may displace sodium and act as a charge-balancing ion to lead to (C,N)-A-S-H gels. The TG analyses were unable to confirm the presence of natron, whose signals arose in some XRD spectra, because, according to Hidalgo et al. [36], the characteristic bands of carbonates arise within the 625–875 °C range.

3.1.3.5 Field Mission Scanning Electron Microscopy (FESEM)

FESEM micrographs of the pastes prepared with 100 wt % CSW, 30 wt % FCC and 100 wt % FCC, alkali-activated with solutions containing 4.37 and 7.28 mol·kg^{-1} of SiO_2, are shown in Figures 3.1-10 to 3.1-13. While the microstructure of the pastes cured at room temperature for 28 days is shown in Figures 3.1-10 and 3.1-11 (at lower and higher magnifications, respectively), that of the pastes cured at 65 °C for 7 days is presented in Figures 3.1-12 and 3.1-13. The compressive strength results obtained for the 100 wt % CSW alkali-activated mortars cured at room temperature (lower than 3.5 MPa after 28 curing days) agree with the characteristics of the pastes, which were weak and soft. As observed in Figures 3.1-10 and 3.1-11, the morphology of the 100 wt % CSW pastes activated at 20 °C differed from that typically formed in N-A-S-H/(C,N)-A-S-H gels (30 wt % or 100 wt % FCC micrographs). The low mechanical properties and the morphology of these pastes suggest that no typical alkali-activation reactions occurred to a great extent. The 100 wt % FCC pastes activated at room temperature with the lowest silica concentration presented a dense homogeneous structure and, in consonance with the XRD spectra,

where peaks attributed to the zeolitic phase natrolite were identified, microcrystals which resembled zeolitic products were distinguished (labeled as ZE in Figure 3.1-11). Although no signals due to zeolites were identified by the XRD analyses in the 30 wt % FCC paste activated at 20 °C with 7.28 mol·kg^{-1} of SiO_2 (Figure 3.1-7b), typical zeolitic-like morphologies were observed at a higher magnification (Figure 3.1-11, labeled as ZE), which denotes that small amount of zeolites may also form under these conditions.

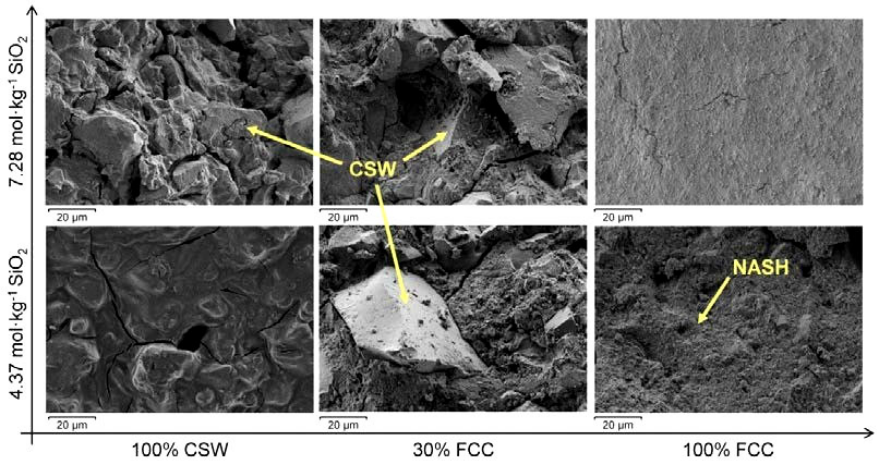

Fig. 3.1-10 Field emission scanning electron images of the CSW/FCC blended pastes prepared with 100 wt % CSW, 30 wt % FCC and 100 wt % FCC, alkali-activated with solutions containing 4.37 and 7.28 mol·kg−1 of SiO_2, and cured at 20 ◦C for 28 days. CSW: ceramic sanitary-ware unreacted particles; NASH: alkali-activated binding gel.

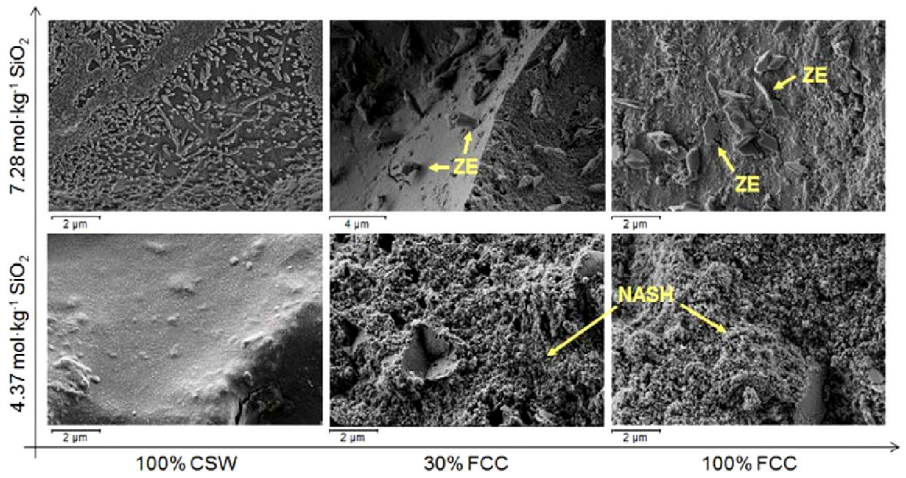

Fig. 3.1-11 . Field emission scanning electron images of the CSW/FCC blended pastes prepared with 100 wt % CSW, 30 wt % FCC and 100 wt % FCC, alkali-activated with solutions containing 4.37 and 7.28 mol·kg−1 of SiO_2, and cured at 20 ◦C for 28 days. Higher magnification. NASH: alkali-activated binding gel; ZE: zeolitic phases.

As observed in Figures 3.1-12 and 3.1-13, the 100 wt % CSW paste and that containing 30 wt % FCC presented a similar microstructure after 7 curing days at 65 ºC, in which unreacted CSW particles, surrounded by reaction products, can be easily distinguished. Variations in the silica concentration or the amount of FCC did not lead to significant differences in the morphology of the newly formed gel. In agreement with the compressive strength results recorded for the 100 wt % FCC mortars, which increased when activated with the 4.37 mol·kg^{-1} of SiO_2 solutions (Figure 3.1-6), the microstructure of these pastes was denser when activated with lower SiO_2 concentrations. Sodium carbonate salt (natron) was also observed with the highest SiO_2 contents (identified with letter N in Figures 3.1-12 and 3.1-13), which denoted excess alkalis in the activating solution. These carbonates have also been previously distinguished in alkali-activated porcelain stoneware tiles [32]. Although

zeolite A, which cubic morphology previously observed Ozer and Soyer-Uzun in alkali-activated metakaolin [37], was identified by XRD tests in the 100 wt % FCC pastes cured at 65 °C, it could not be clearly distinguished by the FESEM analyses.

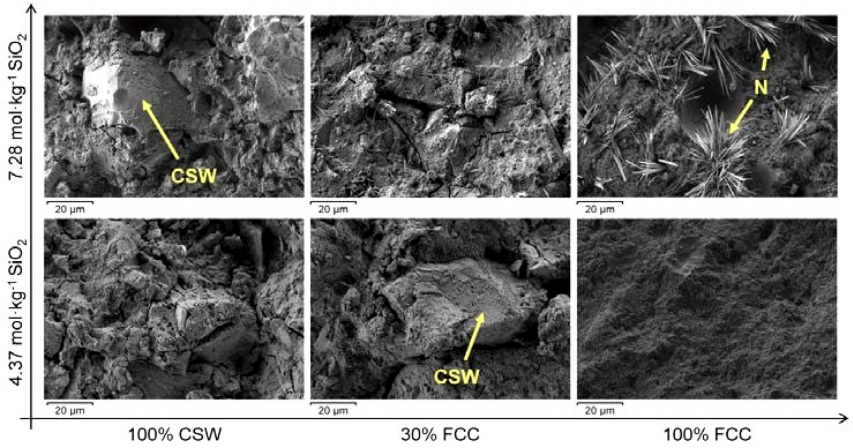

Fig. 3.1-12 Field emission scanning electron images of the CSW/FCC blended pastes prepared with 100 wt % CSW, 30 wt % FCC and 100 wt % FCC, alkali-activated with solutions containing 4.37 and 7.28 mol·kg−1 of SiO_2, and cured at 65 ◦C for 7 days. CSW: ceramic sanitary-ware unreacted particles; N: sodium carbonate Natron.

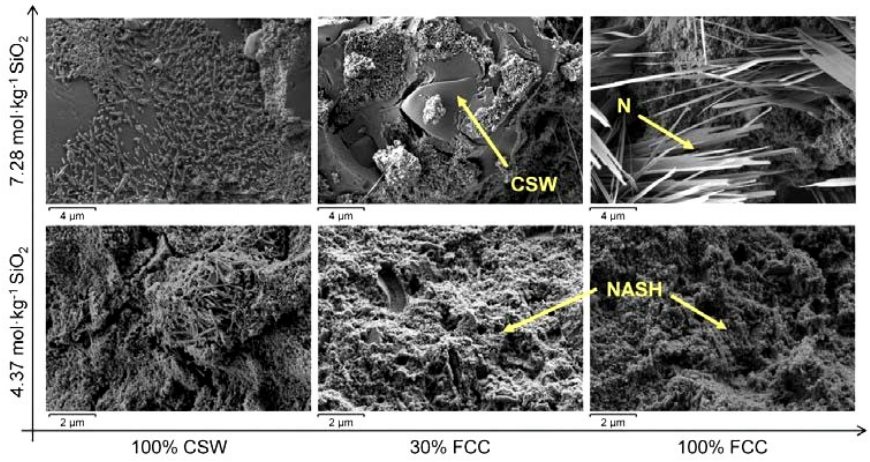

Fig. 3.1-13 Field emission scanning electron images of the CSW/FCC blended pastes prepared with 100 wt % CSW, 30 wt % FCC and 100 wt % FCC, alkali-activated with solutions containing 4.37 and 7.28 mol·kg−1 of SiO_2, and cured at 65 ◦C for 7 days. Higher magnification. CSW: ceramic sanitary-ware unreacted particles; N: sodium carbonate Natron; NASH: alkali-activated binding gel.

3.1.4 Conclusions

The influence of FCC additions (0 wt %–50 wt %) and SiO_2 concentration on the microstructure and compressive strength of alkali-activated ceramic sanitary-ware (CSW) was assessed. The following conclusions were drawn from the results obtained in this research:

The mechanical properties of alkali-activated CSW binders significantly improved with FCC content. Strength values close to 40 MPa were obtained in the mortars blended with 20 wt % FCC cured at 65 ºC for 7 days, and in those that contained 30 wt % FCC, cured at room temperature for 28 days. The compressive strength of these mortars was still higher than 30 MPa when the SiO_2 concentration was lowered from 7.28 to 4.37 mol·kg^{-1}.

The CSW/FCC binders exhibited a wide range of mechanical properties (up to 60.4 MPa after 28 curing days at 20 ºC), which varied depending on the FCC replacing percentage and the silica content in the activating solution. Bigger FCC amounts or higher silica concentrations could be used for special applications, where high strength binders or the use of construction elements in shorter periods are required.

No significant amounts of new crystalline phases were identified in the alkali-activated CSW/FCC blended systems, where the main reaction product formed was a N-A-S-H/(C,N)-A-S-H binding gel. Zeolites were easily distinguished only in alkali-activated pastes developed with 50 wt % or 100 wt % FCC.

A general conclusion is that the partial substitution of CSW by FCC significantly improved the behavior of CSW as a precursor in alkali-activated binders. FCC additions improved the system's mechanical properties and allowed activating CSW at room temperature. However, in order to confirm and totally embrace this reutilization and valorization possibility, further studies on the durability of the developed CSW/FCC-blended systems are required.

References

1.U.S. Geological Survey. Mineral Commodity Summaries 2017. 2017; pp. 44–45. Available online: https: //doi.org/10.3133/70180197 (accessed on 14 March 2018).

2.Imbabi, M.S.; Carrigan, C.; McKenna, S. Trends and developments in green cement and concrete technology. *Int. J. Sustain. Built Environ.* **2012**, *1*, 194–216.

3.Shi, C.; Fernández Jiménez, A.; Palomo, A. The pursuit of an alternative to Portland cement. *Cem. Concr. Res.* **2011**, *41*, 750–763.

4.Puertas, F.; García-Díaz, I.; Barba, A.; Gazulla, M.F.; Palacios, M.; Gómez, M.P. Ceramic wastes as alternative raw materials for Portland cement Clinker production. *Cem. Concr. Compos.* **2008**, *30*, 798–805.

5.Puertas, F.; García-Díaz, I.; Palacios, M.; Gazulla, M.F.; Gómez, M.P.; Orduña, M. Clinkers and cements obtained from raw mix containing ceramic wastes as a raw material. Characterization, hydration and leaching studies. *Cem. Concr. Compos.* **2010**, *32*, 175–186.

6.García de Lomas, M.; Sánchez de Rojas, M.I.; Frías, M. Pozzolanic reaction of a spent fluid catalytic craking catalyst in FCC-cement mortars. *J. Therm. Anal. Calorim.* **2007**, *90*, 443–447.

7.Frías, M.; Rodriguez, O.; Sánchez de Rojas, M.I.; Vilar-Cocina, E.; Rodrigues, M.; Savastano, H. Advances on the development of ternary cements elaborated with biomass ashes coming from different activation process. *Constr. Build. Mater.* **2017**, *136*, 73–80.

8.Deschner, F.; Winnefeld, F.; Lothenbach, B.; Seufert, S.; Schwesing, P.; Dittrich, S.; Goetz-Neunhoeffer, F.; Neubauer, J. Hydration of Portland cement with high replacement by siliceous fly ash. *Cem. Concr. Res.* **2012**, *42*, 1389–1400.

9.Ioannou, S.; Reig, L.; Paine, K.; Quillin, K. Properties of a ternary calcium sulfoaluminate-calcium sulfate-fly ash cement. *Cem. Concr. Res.* **2014**, *56*, 75–83.

10.Srinivasula Reddy, M.; Dinakar, P.; Hanumantha Rao, B. A review of the influence of source material´s oxide composition on the compressive strength of geopolymer concrete. *Microporous Mesoporous Mater.* **2016**, *234*, 12–23.

11.Mellado, A.; Catalán, C.; Bouzón, N.; Borrachero, M.V.; Monzó, J.; Payá, J. Carbon footprint of geopolymeric mortar: Study of the contribution of the alkaline activating solution and assessment of alternative route. *RSC Adv.* **2014**, *4*, 23846–23852.

12.Khan, M.Z.N.; Shaikh, F.A.; Hao, Y.; Hao, H. Synthesis of high strength ambient cured geopolymer composite by using low calcium fly ash. *Constr. Build. Mater.* **2016**, *125*, 809–820.

13.Nath, P.; Sarker, P.K. Effect of GGBFS on setting, workability and early strength properties of fly ash geopolymer concrete cured in ambient condition. *Constr. Build. Mater.* **2014**, *66*, 163–171.

14.Marin, C.; Araiza, J.L.R.; Manzano, A.; Avalos, J.C.R.; Perez, J.J.; Muniz, M.S.; Ventura, E.; Vorobiev, Y. Synthesis and characterization of a concrete based on metakaolin geopolymer. *Inorg. Mater.* **2009**, *45*, 1429–1432.

15.Ranjbar, N.; Mehrali, M.; Behnia, A.; Alengaram, U.J.; Jumaat, M.Z. Compressive strength and microstructural analysis of fly ash/palm oil fuel ash based geopolymer mortar. *Mater. Des.* **2014**, *59*, 532–539.

16.Ye, N.; Yang, J.K.; Liang, S.; Hu, Y.; Hu, J.P.; Xiao, B.; Huang, Q.F. Synthesis and strength optimization of one-part geopolymer based on red mud. *Constr. Buil. Mater.* **2016**, *111*, 317–325.

17.Reig, L.; Soriano, L.; Tashima, M.M.; Borrachero, M.V.; Monzó, J.; Payá, J. Influence of calcium additions on the compressive strength and microstructure of alkali-activated ceramic sanitary-ware. *J. Am. Ceram. Soc.* **2018**.

18.Reig, L.; Borrachero, M.V.; Monzó, J.; Savastano, H.; Tashima, M.M.; Payá, J. Use of ceramic sanitaryware as an alternative for the development of nee sustainable binders. *Key Eng. Mater.* **2016**, *668*, 172–180.

19.Medina, C.; Frías, M.; Sánchez de Rojas, M.I. Microstructure and properties of recycled concretes using ceramic sanitaryware industry waste as coarse aggregate. *Constr. Build. Mater.* **2012**, *31*, 112–118.20. Baraldi, L. World sanitaryware production and exports. *Ceram. World Rev.* **2015**, *114*, 56–65.

20.Trochez, J.J.; Mejía de Gutiérrez, R.; Rivera, J.; Bernal, S.A. Synthesis of geopolymer from spent FCC: Effect of SiO_2/Al_2O_3 and Na_2O/SiO_2 molar ratios. *Mater. Constr.* **2015**, *65*, 65.

21.Schreiber, R.; Yonley, G. The use of spent catalyst as a raw material substitute in cement manufacturing.

22.*ACS Div. Petrol. Chem.* **1993**, *38*, 97–99.

23.Payá, J.; Monzó, J.; Borrachero, M.V.; Velázquez, S. Evaluation of the pozzolanic activity of fluid catalytic cracking catalyst residue (FC3R). Thermogravimetric analysis studies on FC3R-Portland cement pastes. *Cem. Concr. Res.* **2003**, *33*, 603–609.

24.Pacewska, B.; Wilinska, I.; Kubissa, J. Use of spent catalyst from catalytic cracking in fluidized bed as a new concrete additive. *Therm. Acta* **1998**, *322*, 175–181.

25.Chen, H.L.; Tseng, Y.S.; Hsu, K.C. Spent FCC catalyst as a pozzolanic material for high-performance mortar. *Cem. Concr. Comp.* **2004**, *26*, 657–664.

26.Pacewska, B.; Nowacka, M.; Wilinska, I.; Kubissa, W.; Antonovich, V. Studies on the influence of spent FCC catalyst on hydration of calcium aluminate cements at ambient temperature. *J. Therm. Anal. Calorim.* **2011**, *105*, 129–140.

27.Tashima, M.M.; Akasaki, J.L.; Castaldelli, V.N.; Soriano, L.; Monzó, J.; Payá, J.; Borrachero, M.V. New geopolymeric binder based on fluid catalytic cracking catalyst residue (FCC). *Mater. Lett.* **2012**, *80*, 50–52.

28.Tashima, M.M.; Akasaki, J.L.; Melges, J.L.P.; Soriano, L.; Monzó, J.; Payá, J.; Borrachero, M.V. Alkali activated materials based on fluid catalytic cracking catalyst residue (FCC): Influence of SiO_2/Na_2O and H_2O/FCC ratio on mechanical strength and microstructure. *Fuel* **2013**, *108*, 833–839.

29.Rodriguez, E.D.; Bernal, S.A.; Provis, J.L.; Gehman, J.D.; Monzó, J.; Payá, J. Geopolymers based on spent catalyst residue from a fluid catalytic cracking (FCC) process. *Fuel* **2013**, *109*, 493–502.

30.Cheng, H.; Lin, K.L.; Cui, R.; Hwang, C.L.; Cheng, T.W.; Chang, T.M. Effect of solid-to-liquid ratios on the properties of waste catalyst-metakaolin based geopolymers. *Constr. Build. Mater.* **2015**, *88*, 74–83.

31.Cheng, H.; Lin, K.L.; Cui, R.; Hwang, C.L.; Chang, Y.M.; Cheng, T.W. The effects of SiO_2/Na_2O molar ratio on the characteristics of alkali-activated waste catalyst-metakaolin based geopolymers. *Constr. Build. Mater.* **2015**, *95*, 710–720.

32.Reig, L.; Soriano, L.; Borrachero, M.V.; Monzó, J.; Payá, J. Influence of the activator concentration and calcium hydroxide addition on the properties of alkali-activated porcelain stoneware. *Constr. Build. Mater.* **2014**, *63*, 214–222.

33.Pacheco-Torgal, F.; Jalali, S. Reusing ceramic wastes in concrete. *Constr. Build. Mater.* **2010**, *24*, 832–838.

34.Fernández-Jiménez, A.; Palomo, A.; Sobrados, I.; Sanz, J. The role played by the reactive alumina content in the alkaline activation of fly ashes. *Microporous Mesoporous Mater.* **2006**, *91*, 111–119.

35.Bernal, S.A.; Gutierrez, R.M.; Provis, J.L.; Rose, V. Effect of silicate modulus andmetakaolin incorporation on the carbonation of alkali silicate-activated slags. *Cem. Concr. Res.* **2010**, *40*, 898–907.

36.Hidalgo, A.; García, J.L.; Alonso, M.C.; Fernández, L.; Andrade, C. Microstructure development in mixes of calcium aluminate cement with silica fume or fly ash. *J. Therm. Anal. Calorim.* **2009**, *96*, 335–345.

37.Ozer, I.; Soyer-Uzun, S. Relations between the structural characteristics and compressive strength in metakaolin based geopolymers with different molar Si/Al ratios. *Ceram. Int.* **2015**, *41*, 10192–10198.

3.2 The Compressive Strength and Microstructure ofAlkali-Activated Binary Cements Developed byCombining Ceramic Sanitaryware with Fly Ash or Blast Furnace Slag

Juan Cosa , Lourdes Soriano, María Victoria Borrachero, Lucía Reig , Jordi Payá and José María Monzó. Minerals 2018, 8, 337

Abstract: The properties of a binder developed by the alkali-activation of a single waste material can improve when it is blended with different industrial by-products. This research aimed to investigate the influence of blast furnace slag (BFS) and fly ash (FA) (0–50 wt %) on the microstructure and compressive strength of alkali-activated ceramic sanitaryware (CSW). 4 wt % $Ca(OH)_2$ was added to the CSW/FA blended samples and, given the high calcium content of BFS, the influence of BFS was analyzed with and without adding $Ca(OH)_2$. Mortars were used to assess the compressive strength of the blended cements, and their microstructure was investigated in pastes by X-ray diffraction, thermogravimetry, and field emission scanning electron microscopy. All the samples were cured at 20 ◦C for 28 and 90 days and at 65 ◦C for 7 days. The results show that the partial replacement of CSW with BFS or FA allowed CSW to be activated at 20 ◦C. The CSW/BFS systems exhibited better mechanical properties than the CSW/FA blended mortars, so that maximum strength values of 54.3 MPa and 29.4 MPa were obtained in the samples prepared with 50 wt % BFS and FA, respectively, cured at 20 ◦C for 90 days.

Keywords: sustainable construction materials; waste management; alkali-activated binder; fly ash; blast furnace slag; ceramic sanitaryware; mechanical strength; microstructure

3.2.1. Introduction

Portland cement is the most commonly used synthetic construction material. Although its properties and behavior are well-known, the greenhouse gases emitted during its production, together with the natural resources used, have motivated new more eco-efficient binders, such as alkali-activated cements, to be developed. As explained by Zedan et al. [1], alkali-activated binders may be classified into two main types: low-calcium systems, which generally require applying temperature to set; and calcium-based binders, which usually harden at room temperature. While N–A–S–H gel mainly forms in the former, the activation of high-calcium systems principally brings about C–A–S–H gel [2,3]. Both gels may co-exist in the presence of calcium, with calcium silicate hydrate (C–A–S–H) being favored at a high pH (>12) if sufficient calcium is provided [4].

Alkali-activated fly ash (FA) and blast furnace slag (BFS) may be considered the models for lowand high-calcium binders, respectively [3]. FA is obtained by the electro-static separation of dust from fuel gases in coal thermoelectric plants [5] and, according to [6,7], it is estimated that approximately 750–780 million tons are produced yearly. Granulated BFS is formed by rapidly cooling melted slag during iron production [8]. As reported by the World Steel Association [9], 1629.6 million tons of Steel were produced worldwide in 2016, of which 74.3% are made in blast furnaces and the remaining 25.7% in electric furnaces. Consequently, approximately 300–360 million tons of iron slag were produced globally in blast furnaces in 2016, and 160–240 million tons of steel slag were generated in electric arc and basic oxygen furnaces [10].

In the last few decades, the use of different silico aluminate waste materials as a precursor in alkali-activated binders has been widely investigated [11,12]. Reusing waste materials as a precursor positively contributes to sustainable development because it limits the mining of natural resources, reduces the visual impact caused by accumulated waste, and diminishes the emissions associated with Portland cement manufacture [13,14]. Ceramic materials are a very interesting option to be explored to develop alkali-activated cements as they are chemically inert and present a long biodegradation period (up to 4000 years) [15]. Among them, ceramic sanitaryware waste (CSW) units are expected to present quite a homogeneous chemical and mineralogical composition since they are generally sintered within a narrow range of calcination temperatures (1200–1280 ºC [16]). Moreover, CSW units (i.e., washbasins, lavatories, or bidets) can be easily separated from construction and demolition waste (CDW), which implies that they will present fewer impurities, such as gypsum or Portland cement. As reported by Baraldi [17], nearly 349.3 million CSW units were globally produced in 2014, of which almost 12% (41.6 million) was manufactured in the European Union.

CSW was successfully activated in a previous study by Reig et al. [18], where maximum strength values of 36 MPa were obtained in mortars cured at 65 °C for 7 days. However, addition of $Ca(OH)_2$ and applying temperature to cure samples proved essential to successfully activate this ceramic waste material, which limited its use mainly to prefabricated applications. In order to improve the properties of alkali-activated binders developed using a single material as a precursor, several studies have lately combined low-calcium precursors, like CSW, with different sources of calcium and reactive Al_2O_3, such as BFS [1,2,19–23], FA [6], calcium aluminate cement (CAC) or Portland cement (PC) [24,25]. Robayo-Salazar et al. [19] observed that the heat of reaction in an alkali-activated natural pozzolan/BFS binary cement increased with BFS addition, which

accelerated the kinetics of the process and, consequently, favored the activation of the pozzolan at room temperature, as well as strength development. A very positive influence of PC, CAC, and $Ca(OH)_2$ on the microstructure and mechanical properties of alkali-activated CSW is reported in [24], where compressive strength values of 40.06 MPa, 64.41 MPa, and 56.62 MPa are reported in mortars containing 6 wt % $Ca(OH)_2$, 10 wt % PC and 10 wt % CAC, respectively (all cured at 65 °C for 7 days). However, the natural resources used, and the large amounts of CO_2 emitted to the atmosphere during CAC or PC production, motivated a later study, which explored the influence of spent fluid catalytic cracking waste (an industrial by-product) on the microstructure and compressive strength of alkali-activated CSW [26]. FCC significantly improves the reactivity of CSW, and compressive strength values of 40 MPa and 60.4 MPa have been reported in the mortars cured at 20 °C for 28 days, blended with 30 wt % and 50 wt % FCC, respectively.

The present study aims to investigate the influence of BFS and FA (0–50 wt % each), together with the addition of $Ca(OH)_2$, on the compressive strength and microstructure of alkali-activated CSW.

3.2.2. Experimental Process

3.2.2.1. Materials

CSW units were supplied by the company Ideal Standard, located in Valencia (Spain). Units rejected due to production defects were broken with a hammer and crushed in a jaw crusher (BB200 by Retsch) to obtain particles smaller than 2 mm. Crushed particles were formed mainly by a dense ceramic body and generally contained part of the glaze that covered the CSW unit.

These particles homogenized after their particle size was reduced when milled in a jars turner roller (Roller 1 by Gabrielli), for which 5-L volume cylindrical alumina jars were used. Each jar was filled with 1500 g of CSW and 6500 g of alumina balls to be rotated for 6 h at 190 rpm for the first 10 min and at 140 rpm for the remaining time.

FA was supplied by Balalva S.L. (Onda, Spain), and was produced in the thermoelectric power plant in Escucha (Teruel, Spain). Particles were milled in an industrial mill for 10 h, which were used as received. BFS was supplied by the cement company Cementval S.L. (Sagunto, Spain). This waste was dry-milled in a laboratory for 30 min using porcelain jars filled with 450 g of BFS and 98 alumina balls. Sodium hydroxide pellets (98% purity, supplied by Panreac), water and waterglass (supplied by Merck, with the following composition: 64% H_2O, 28% SiO_2, and 8% Na_2O) were used to prepare the activating solutions. 4 wt % $Ca(OH)_2$ (95% purity) was used as an addition to the 100 wt % CSW and some blended samples (specified in the next section).

3.2.2.2. Experimental Process and Tests Performed

Before using the CSW, FA and BFS waste materials as precursors to develop alkali-activated binary cements, they were characterized to determine the morphology, particle size distribution (PSD), amorphous content, and the chemical and mineralogical composition of the milled powders.

The shape of particles was observed by field emission scanning electron microscopy in an FESEM ULTRA 55 (ZEISS, Oberkochen, Germany). Powders were carbon-coated prior to their observation, and images were taken at 2 kV. PSD was determined by laser diffraction in a Mastersizer 2000 (Malvern Instruments, Malvern, UK). Powder was dispersed in water and stirred at 1200 rpm and, in order to disperse possible powder agglomerations, a 1-min ultrasound was applied. The amorphous

contents of CSW, FA, and BFS were determined following Standard UNE EN 196-2:2006, and their chemical composition was assessed by X-ray fluorescence (XRF) in a Magix Pro spectrometer (Philips, Netherland). Powder X-ray diffraction (XRD) analyses were performed in a Brucker AXS D8 Advance (Billerica, MA, USA), from 10 to 70 2θ degrees. Cu Kα radiation at 20 mA and 40 kV was used, with a 2-s accumulation time in a 0.02-angle step.

Three different systems were designed to investigate the influence of BFS and FA, together with the addition of $Ca(OH)_2$, on the alkali-activation of CSW:

- System 1: 0 to 50 wt % CSW was replaced with BFS, a high-calcium waste material. A 100 wt % BFS sample was also prepared for comparison purposes, and no $Ca(OH)_2$ was added to this system.

- System 2: 0 to 50 wt % CSW was replaced with a low-calcium FA. 4 wt % $Ca(OH)_2$ (amount determined according to the previous results reported in [18,27]) was added to these CSW blended pastes and mortars. A 100 wt % FA sample was also prepared as a reference (no $Ca(OH)_2$ was added to this sample).

- System 3: 0 to 50 wt % CSW was replaced with BFS and 4 wt % $Ca(OH)_2$ was added to these blended samples. The microstructure and mechanical properties of this system were compared with those observed in the alkali-activated CSW/BFS with no added $Ca(OH)_2$ (System 1) and the alkali-activated CSW/FA binders (System 2).

Table 3.2-1 summarizes the three different developed systems, designation of samples, percentages of replacement of CSW with FA or BFS, and $Ca(OH)_2$ addition. Samples were named according to the waste material and the CSW replacement percentage, and letter "C" denoted the addition of 4 wt % $Ca(OH)_2$. Thus BFS/30, C-FA/50 and C-BFS/40 corresponded to the CSW samples blended with 30 wt % BFS, 50 wt % FA with 4 wt % $Ca(OH)_2$, and 40 wt % BFS with 4 wt % $Ca(OH)_2$, respectively.

Tab. 3.2-1 Designation of samples, ceramic sanitaryware (CSW) replacement with blast furnace slag (BFS), or fly ash (FA), and samples with $Ca(OH)_2$ addition.

System 1. BFS without $Ca(OH)_2$				**System 2. FA with $Ca(OH)_2$**				**System 3. BFS with $Ca(OH)_2$**			
Sample	**Mat.**	**CSW Replac. Wt %**	**$Ca(OH)_2$ Addition wt %**	**Sample**	**Mat.**	**CSW Replac. Wt %**	**$Ca(OH)_2$ Addition wt %**	**Sample**	**Mat.**	**CSW Replac. Wt %**	**$Ca(OH)_2$ Addition wt %**
100CSW-C		0	4	100CSW-C		0	4	100CSW-C		0	4
BFS/10		10	-	C-FA/10		10	4	C-BFS/10		10	4
BFS/20	Blast	20	-	C-FA/20		20	4	C-BFS/20	Blast	20	4
BFS/30	Furnace	30	-	C-FA/30	Fly	30	4	C-BFS/30	Furnace	30	4
BFS/40	Slag	40	-	C-FA/40	Ash	40	4	C-BFS/40	Slag	40	4
BFS/50	(BFS)	50		C-FA/50	(FA)	50	4	C-BFS/50	(BFS)	50	4
BFS/100		100	-	FA/100		100	-	BFS/100		100	-

The compressive strength (σ_c) of the blended systems was assessed in mortars according to Standard UNE EN 196-1, and pastes were used to investigate microstructural evolution, by XRD, FESEM, and thermogravimetric analyses (TG). The XRD and FESEM tests were run according to the experimental processes described at the beginning of this section, and the TG experiments were run in a Mettler Toledo TGA 850 thermobalance, from 35 ºC to 600 ºC, at a heating rate of 10 $ºC \cdot min^{-1}$. Tests were performed in a nitrogen atmosphere at a flow gas rate of 75 $mL \cdot min^{-1}$. To better distinguish the thermogravimetric events, aluminum-sealed crucibles (100-µL volume) with a pinholed lid were used, which allowed a self-generated atmosphere to be created.

3.2.2.3. Mix Proportions and Preparing Pastes and Mortars

The mix proportions, the SiO_2/Na_2O molar ratio and the curing conditions used herein are summarized in Table 3.2-2. The concentrations of Na_2O and SiO_2 in the activating solution (defined in molality terms, moles per kg of water) were taken from previous studies on the alkali-activation of CSW [18], where the best compressive strength results (36 MPa after 7 curing days at 65 °C) were achieved with the solutions containing 3.75 and 7.28 mol·kg^{-1} of Na_2O and SiO_2, respectively. A water/binder ratio of 0.45 was used to prepare all the samples. Water was provided by the sodium silicate solution and the binder was formed by CSW, and its partial replacement with FA or BFS (calcium hydroxide was used as an addition to the binder in the samples indicated in Table 3.2-1). Pastes and mortars were cured at 20 °C at 95% relative humidity in a temperature- and humidity-controlled chamber, and at 65 °C in a thermostatically controlled bath inside a sealed box floating in water (100% RH).

Tab. 3.2-2 The mix proportions, ratios and curing conditions used to assess the influence of BFS and FA on the alkali-activated CSW blended systems.

w/b [(a)]	Na_2O mol·kg^{-1}	SiO_2 mol·kg^{-1}	SiO_2/Na_2O Na_2O mol·kg$_{binder-1}$	SiO_2 mol·kg$_{binder-1}$	Curing Conditions
0.45	3.75	7.28	1.941.69	3.28	7 days at 65 °C 28 and 90 days 20 °C

[(a)] Water (w), provided by the sodium silicate solution; binder (b) composed of CSW and the different replacements with BFS or FA.

CSW, $Ca(OH)_2$, and the corresponding amount of FA or BFS were mixed until a homogeneous blend was obtained. To prepare the alkali-activating solutions, NaOH pellets were dissolved in the required amount of

waterglass. Solutions were cooled at room temperature before being used to prepare pastes and mortars. The mortar samples sized 40 × 40 × 160 mm^3 were prepared using siliceous sand with a fineness modulus of 4.3 at a binder/sand ratio of 1:3. These prismatic samples were wrapped in plastic film until testing age to avoid loss of moisture and to prevent efflorescence formation.

3.2.2.4. Further Studies on the Influence of BFS and $Ca(OH)_2$ in the Alkali-Activated CSW Blended Systems

After analyzing the influence of BFS, FA, and $Ca(OH)_2$ on the compressive strength of the alkali-activated CSW blended mortars, further research was conducted to better understand the role of BFS and $Ca(OH)_2$ in the CSW/BFS systems. The following new mortars were prepared:

- a 100 wt % BFS mortar with a higher Na_2O concentration (7.5 $mol \cdot kg^{-1}$ instead of 3.75 $mol \cdot kg^{-1}$);

- 50 wt % BFS mortars blended with two different high-crystallinity materials: kephalite (and alucite, silicoaluminate in nature) and sikron (flour quartz, siliceous in nature). Both were prepared without $Ca(OH)_2$ and with the addition of 4 wt %;

- 50 wt % XXX/BFS mortars (where XXX: CSW or kephalite), with 0, 4 and 8 wt % $Ca(OH)_2$;

- a 100 wt % kephalite with the addition of 4 wt % $Ca(OH)_2$.

All these mortars (except the new 100 wt % BFS) were prepared using the mix proportions summarized in Table 3.2-2. As the objective of these additional tests was to acquire additional data to help corroborate some hypotheses, these mortars were cured only at 65 °C for 7 days (the

curing condition that generally provided the best compressive strength results).

3.2.3.Results

3.2.3.1. Characteristics of the Waste Materials

Figure 3.2-1 shows the granulometric distribution of the milled powders, whose main parameters are summarized in Table 3.2-3 (the d_{10}, d_{50} and d_{90} values represent the percentages in volume of particles below the indicated diameter). All the materials had a mean diameter under 32 μm, 90 vol % under 75 μm and 10 vol % under 3 μm. CSW and BFS showed similar granulometric distributions, where the CSW particles were slightly larger than BFS, and FA was the finest powder used. As observed by Temuujin et al. [28], a reduction in particle size may increase the dissolution rate of particles, facilitating the binder setting and leading to improved compressive strength results.

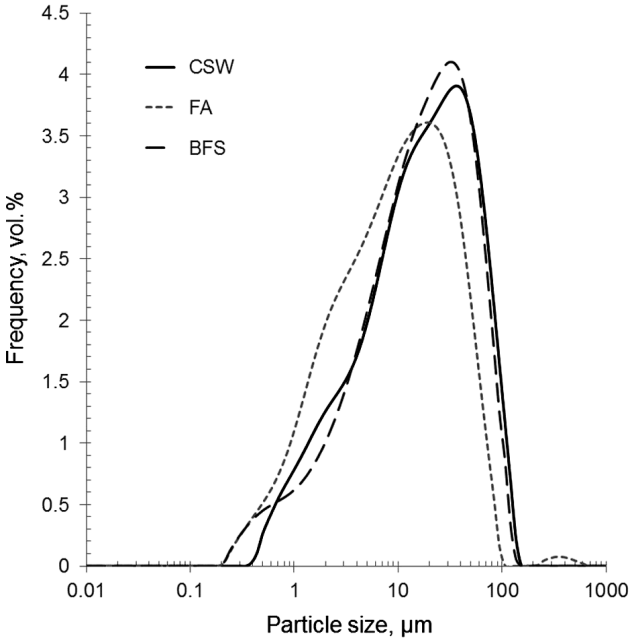

Fig. 3.2-1 Granulometric distribution of the milled CSW, BFS, and FA particles.

Tab. 3.2-1 Main granulometric parameters of the milled waste materials.

Waste Materials	**d_{10}, µm**	**d_{50}, µm**	**d_{90}, µm**	**Mean Diameter, µm**
CSW	2.92	22.38	73.32	31.24
BFS	2.78	20.60	66.16	28.54
FA	2.09	11.52	47.75	21.07

The morphology of the milled CSW, BFS, and FA powders is presented in Figure 3.2-2. The CSW fragments were dense, irregular, and presented smooth surfaces. The BFS powder also had an irregular morphology, which was attributed to the decomposition of the slag while being rapidly

cooled by a powerful flow of cold water, and to the milling conducted to reduce its particle size. The milled FA powder was composed of a combination of rounded and irregularly shaped FA particles. As explained by Ranjbar and Kuenzel [7], spherical particles enhance workability, as their smaller surface area reduces the water required to wet particles.

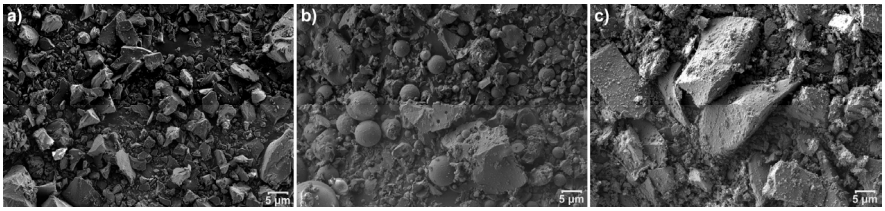

Fig. 3.2-1 Images of the milled materials used as a precursor: (a) CSW; (b) FA; (c) BFS.

The XRD spectra of the CSW, BFS, and FA waste materials are shown in Figure 3.2-3. Quartz (Q, SiO_2, Powder Diffraction File (PDF) #331161) and mullite (M, $Al_6Si_2O_{13}$, PDF#150776) were the main crystalline compounds distinguished in CSW, along with small amounts of anorthite, a calcium feldspar (A, $CaAl_2Si_2O_8$, PDF#411486). Crystalline quartz and mullite were also identified in FA, together with iron oxide maghemite (F, Fe_2O_3PDF#251402) and traces of gypsum (G, $CaSO_4{\cdot}2H_2O$ PDF#330311). The spectra of both CSW and FA deviated from the baseline from 17 to 32 2θ degrees, which indicates the presence of some amorphous phases. BFS was essentially amorphous to XRD (halo located within the range of 23–37 2θ degrees) and presented peaks that were attributed to the crystalline phases quartz and calcite (C, $CaCO_3$, PDF#050586). As observed by Ismail et al. [29], the different location of the amorphous hump of BFS compared with that of FA or CSW denotes structural differences in the amorphous phases of the waste materials.

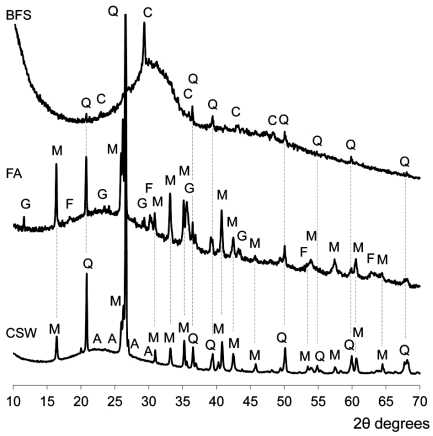

Fig. 3.2-2 Mineralogical composition of the CSW, BFS, and FA raw materials. Quartz (Q, SiO_2); Mullite (M, $Al_6Si_2O_{13}$); Anorthite (A, $CaAl_2Si_2O_8$); Calcite (C, $CaCO_3$); Gypsum (G, $CaSO_4{\cdot}2H_2O$); Maghemite (F, Fe_2O_3).

Table 3.2-4 provides the chemical composition and amorphous content of the CSW, BFS, and FA waste materials used as precursors. CSW and FA exhibited high SiO_2 and Al_2O_3 contents (89.06 and 75.71 wt %, the sum of CSW and FA, respectively), which were significantly lower in BFS (40.64 wt %).

FA was classified as class F according to the ASTM C 618-08a specifications as it presented a CaO content below 15 wt %. Conversely, the 40.35 wt % CaO present in BFS motivated us to investigate the influence of $Ca(OH)_2$ additions when replacing CSW with BFS (Systems 1 and 3, without and with $Ca(OH)_2$, respectively). In line with the XRD results reported in Figure 3.2-3, 98.6 wt % of BFS was in an amorphous state, while the production process of the CSW units gave the highest amount of crystalline stable phases.

Tab. 3.2-2 Chemical composition and amorphous content of CSW, BFS, and FA (wt %).

Waste Materials	Al_2O_3 SiO_2	CaO	Fe2O3 K2O	MgO	Na_2O	SO_3	Other	L	Amorph. Content
CSW	23.60	66 1.20	1.30	2.0.70	2.40	0.10	1.80	0.2	45.6
FA	25.80	49 3.84	13.94	2.1.06	-	1.00	0.01	1.9	71.4
BFS	10.60	3040.35	1.30	0.7.47	0.87	1.94	1.30	5.5	98.6

[1] Determined at 950 °C.

3.2.3.2. Compressive Strength

Figure 3.2-4 summarizes the compressive strength results of the alkali-activated CSW/BFS and CSW/FA blended mortars cured at 65 °C for 7 days, and at 20 °C for 28 and 90 days. The 100 wt % FA mortars and those prepared with 10 wt % BFS without $Ca(OH)_2$, were ruled out because they had not hardened after 2 curing days at 20 °C. Authors like Temuujin et al. [28] have successfully activated FA at room temperature, and achieved up to 45 MPa after the mechanical activation of the ash. The differences with the 100 wt % FA mortars developed herein, which did not harden at 20 °C, were attributed mainly to the mix proportions in the alkali-activating solution, which had been optimized for the CSW precursor, but were most probably not optimum for FA. Additionally, the FA mechanically activated by Temuujin et al. [28] most probably had a smaller particle size, which would improve its dissolution rate. Another factor that could have influenced the hardening of the 100 wt % FA mortars is the absence of calcium, which would have accelerated the reaction kinetics.

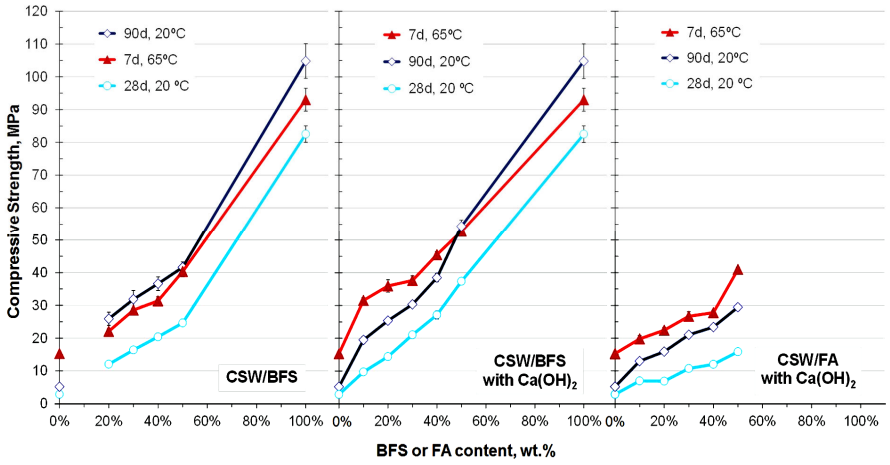

Fig. 3.2-3 Evolution of compressive strength with the BFS and FA contents in the alkali-activated CSW mortars cured at 65 °C for 7 days and at 20 °C for 28 and 90 days.

Addition of FA or BFS considerably improved the compressive strength of the alkali-activated CSW mortars, and allowed this ceramic waste to be activated at 20 ºC, which significantly extended its reuse possibilities as a precursor. A wide range of mechanical properties was obtained, depending on the replacement percentage of CSW with BFS or FA, and also on the curing conditions. For a given replacement percentage, improvement of strength became more significant in the CSW/BFS systems than in the CSW/FA ones. This was attributed to the high amorphous content and reactivity of BFS, which provided strength results over 80 MPa after 28 curing days at 20 ºC (100 wt % BFS). Although the FA blended mortars cured at 20 ºC exhibited the poorest mechanical performance, the obtained strength results when cured at 65 ºC were similar to those provided by the BFS blended systems with no $Ca(OH)_2$ addition. Unlike the BFS mortars, the CSW/FA systems showed a synergistic effect, since the 100 wt % FA mortars did not set at 20 ºC, and the strength of the 100 wt % CSW mortars improved when partially

replaced with FA. Provided that the calcium and Al_2O_3 contents in FA and CSW were similar (Table 3.2-4), the improved strength observed with increasing FA contents was attributed to the higher amorphous contents of FA.

The BFS blended mortars with no $Ca(OH)_2$ addition had similar strength results after 7 curing days at 65 °C or 90 days at 20 °C. The loss of strength of the CSW/BFS mortars (compared with the 100 wt % BFS mortar) generally came close to, or was even higher than, the CSW percentage in the system (except for the C-BFS mortars cured at 65 °C). By way of example, the strength of the mortars prepared with 30 wt % or 50 wt % BFS (without $Ca(OH)_2$) diminished by approximately 70% and 60%, respectively, after 7 curing days at 65 °C or 90 days at 20 °C. Similarly, the C-BFS-blended mortars cured at 20 °C for 90 days also exhibited strength loss values of 71.1% and 48.1% when prepared with 70 wt % and 50 wt % CSW, respectively. The addition of $Ca(OH)_2$ is thought to accelerate the process kinetics since it improved the mechanical properties of the CSW/BFS mortars cured at 65 °C or at 20 °C for 28 days, but hardly influenced those of the mortars cured for longer periods (similar strength values were obtained with and without $Ca(OH)_2$ in the CSW/BFS mortars cured at 20 °C for 90 days).

3.2.3.3. Further Results on the Influence of BFS and $Ca(OH)_2$ in the Alkali-Activated CSW Blended Systems

As described in Section 3.2.3.2 above, the loss of strength observed in the CSW/BFS blended mortars, compared with the 100 wt % BFS reference sample, came close to the CSW content in the system. This suggests that CSW could act as an inert mineral addition when blended with BFS and, consequently, the activator would be consumed mainly by BFS, which would lead to excess sodium and silica for the diluted amount

of BFS in the blended samples. $Ca(OH)_2$ is also thought to accelerate the activation reactions in CSW/BFS systems, particularly those cured at 65 °C, or at 20 °C for 28 days. Figure 3.2-5 shows the compressive strength results of the mortars prepared to corroborate these hypotheses. The strengths of the 100 wt % CSW and 100 wt % BFS mortars, which are presented in Figure 3.2-4, are also included as references.

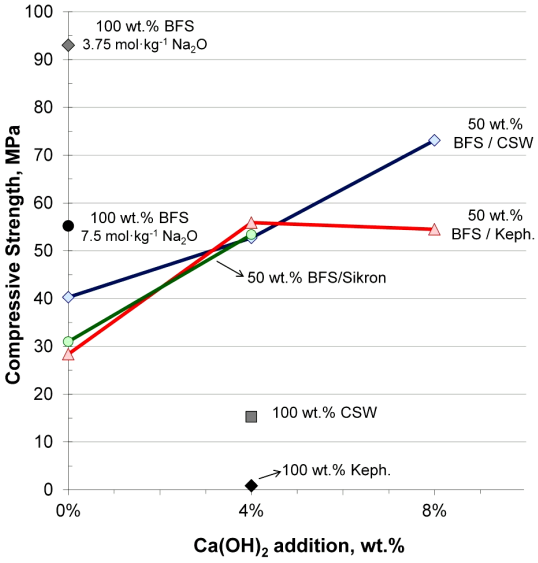

Fig. 3.2-5 Compressive strength of the new mortars developed to further investigate the influence of BFS and $Ca(OH)_2$ on alkali-activated CSW blended systems.

The strength of the 100 wt % BFS mortar diminished from 93.0 MPa to 55.2 MPa when the sodium concentration was increased from 3.75 $mol \cdot kg^{-1}$ to 7.5 $mol \cdot kg^{-1}$. This suggests that, given the predominantly amorphous nature of BFS, this waste material consumed mainly the activating solution first, which led to excess sodium and silica for the amount of BFS in the blended system.

The 50 wt % BFS mortars prepared with 4 wt % $Ca(OH)_2$ exhibited similar compressive strength results, no matter what the material used to replace BFS (CSW, kephalite or sikron). However, when no $Ca(OH)_2$ was added to the system, slightly better strength results were obtained in the 50 wt % BFS/CSW systems than in those blended with sikron or kephalite. Increasing the addition of $Ca(OH)_2$ to 8 wt % favored the reactivity of the CSW/BFS mortars, which improved strength by 20.4 MPa, but did not affect that of the BFS/Kephalite sample. Additionally, 0.86 MPa were given by the 100 wt % kephalite mortar, which were remarkably reduced compared with the 15.3 MPa provided by the corresponding 100 wt % CSW sample. All these results indicate some reactivity of the ceramic waste, which contributed to develop strength. Conversely, as suggested by Perná and Hanzlicek [20], although microstructural analyses would confirm the exact role of kephalite and sikron in the 50 wt % BFS blended mortars, these high crystallinity materials most probably acted as fillers, and were merely encapsulated in the binding matrix without creating any chemical bonds.

3.2.3.4. X-ray Diffraction (XRD) Studies

The XRD spectra for the CSW/BFS (with and without $Ca(OH)_2$) and the CSW/FA blended pastes, cured at 20 °C for 28 days and at 65 °C for 7 days, are reported in Figures 3.2-6 to 3.2-8. The signals attributed to crystalline quartz (Q, SiO_2, PDF#331161) and mullite (M, $Al_6Si_2O_{13}$, PDF#150776), which were previously identified in the raw CSW and FA materials, also arose in the diffractograms of the 100 wt % CSW, 100 wt % FA and CSW/FA blended pastes. The peaks attributed to iron oxide maghemite (F, Fe_2O_3 PDF#251402) were observed in the 100 wt % FA paste, and the signals due to anorthite (A, $CaAl_2Si_2O_8$, PDF#411486), this being the calcium feldspar identified in the raw CSW waste, arose in the 100 wt % CSW activated pastes and those containing 90 wt % CSW.

Calcite, which was distinguished in the original BFS, was also identified in all the activated pastes containing this waste. This indicates that, given their stability, these crystalline phases scarcely participated in the activation reactions. Calcium silicate rankinite (R, $Ca_3Si_2O_7$, PDF#220539) emerged in the spectra of the 100 wt % BFS pastes (with and without calcium addition), and small amounts of Natron (N, $Na_2CO_3{\cdot}10H_2O$, PDF#150800) formed in the 100 wt % CSW activated paste. This sodium carbonate has also been noted in previous works conducted into the alkali-activation of CSW [24,26], and has been attributed to the existence of non reacted reagents or to the carbonation of pastes. Although, as described by Marjanovic et al. [2], hydrotalcite gel usually forms in alkali-activated 100 wt % BFS when the original BFS contains more than 5% MgO (the BFS used in our study had 7.47 wt % MgO; see Table 3.2-4) and is activated with sodium silicate solutions, no signals associated with this compound were clearly distinguished in any activated paste. The absence of hydrotalcite was attributed to the fact that small amounts formed, or it was poorly crystalline, which makes XRD identification difficult.

Addition of 4 wt % $Ca(OH)_2$ to the CSW/BFS system did not significantly modify the formed crystalline phases, and no major differences were observed between the crystalline compounds formed when cured at 20 °C and at 65 °C (in neither BFS nor the FA systems). No signals due to $Ca(OH)_2$, which was added to the samples indicated in Table 3.2-1, were distinguished in the XRD patterns of the activated pastes. This finding indicates that calcium hydroxide was consumed during the activation process, and was incorporated into the newly-formed alkali-activated gel.

A deviation from the baseline toward higher 2θ values was observed in the activated pastes compared with the original materials, especially in the CSW/BFS blended pastes, which exhibited a more marked deviation with increasing BFS contents: from 17–32 2θ degrees in the raw CSW to

19–38 2θ degrees in the activated 50 wt % CSW/BFS paste. As explained by Dzunuzovic et al. [30], this displacement denotes the formation of bigger amounts of amorphous binding gel due to alkali-activation reactions. These results fall in line with those previously reported by Zedan et al. [1], who also observed that the amorphous content in alkali-activated ceramic/BFS blends increased with the replacement percentage of the ceramic material with BFS.

A low-intensity band centered at 29.5 2θ degrees emerged in the spectra of the pastes that contained 30 wt % or 50 wt % BFS. This band was not distinguished in the 10 wt % BFS samples, where sodium carbonate thermonatrite (T, $Na_2CO_3 \cdot H_2O$, PDF#080448) formed instead. The band of 29–30 2θ degrees broadened and its intensity increased with higher BFS contents. This denotes a higher amorphous gel content and is in tune with the improved compressive strength results reported in Figure 3.2-4.

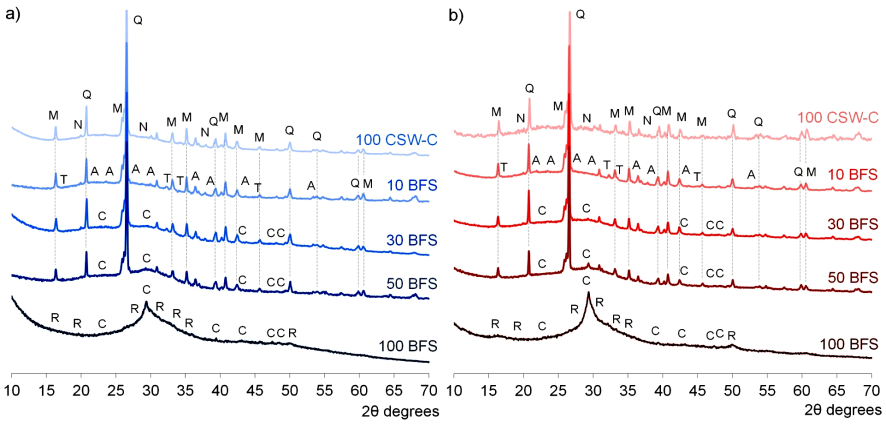

Fig. 3.2-4 The powdered X-ray diffraction (XRD) spectra for the CSW/BFS blended pastes prepared with 10, 30, and 50 wt % BFS, cured at: (a) 20 ˚C for 28 days; (b) 65 ˚C for 7 days.

Quartz (Q, SiO_2); Mullite (M, $Al_6Si_2O_{13}$); Calcite (C, $CaCO_3$); Anorthite (A, $CaAl_2Si_2O_8$); Natron (N, $Na_2CO_3{\cdot}10H_2O$); Rankinite (R, $Ca_3Si_2O_7$); Thermonatrite (T, $Na_2CO_3{\cdot}H_2O$).

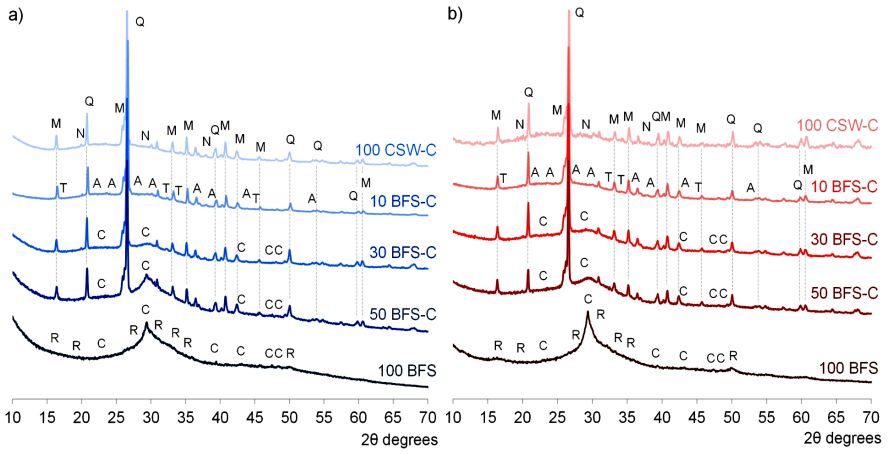

Fig. 3.2-5 The XRD spectra for the CSW/BFS blended pastes that contained 4 wt % $Ca(OH)_2$ and prepared with 10, 30 and 50 wt % BFS, cured at: (a) 20 ˚C for 28 days; (b) 65 ˚C for 7 days. Quartz (Q, SiO_2); Mullite (M, $Al_6Si_2O_{13}$); Calcite (C, $CaCO_3$); Anorthite (A, $CaAl_2Si_2O_8$); Natron (N, $Na_2CO_3{\cdot}10H_2O$); Rankinite (R, $Ca_3Si_2O_7$); Thermonatrite (T, $Na_2CO_3{\cdot}H_2O$).

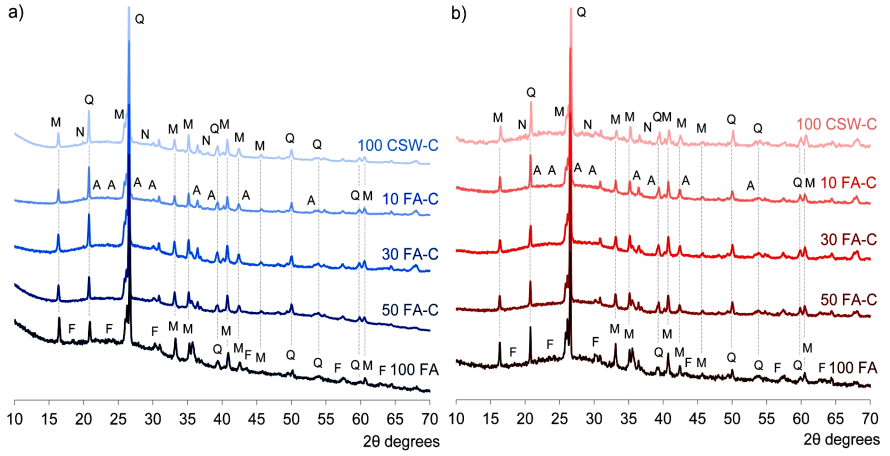

Fig. 3.2-6 The XRD spectra for the CSW/FA blended pastes that contained 4 wt % $Ca(OH)_2$ and prepared with 10, 30 and 50 wt % FA, cured at: (a) 20 °C for 28 days; (b) 65 °C for 7 days. Quartz (Q, SiO_2); Mullite (M, $Al_6Si_2O_{13}$); Anorthite (A, $CaAl_2Si_2O_8$); Natron (N, $Na_2CO_3{\cdot}10H_2O$); Maghemite (F, Fe_2O_3).

3.2.3.5 Thermogravimetric Analyses

The results of the differential thermogravimetric analyses (DTG) for the alkali-activated CSW/FA and CSW/BFS (with and without $Ca(OH)_2$) pastes, prepared with 0, 10, 30, 50, and 100 wt % FA or BFS, are depicted in Figures 3.2-9 to 3.2-11. The DTG analyses of the 100 wt % CSW, FA, and BFS pastes were also taken as references. Figures 3.2-9 and 3.2-10 depict the DTG curves for the pastes cured at 20 °C for 28 and 90 days, respectively, and Figure 3.2-11 presents those of the samples cured at 65 °C for 7 days. The total recorded mass loss is indicated in the figure as a percentage. All the DTG curves showed a main band within the 100–200 °C range, which was attributed to the dehydration of the gel formed during the activation reactions [31,32]. In the CSW/BFS blended pastes (both with and without $Ca(OH)_2$), this dehydration band slightly displaced toward higher temperatures with increasing BFS contents: from 130 °C in the 100 wt % CSW pastes to 145 °C in the 100 wt % BFS pastes cured at 20 °C, and from 125 °C to 150 ºC in those cured at 65 °C. Although this displacement was not observed in the CSW/FA systems cured at 20 °C (Figures 3.2-9 and 3.2-10), and all bands centered approximately at 130 °C (no matter what the FA content), the CSW/FA blended pastes slightly moved when cured at 65 °C compared with the 100 wt % activated CSW or FA (Figure 3.2-11). This shift toward higher temperatures was generally accompanied by higher mass loss values and, in agreement with Moraes et al. [32], both indicate changes in the gel formed during the activation process, which denotes the formation of phases with strongly bonded water. These

results also coincide with those previously reported by Zedan et al. [1], who observed an increase in the chemically bonded water with rising BFS contents in alkali-activated ceramic waste/BFS blends (10 and 30 wt % replacements). The higher recorded mass loss with increasing BFS contents well agrees with the positive evolution of the compressive strength results reported in Figure 3.2-4, and also with the higher amorphous contents in the binding matrix denoted by the XRD spectra (Figures 3.2-5 and 3.2-6). Similarly, higher mass loss values were recorded in the CSW/FA blended pastes cured at 20 ºC for 90 days, which also exhibited higher mass loss values compared with the 100 wt % FA or CSW pastes. As expected [18,33], these values significantly improved when cured at 65 ºC, which indicates that the reactivity of these low-calcium precursors improved with thermal curing.

A new dehydration band arose on the 100 wt % BFS thermogravimetric curves with and without $Ca(OH)_2$, which shifted from 435 ºC in the pastes cured at 20 ºC for 28 days, to 445 ºC in those cured at 65 ºC for 7 days. According to previous studies by Moraes et al. [32] and Jin et al. [34], this band denotes the formation of small amounts of hydrotalcite, which are commonly observed in alkali-activated 100 wt % BFS [2,32,34,35]. In agreement with the XRD spectra (Figures 3.2-6 to 3.2-8), no signals due to $Ca(OH)_2$, whose bands typically arose within the 520–580 ºC range [27], were distinguished in any activated pastes. This indicates that calcium participates in the activation reactions. Nor was it possible to confirm the existence of natron by the TG analyses as the signals because this sodium carbonate emerged within the 625–875 ºC range [36].

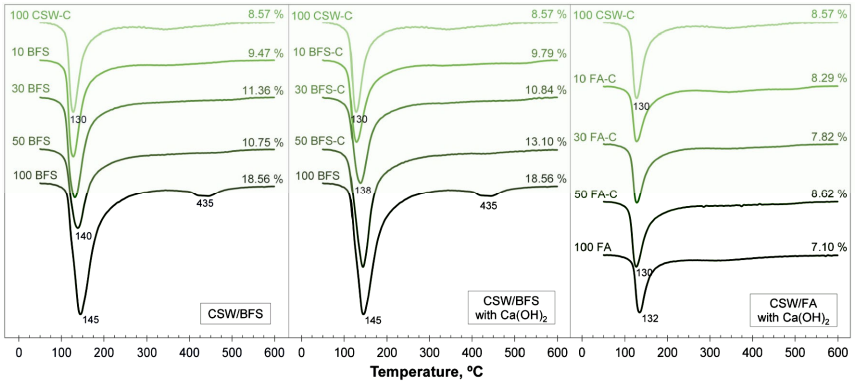

Fig. 3.2-7 The differential thermogravimetric curves for the alkali-activated CSW blended pastes cured at 20 ◦C for 28 days. Total mass loss is indicated as a percentage.

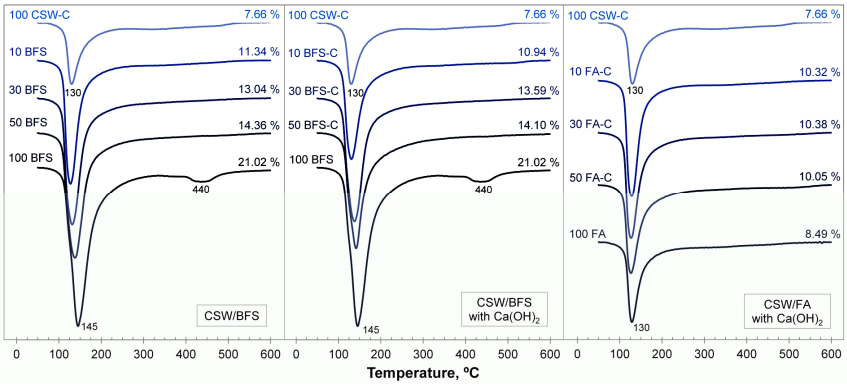

Fig. 3.2-8 The differential thermogravimetric curves for the alkali-activated CSW blended pastes cured at 20 ◦C for 90 days. Total mass loss is indicated as a percentage.

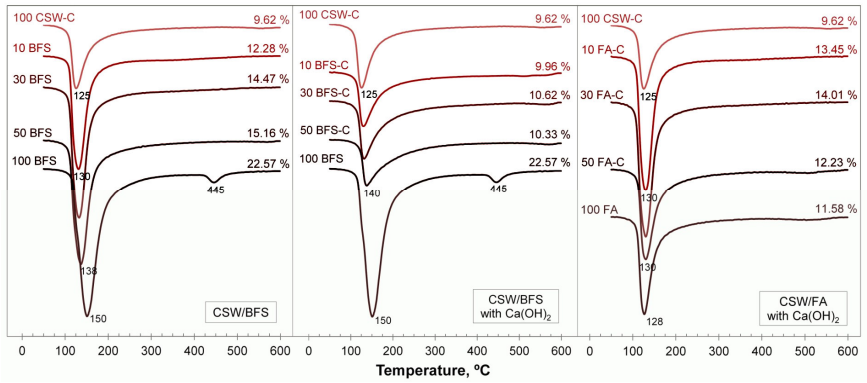

Fig. 3.2-9 The differential thermogravimetric curves for the alkali-activated CSW blended pastes cured at 65 °C for 7 days. Total mass loss is indicated as a percentage.

3.2.3.6. Field Emission Scanning Electron Microscopy (FESEM)

The FESEM micrographs of the alkali-activated pastes prepared with 100 wt % CSW, BFS, and FA are shown in Figure 3.2-12, and those of the pastes containing 30 wt % BFS (with and without $Ca(OH)_2$) and 30 wt % FA are presented in Figure 3.2-13. They were all cured at 20 °C for 28 days and at 65 °C for 7 days. The 90-day micrographs are not presented because the microstructure was similar to that observed after 28 curing days.

As observed in Figures 3.2-12 and 3.2-13, some FA particles exhibit an unaltered dense surface, while others show a partially reacted outer layer, in which the amorphous part of ash reacts and reveals its crystalline phases. As expected, as the 100 wt % FA mortar did not set at 20 ºC, the spherical FA particles observed in this paste (Figure 3.2-12) remained mainly unreacted. Conversely in agreement with the mechanical properties exhibited by the CSW/FA blended systems (Figure 3.2-4), the 30 wt % FA pastes showed some FA particles with a disintegrated external layer which, according to Khan et al. [37], denotes

some FA reaction. These results agree with those previously reported by Rodríguez et al. [38],

who associated smooth spherical particles with undissolved FA, and dendritic or rectangularly-shaped structures with crystalline low-solubility phases in partially reacted FA particles.

The 100 wt % BFS pastes (Figure 3.2-12) had the densest microstructure, formed mainly by C–S–H/C–A–S–H gel [19,20,35], and was similar no matter what the curing conditions were (65 ºC or 20 ºC). These results also fall in line with the compressive strength results reported in Figure 3.2-4, and agree with those previously reported by Pan et al. [20], who also observed a denser microstructure in the 100 wt % BFS pastes compared with that presented by the alkali-activated 50 wt % FA/BFS blends. The 100 wt % CSW pastes (Figure 3.2-12) were composed mainly of unreacted or partially reacted irregularly-shaped CSW particles surrounded by the newly-formed N–A–S–H/N–(C)–A–S–H gel. Although the microstructure of the 30 wt % BFS pastes (with and without $Ca(OH)_2$) was formed mainly by an amorphous-binding matrix, it was not possible to distinguish the type of gel that formed from its morphology. Small amounts of particles with a fibrous morphology were identified in the 30 wt % CSW/BFS pastes prepared with 4 wt % $Ca(OH)_2$, which were attributed to hydrotalcite ($Mg_6Al_2(CO_3)_{16}{\cdot}4H_2O$). Although the signals due to hydrotalcite were identified only on the DTG curves of the 100 wt % BFS activated pastes, and could not be clearly distinguished in the XRD spectra of the CSW/BFS blended systems, this finding was attributed to the high amorphous content in the CSW/BFS binding matrix, and to the fact that hydrotalcite probably presented poor crystallinity or small amounts formed.

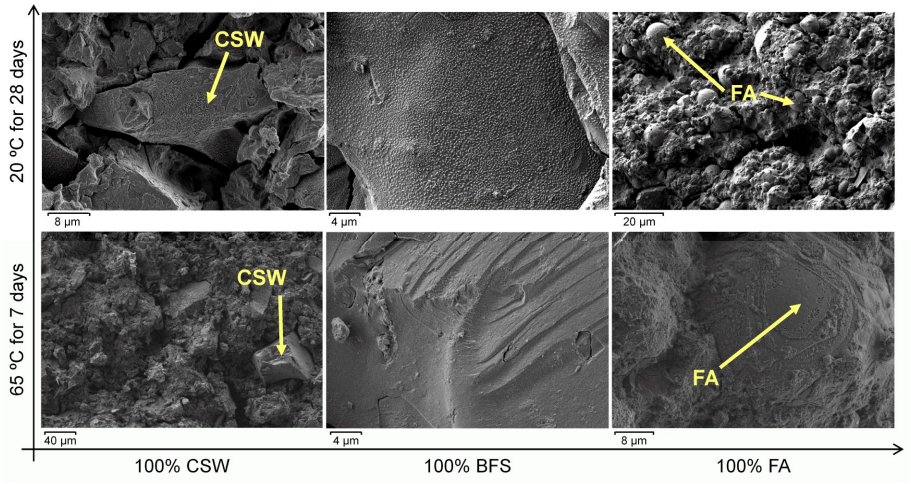

Fig. 3.2-10 The field emission scanning electron images of the 100 wt % CSW, BFS, and FA alkali-activated pastes cured at 20 ˚C for 28 days and at 65 ˚C for 7 days. CSW: ceramic sanitaryware particles; FA: fly ash particles, N–(C)–A–S–H/C–S–H/C–A–S–H: alkali-activated gels.

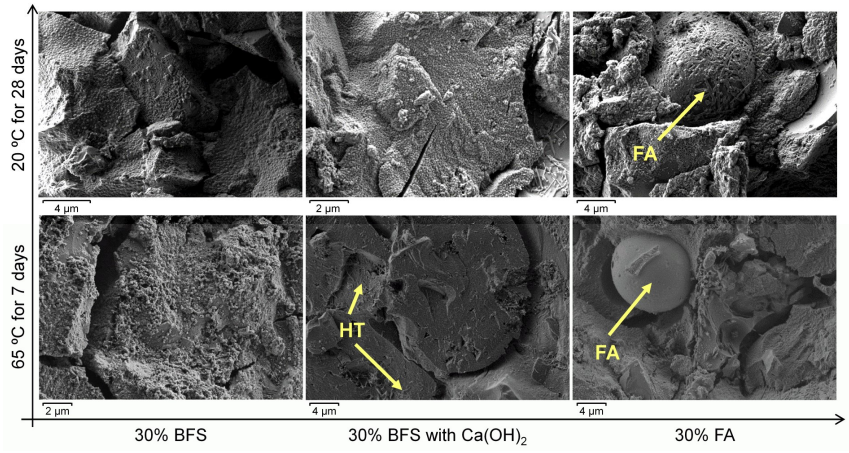

Fig. 3.2-11 The field emission scanning electron images of the CSW blended pastes prepared with 30 wt % BFS (with and without $Ca(OH)_2$) and 30 wt % FA, cured at 20 °C for 28 days and at 65 °C for 7 days. FA: fly ash particles, HT: hydrotalcite, N–(C)–A–S–H: alkali-activated gel.

3.2.4. Discussion

3.2.4.1. Strength of the CSW/BFS and CSW/FA Blended Mortars

The partial replacement of CSW with BFS or FA allowed this ceramic waste to be activated at 20 ºC and generated mortars with a wide range of mechanical properties, depending on the percentage of replacement and the curing conditions. Authors like Zedan et al. [1] or Najimi et al. [3] have attributed the better mechanical properties obtained with increasing amounts of BFS to the amorphous calcium aluminosilicates provided by BFS, which enhance the possibilities of forming hydration products. Robayo-Salazar et al. [19] have also observed how the reaction heat increases with higher BFS additions, which not only accelerated the process kinetics, but also favored the activation of a pozzolan at room temperature. The wide range of compressive strength results obtained falls in line with the previous study by Najimi et al. [3], who also observed a wide variation in the compressive strength results of natural pozzolan/BFS blended mortars (20 to 47 MPa after 28 days at 20 °C), depending on the BFS content (30, 50 or 70 wt %) and the mix proportions of the activating solutions. Robayo-Salazar et al. [19] also observed how BFS activated a natural volcanic pozzolan at room temperature, and reported improved strength values with increasing BFS contents (up to 30 wt %, which provided 37.24 MPa in the mortars cured at 20 ºC for 28 days). Similarly, Pan et al. [20] also found that adding BFS allowed FA to activate at room temperature, and these authors reported strength values of 29 MPa in the 50 wt % FA/BFS mortars cured at room temperature for 28 days. In the study by Zedan et al. [10], the

strength of alkali-activated ceramic waste mortars cured for 28 days also improved by going from 10 MPa to almost 40 MPa when blended with 30 wt % BFS.

The obtained results significantly extend the field of applications of alkali-activated CSW blended cements. However, FA and BFS are valuable by-products that can be easily reused in different construction applications, and are employed mainly as pozzolanic admixtures in Portland cement [5,6,8,39,40]. Although 13.6 million tons of steel were produced in Spain in 2016 (16th highest steel production country), only 4.6 MT were manufactured in blast furnaces (33.9%), and the remaining 66.1% (9.0 MT) was produced in electric furnaces [9]. Nowadays, Spanish iron blast furnaces operate only in Gijón (north Spain), and the amount of BFS consumed by Spanish cement companies is larger than that produced [8], which implies that some BFS is imported. Consequently, it is recommended to use as small as possible BFS or FA amounts, depending on the specific use of the binder. In this sense, the CSW mortars containing 20–30 wt % BFS or FA exhibited compressive strength values within the 22.1–37.6 MPa range after 7 curing days at 65 ◦C, and 6.9–21.1 MPa after 28 days at 20 ◦C. These binders can be used mainly in low-strength applications (e.g., nonstructural concrete or blocks) or prefabricated systems (where temperature can be easily applied to cure samples). For high-strength applications, the C-BFS40 and C-BFS50 systems can be selected with strength values that come close to 30 and 40 MPa after 28 curing days at 20 ◦C. However, as these mortars use large amounts of BFS, CSW can alternatively be blended with CAC, PC [24] or fluid catalytic cracking waste (FCC, an industrial by-product) [26] when high strength binders or shorter curing periods are required. Compressive strength values of 66.3 MPa and 78.6 MPa have been reported in alkali-activated CSW mortars blended with 15 wt % PC or 20 wt % CAC, respectively (cured at 65 ◦C for 7 days). However, as highlighted by the authors [24], CAC or PC production implies the use of

natural resources and requires vast amounts of energy. Thus, an alternative with a higher added value would be to blend CSW with FCC [26], which gave compressive strength results that came close to 40 MPa in the mortars cured at 20 ◦C for 28 days (made with 30 wt % FCC and the same mix proportions as those used herein).

3.2.4.2. Types of Gels Formed

As Ranjbar et al. described [7], during the synthesis of geopolymers, the aluminate and silicate monomers released from dissolved precursors form dissolved species. They cross-link to form oligomers, which arrange to form an aluminosilicate gel. Si and Al are tetrahedrally bonded with oxygen so that the basic monomer units (AlO_4^-) are negatively charged [41]. Although these charges are balanced by the alkali cations in the system (Na^+), they may also be balanced by Ca^{2+} in the presence of reactive calcium. Thus, in the presence of calcium, different types of gels may co-exist in the binding matrix. Ismail et al. [29], who investigated the effect of FA on BFS blended systems, observed that the structure of silicate-activated slag pastes was formed mainly by a C–A–S–H gel, activated fly ash was composed chiefly by a N–A–S–H gel, and both gels co-existed in slag-fly ash blended binders. Marjanovic et al. [2] observed that the co-existence of both N–A–S–H and C–A–S–H gels strongly depends on both the blend proportions and the activator concentration. Previous studies into the alkali-activation of blended precursors [2,29,32,35] suggest that N–A–S–H or low-calcium N–(C)–A–S–H gels most probably formed in the 100 wt % CSW or CSW/FA blended systems, and that N–(C)–A–S–H gels presumably arose in the CSW/BFS binders, with bigger amounts of calcium and closer to C–S–H/C–A–S–H with increasing slag contents.

The signal at 29.5 2θ degrees in the diffraction pattern of alkali-activated slag has been attributed by authors like Burciaga-Díaz et al. [35] and Pan el al. [20] to the formation of a poorly crystalline calcium silicate hydrate C–S–H with partial replacement of Si with Al (C–A–S–H). In the study by Pan et al. [20], a C–S–H binding gel was formed mainly in alkali-activated 100 wt % BFS, and the partial replacement of FA with BFS gave a combination of N–A–S–H and C–A–S–H gels. As observed by these authors [20], as the C–S–H gel formed in pore solutions with high SiO_2 concentrations, it presented a lower CaO/SiO_2 ratio compared with the C–S–H gel that typically forms in PC. No signals within the 29–30 2θ degrees range arose in the spectra of the CSW/FA systems studied herein. Given the low CaO content in the original CSW and FA (lower than 4 wt %; see Table 3.2-4), a N–A–S–H or a N–(C)–A–S–H gel was expected to form, with calcium provided mainly by the 4 wt % $Ca(OH)_2$ addition. The XRD results agree with those obtained by DTG as the main dehydration band slightly displaced toward higher temperatures with increasing BFS contents, and hardly moved in the CSW/FA blended systems cured at 20 °C, but exhibited a minor displacement when these CSW/FA blended pastes were cured at 65 °C. As observed by Ismail et al. [29] and Djobo et al. [41], these higher dehydration temperatures denote a modification in the gel structure, with free water more tightly bound or with smaller pores. Thus, in the CSW/BFS blended cements, the slightly higher dehydration temperatures would be attributed to the incorporation of calcium into the binding gel, while they would be explained by the formation of a more cross-linked structure with smaller pores in the CSW/FA pastes cured at 65 °C.

3.2.4.3. Role of Calcium in the Kinetics of the Process

In agreement with the results reported in [24,26], where no $Ca(OH)_2$ was identified after the activation of CSW [24] or CSW/FCC blends [26], no signals due to $Ca(OH)_2$ arose in the XRD spectra or DTG curves of the

alkali-activated CSW blended pastes. This indicates that $Ca(OH)_2$ was consumed during the alkali-activation reactions. In line with the obtained results, Chen et al. [4] observed that adding calcium to metakaolin geopolymers enhanced the rate and extent of MK dissolution. The higher dissolution rates of the precursor increased the Al concentration in the solution as Al tends to dissolve faster than Si [4]. As explained by Ranjbar et al. [7], the bigger amounts of $Al(OH)_4^-$ species available for condensation at early ages improve the condensation rate between silicate and aluminate species, rather than only between silicate species. Since the condensation between silicate species is slower than that between silicate and aluminate species [42], this accelerates the reaction kinetics, and originates higher initial strength and shorter setting times [4,7]. Briefly, the higher dissolution rates promoted by adding $Ca(OH)_2$ increases the Al concentration in the solution, which strongly influences the setting time of the developed mortars due to accelerated gel formation. However as pointed out by Silva et al. [42], the Si present in the alkali-activated systems determines the type of silica-aluminate structures that form, and is responsible for a higher later strength development.

3.2.4.4. Future Research

The further research conducted (Sections 3.2.2.4 and 3.2.3.3) confirmed that BFS mainly reacted with the activating solution in the 50 wt % BFS blended mortars prepared with 4 wt % $Ca(OH)_2$. This resulted in an excess of alkalis for the amount of BFS in the blended cements, which consequently diminished the mechanical properties of these mortars. As observed by Silva et al. [42], the properties of an alkali-activated binder may significantly be improved by making minor changes in the Si and Al concentrations available during synthesis. Hence the obtained results open up a new interesting research line to be explored in order to

optimize the mix proportions in the activating solutions, depending on the amount of BFS or FA in the CSW blended systems.

3.2.5. Conclusions

The present research investigated the effect of partially replacing CSW with BFS or FA, together with the influence of $Ca(OH)_2$ additions, on the microstructure and compressive strength of alkali-activated CSW blended cements. Based on the results, the following conclusions can be drawn:

- The compressive strength of the 100 wt % CSW mortars improved with BFS or FA content. The best results were provided by the CSW/BFS blended systems with the $Ca(OH)_2$ addition, which reached almost 55 MPa after 90 curing days at 20 °C or 7 days at 65 °C.

- The BFS mortars presented better strength results than FA, especially when cured at 20 °C.

- BFS mainly reacted with the activating solution in the CSW/BFS blended cements, which led to a significant loss of strength compared to the 100 wt % BFS sample. This was attributed to excess reagents for the diluted amount of BFS in the system.

- Although 4 wt % $Ca(OH)_2$ was consumed mainly by BFS in the CSW/BFS blended systems, the 8 wt % additions promoted the reactivity of CSW, which also conferred the binder strength.

- No significant new crystalline phases were identified in the CSW blended cements, and $Ca(OH)_2$ reacted during the alkali-activation process.

- Although it was not possible to clearly differentiate the different types of gel that formed, N–A–S–H and low-calcium N–(C)–A–S–H gels most probably formed in the CSW/FA blended systems, and a combination of N–(C)–A–S–H/C–S–H/C–A–S–H gels formed in the CSW/BFS binary cements.

The combination of CSW with BFS or FA significantly broadens the possibilities of reusing and valorizing a ceramic waste generated in large quantities worldwide as a precursor in alkali-activated blended cements. The new low-CO_2 binders developed are a potential alternative to Portland cement to help preserve the environment.

References

1. Zedan, S.R.; Mohamed, M.R.; Ahmed, D.A.; Mohammed, A.H. Alkali activated ceramic waste with or without two different calcium sources. *Adv. Mater. Res.* **2015**, *4*, 133–144.

2. Marjanovic´, N.; Komljenovic´, M.; Bašc˘arevic´, Z.; Nikolic´, V.; Petrovic´, R. Physical-mechanical and microstructural properties of alkali-activated fly ash-blast furnace slag blends. *Ceram. Int.* **2015**, *41*, 1421–1435.

3. Najimi, M.; Ghafoori, N.; Sharbaf, M. Alkali-activated natural pozzolan/slag mortars: A parametric study. *Constr. Build. Mater.* **2018**, *164*, 625–643.

4. Chen, X.; Sutrisno, A.; Struble, L.J. Effects of calcium on setting mechanism of metakaolin-based geopolymer. *J. Am. Ceram. Soc.* **2018**, *101*, 957–968.

5. CEDEX, Center for Studies and Experimentation of Public Works-Ministerio de Fomento. Gobierno de España: Catálogo de Residuos.Ficha Técnica Cenizas Volantes De Carbón Y Cenizas De Hogar o Escorias. 2011. Available online:

http://www.cedexmateriales.es/catalogo-de-residuos/24/diciembre- 2011/ (accessed on 4 August 2018). (In Spanish)

6. Toniolo, N.; Boccaccini, A.R. Fly ash-based geopolymers containing added silicate waste. A review. *Ceram. Int.* **2017**, *43*, 14545–14551.

7. Ranjbar, N.; Kuenzel, C. Cenospheres: A review. *Fuel* **2017**, *207*, 1–12.

8. CEDEX, Center for Studies and Experimentation of Public Works-Ministerio de Fomento. Gobierno de España: Catálogo de Residuos. Ficha Técnica Escorias De Horno Alto. 2011. Available online: http://www.cedexmateriales.es/catalogo-de-residuos/39/escorias-de-horno-alto/ (accessed on 4 August 2018). (In Spanish)

9. World Steel Association, World Steel in Figures 2017. Available online: https://www.worldsteel.org (accessed on 4 August 2018).

10. US Geological Survey, Mineral Resources Program, Iron and Steel Slag. Available online: ttps://minerals.usgs.gov/minerals/pubs/commodity/iron_&_steel_slag/mcs-2017-fesla.pdf (accessed on 4 August 2018).

11. Pacheco-Torgal, F.; Castro-Gomes, J.; Jalali, S. Alkali-activated binders: A review. Part 2. About materials and binders manufacture. *Constr. Build. Mater.* **2008**, *22*, 1315–1322.

12. Mehta, A.; Siddique, R. An overview of geopolymers derived from industrial by-products. *Constr. Build. Mater.* **2016**, *127*, 183–198.

13. Mellado, A.; Catalán, C.; Bouzón, N.; Borrachero, M.V.; Monzó, J.; Payá, J. Carbon footprint of geopolymeric mortar: Study of the contribution of the alkaline activating solution and assessment of alternative route. *RSC Adv.* **2014**, *4*, 23846–23852.

14. Mohammed, S. Processing, effect and reactivity assessment of artificial pozzolans obtained from clays and clay wastes: A review. *Constr. Build. Mater.* **2017**, *140*, 10–19.

15. Halicka, A.; Ogrodnik, P.; Zegardlo, B. Using ceramic sanitary ware waste as concrete aggregate. *Constr. Build. Mater.* **2013**, *48*, 295–305.

16. Bernasconi, A.; Diella, V.; Pagani, A.; Pavese, A.; Francescon, F.; Young, K.; Stuart, J.; Tunnicliffe, L. The role of firing temperature, firing time and quartz grain size on phase-formation, thermal dilatation and water absorption in sanitary-ware vitreous bodies. *J. Eur. Ceram. Soc.* **2011**, *31*, 1353–1360.

17. Baraldi, L. World sanitaryware production and exports. *Ceram. World Rev.* **2015**, *114*, 56–65.

18. Reig, L.; Borrachero, M.V.; Monzó, J.; Savastano, H.; Tashima, M.M.; Payá, J. Use of ceramic sanitaryware as an alternative for the development of new sustainable binders. *Key Eng. Mater.* **2016**, *668*, 172–180.

19. Robayo-Salazar, R.A.; de Gutiérrez, M.; Puertas, F. Study of synergy between a natural volcanic pozzolan and a granulated blast furnace slag in the production of geopolymeric pastes and mortars. *Constr. Build. Mater.* **2017**, *157*, 151–160.

20. Pan, Z.; Tao, Z.; Cao, Y.F.; Wuhrer, R.; Murphy, T. Compressive strength and microstructure of alkali-activated fly ash/slag binders at high temperature. *Cem. Concr. Compos.* **2018**, *86*, 9–18.

21. Tashima, M.M.; Reig, L.; Santini, M.A.; B Moraes, J.C.; Akasaki, J.L.; Payá, J.; Borrachero, M.V.; Soriano, L. Compressive Strength and Microstructure of Alkali-Activated Blast Furnace Slag/Sewage Sludge Ash (GGBS/SSA) Blends Cured at Room Temperature. *Waste Biomass Valorization* **2017**, *8*, 1441–1451.

22. Perná, I.; Hanzlíc̆ek, T. The setting time of a clay-slag geopolymer matrix: The influence of blast-furnace-slag addition and the mixing method. *J. Clean. Prod.* **2016**, *112*, 1150–1155.

23. El-Naggar, M.R.; Amin, M. Impact of alkali cations on properties of metakaolin and metakaolin/slag geopolymers: Microstructures in relation to sorption of 134Cs radionuclide. *J. Hazard. Mater.* **2018**, *344*, 913–924.

24. Reig, L.; Soriano, L.; Tashima, M.M.; Borrachero, M.V.; Monzó, J.; Payá, J. Influence of calcium additions on the compressive strength and microstructure of alkali-activated ceramic sanitary-ware. *J. Am. Ceram. Soc.* **2018**, *101*, 3094–3104.

25. García-Lodeiro, I.; Fernández-Jiménez, A.; Palomo, A. Variation in hybrid cements over time. Alkaline activation of fly ash-portland cement blends. *Cem. Concr. Res.* **2013**, *52*, 112–122.

26. Cosa, J.; Soriano, L.; Borrachero, M.; Reig, L.; Payá, J.; Monzó, J. Influence of Addition of Fluid Catalytic Cracking Residue (FCC) and the SiO_2 Concentration in Alkali-Activated Ceramic Sanitary-Ware (CSW) Binders. *Minerals* **2018**, *8*, 123.

27. Reig, L.; Soriano, L.; Borrachero, M.V.; Monzó, J.; Payá, J. Influence of the activator concentration and calcium hydroxide addition on the properties of alkali-activated porcelain stoneware. *Const. Build. Mater.* **2014**, *63*, 214–222.

28. Temuujin, J.; Williams, R.P.; van Riessen, A. Effect of mechanical activation of fly ash on the properties of geopolymer cured at ambient temperature. *J. Mater. Process. Technol.* **2009**, *209*, 5276–5280.

29. Ismail, I.; Bernal, S.A.; Provis, J.L.; San Nicolas, R.; Hamdan, S.; Van Deventer, J.S.J. Modification of phase evolution in alkali-activated blast furnace slag by the incorporation of fly ash. *Cem. Concr. Compos.* **2014**, *45*, 125–135.

30. Džunuzovic´, N.; Komljenovic´, M.; Nikolic´, V.; Ivanovic´, T. External sulfate attack on alkali-activated fly ash-blast furnace slag composite. *Constr. Build. Mater.* **2017**, *157*, 737–747.

31. Fernández-Jiménez, A.; Palomo, A.; Sobrados, I.; Sanz, J. The role played by the reactive alumina content in the alkaline activation of fly ashes. *Microporous Mesoporous Mater.* **2006**, *91*, 111–119.

32. Moraes, J.C.B.; Tashima, M.M.; Melges, J.L.P.; Akasaki, J.L.; Monzó, J.; Borrachero, M.V.; Soriano, L.; Payá, J. Optimum Use of Sugar Cane Straw Ash in Alkali-Activated Binders Based on Blast Furnace Slag. *J. Mater. Civ. Eng.* **2018**, *30*, 4018084.

33. Rashad, A.M. A comprehensive overview about the influence of different admixtures and additives on the properties of alkali-activated fly ash. *Mater. Des.* **2014**, *53*, 1005–1025.

34. Jin, F.; Gu, K.; Al-Tabbaa, A. Strength and hydration properties of reactive MgO-activated ground granulated blastfurnace slag paste. *Cem. Concr. Compos.* **2015**, *57*, 8–16.

35. Burciaga-Díaz, O.; Escalante-García, J.I. Comparative performance of alkali activated slag/metakaolin cement pastes exposed to high temperatures. *Cem. Concr. Compos.* **2017**, *84*, 157–166.

36. Hidalgo, A.; García, J.L.; Alonso, M.C.; Fernández, L.; Andrade, C. Microstructure development in mixes of calcium aluminate cement with silica fume or fly ash. *J. Therm. Anal. Calorim.* **2009**, *96*, 335–345.

37. Khan, M.Z.N.; Shaikh, F.; uddin Ahmed Shaikh, F.; Hao, Y.; Hao, H. Synthesis of high strength ambient cured geopolymer composite by using low calcium fly ash. *Constr. Build. Mater.* **2016**, *125*, 809–820.

38. Rodríguez, E.D.; Bernal, S.A.; Provis, J.L.; Paya, J.; Monzo, J.M.; Borrachero, M.V. Effect of nanosilica-based activators on the performance of an alkali-activated fly ash binder. *Cem. Concr. Compos.* **2013**, *35*, 1–11.

39. Dwivedi, A.; Jain, M.K. Fly ash–waste management and overview: A Review. *Recent Res. Sci. Technol.* **2014**, *6*, 30–35.

40. Ministry of Public Works. *RC-16. Instrucción para la Recepción de Cementos (CementReceptionInstruction)*; Ministry of Public Works: Madrid, Spain, 2016.

41. Djobo, J.N.Y.; Tchakouté, H.K.; Ranjbar, N.; Elimbi, A.; Tchadjié, L.N.; Njopwouo, D. Gel Composition and Strength Properties of Alkali-Activated Oyster Shell-Volcanic Ash: Effect of Synthesis Conditions. *J. Am. Ceram. Soc.* **2016**, *99*, 3159–3166.

42. Silva, P.D.; Sagoe-Crenstil, K.; Sirivivatnanon, V. Kinetics of geopolymerization: Role of Al_2O_3 and SiO_2. *Cem. Concr. Res.* **2007**, *37*, 512–518.

4. Aplicación en suelos

4.1 Stabilization of soil by means alternative alkali-activated cement prepared with spent FCC catalyst

Juan Cosa, Lourdes Soriano, María Victoria Borrachero, Jordi Payá, José María Monzó (2020) **International Journal of Applied Ceramic Technology. 17(1):190-196.**

Abstract: Alkali-activated cements are widely studied as alternative and sustainable binder in soil stabilization. When traditional methods are employed to make cylindrical specimens using soil stabilized with alkali-activated cement (AAC), certain slenderness and buckling problems arise. In this research work, a mold was designed and constructed, which allowed small cubic specimens to be made (40x40x40 mm^3). With the newly designed mold, cubic samples of soil stabilized with Portland cement (OPC) and alternative AAC (based on spent fluid catalytic cracking catalyst FCC) were prepared from which compressive strength was obtained. Cylindrical specimens were also prepared using the same binders as in the previous case to obtain their compressive strength. The results obtained in both cases were compared. Greater resistances for cubic samples were achieved. The cubic specimens were selected for being better in terms of standard deviation of compressive strength for AAC stabilized soil. The obtained compressive strength and standard deviation results were compared between the soil specimens stabilized with different stabilizers cured at 7, 14, 28 and 90 days. The method allows small-sized cubic specimens to be prepared. It improves ergonomics. It also facilitates a large number of specimens being obtained with a small amount of sample. Soil stabilized with AAC yielded higher compressive strength after 90 days compared to that with OPC.

Keywords: Sustainable construction materials, Waste reuse, Alkali-activated cement, Soil stabilization.

4.1.1 Introduction

Large-sized and heavy cubic or cylindrical specimens are normally used to study stabilized soils for their use on road surfaces UNE 12390-1 [1] and in compressed earth blocks (CEB), where even the same block is used, as in UNE 41410 [2]. In some standards, smaller sized cylindrical specimens are used; e.g. ASTM STP 479 [3]. In this study, the Harvard miniature mold was used (see Fig. 4.1-1), but cylindrical samples have some problems as cubic ones do, such as possible buckling when some compression is exercised. They do not usually have the same base (Ø 3.8 cm) and height (7.6 cm) dimensions, and thus present certain slenderness, and possibly defects on the upper face that do not guarantee total flatness. When utilizing soil stabilization with alkali-activated cement (AAC), we may come across very plastic optimum dry density, which causes specimens to deform while unmolding at the end of compaction, an effect that is more pronounced in cylindrical specimens (see Fig. 4.1-2)

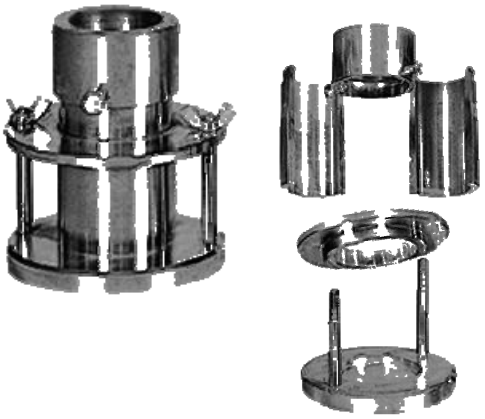

Fig. 4.1-1 Mold used for cylindrical specimens.

Fig. 4.1-2 Cylindrical specimen deformed when unmolding by sample plasticity.

A mold was designed and constructed for a sample size of 40x40x40 mm^3 because it is a size that is suitable for the load cell of the compressive strength test (Fig. 4.1-3) usually employed for OPC mortar testing (UNE-EN 196- 1 [4]).

Fig. 4.1-3 A cubic specimen in a compressive strength test.

Apart from solving the raised problems, the use of specimens with these characteristics helps many specimens to be obtained with small material samples because it is possible to use many specimens for some studies. Indeed, we have even accounted for more than 700 in some studies. This specimen type allows numerous variables to be studied, and a little raw material to be used to manufacture specimens, which also cuts economic and environmental costs by reducing the generated material and waste. Besides, ergonomics in handling is improved by reduced weight.

Different soil stabilizer types exist. The most commonly used one is Portland cement (OPC) [5]. As an alternative to it, several solutions are used, including blends of lime-pozzolana [5]. We found plenty of documents about using stabilizers for soils with OPC, lime, or with both, along with the methodology followed to prepare large-sized specimens in Standards NLT -310/90 [6] and UNE EN 13286, parts 50, 51, 52 and 53 [7]. Finding bibliography on the stabilization of soils with AAC is less common [8-13], where sodium silicate is frequently used as an activator. What is even less common is using AAC, whose activator is obtained from waste [14-17], where sodium silicate can be synthesized from mixtures of rice husk ash and sodium hydroxide and can, thus, considerably reduce CO_2 emissions [18,19].

To fulfill the research objectives, a mold (100x80x100 mm^3) for the cubic specimens was designed and made with a central filling gap (base of 40x40 mm^2 and 100 mm high) that allows layers of the material to be placed and their subsequent compaction.

In this article, the results of soils stabilized with AAC and those stabilized with OPC were compared to determine a simple protocol to prepare small-sized cubic specimens as a step prior to preparing the larger specimens normally used in current standards. The dispersion of the results was studied by calculating the standard deviation for each employed stabilizer, and for the two studied specimen types: cubic and cylindrical.

4.1.2. Experimental Section

4.1.2.1. Mold design and compaction procedures

Mold height must exceed 40 mm to be able to contain the soil volume before being compacted, with a cubic steel cube of 39x39x39 mm (dice). As shown in Figure 4.1-4, a removable cubic mold of 100x80x100 mm was designed with four screws on its front and two on its lower part, and with a central filling gap (40x40 mm base and 100 mm high) that allows layers of the material to be placed and serves as a guide for the cube. The mold base was made of a 10 mm-thick steel sheet.

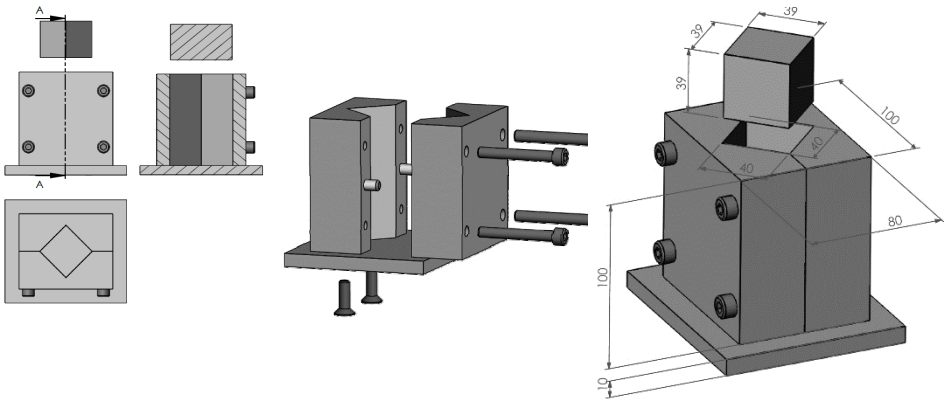

Fig. 4.1-4 Mold design of variable height.

When performing the AAC cylindrical specimens according to ASTM STP 479 [3], humidity was above optimum in these specimens. This behavior may be attributed to the difference of rheology of material compared to soil or OPC stabilized soil. An error due to deformation occurred when unmolding, and sometimes the specimen buckles in the simple compressive strength test. The upper face of specimens does not offer the desired flatness and is inclined due to deformation (see Fig. 4.1-2). For this reason, a decision was made to design a mold for the specimens measuring 40x40x40 mm^3 following a procedure to manufacture similar specimens to cylindrical specimens, and with the same dimensions on all sides to solve flatness and slenderness problems.

Standard UNE 103 501 [20] (which corresponds to ASTM D 1557 [21]) was used as the basis. The aims here were to specify the method to determine the dry and wet density ratio in soil for a compaction energy of 2632 J/cm^3, and to define the maximum dry density and its corresponding or optimal humidity, which can be obtained in the laboratory.

The cylindrical specimens were made in five layers of filling. By following Equation 1, it was possible to apply an approximate energy of 2632 J/cm^3 by dropping a 1.5-kilogram mass from 20 cm in height and with 15 blows.

$$\frac{Blows\ (15) \times Layers\ (5) \times Rammer\ weight\ (1.5\ kg \times 9.81) \times Rammer\ fall\ (0.20\ m)}{Vol.\ (86\ cm^3)} \approx 2632\ J/cm^3$$

Equation 1. Compaction of cylindrical specimens.

The cube specimens were made in three layers of filling, as seen in Table 4.1-1, following a similar procedure to that used in the modified proctor. With Equation 2, which allows the energy applied while preparing cubic specimens to be calculated, a 1.5-kilogram mass was dropped from 20 cm in height and with 19 blows.

$$\frac{Blows\ (19) \times Layers\ (3) \times Rammer\ weight\ (1.5\ kg \times 9.81) \times Rammer\ fall\ (0.20\ m)}{Vol.\ (64\ cm^3)} \approx 2632\ J/cm^3$$

Equation 2. Compaction of cube specimens.

To cure samples, a temperature of 22ºC and 50% relative humidity were chosen for all curing times (7, 14, 28 and 90 days).

Tab. 4.1-1 Cubic mold, the specimens manufacturing diagram.

Step 1-	Introduce a layer of mixture soil with the stabilizer
Step 2-	Introduce the dice

Step 3-	Apply 15 blows with the 1.5-kilogram mass
Step 4-	Extract the dice

Repeat steps 1 to 4 to complete the three layers

Step 5-	Loosen the mold's screws by completely removing the two lower screws
Step 6-	Remove the lower plate
Step 7-	Press the dice to remove the specimen from the bottom of the mold

4.1.2.2. Materials

The Spanish company PAVASAL, S.A. supplied the soil used to prepare the samples. This soil is that normally used to produce road surfaces. Thermogravimetry (35 to 1000 ° C) of a soil sample was carried out to determine its nature. Figure 4.1-5 shows the TG soil curve. Here we observe loss of mass in the curve starting at 700ºC, which indicates the presence of dolomite (two mass loss steps overlapped in the range 700-950ºC).

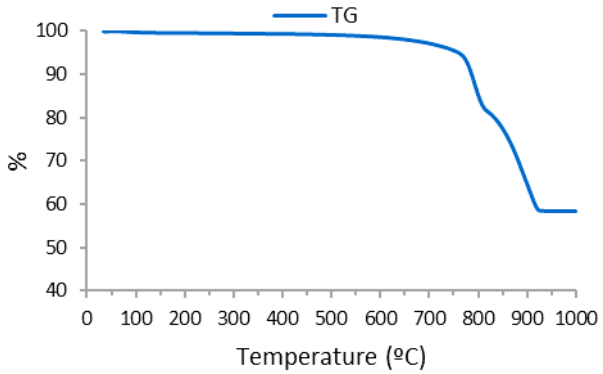

Fig. 4.1-5 Thermogravimetric curve (TG) for used soil.

For the thermogravimetric analysis, a Mettler Toledo TGA 850 module was used, along with an alumina crucible, at a heating rate of 20°C/min in an air atmosphere (gas flow 75 mL/min).

The water used to prepare samples came from the drinking water distribution network of the Universitat Politècnica de València (UPV), Spain.

The employed Portland cement (OPC) was gray cement type CEM I-52R, whose chemical composition is provided in Table 4.1-2. It was supplied by the company Lafarge Asland (Spain). The classification of this cement corresponds to that referred to in Standard UNE-EN 197-1 [22].

The spent catalyst from the catalytic cracking process (FCC), whose chemical composition is provided in Table 4.1-2, was petrochemical industry waste. The company OMNYA Clariana S.A. (Tarragona, Spain) supplied it.

Tab. 4.1-2 Chemical compositions of OPC and FCC. * Loss upon ignition determined at 950ºC.

% Mat.	SiO_2	Al_2O_3	Fe_2O_3	CaO	MgO	SO_3	K_2O	Na_2O	P_2O_5	TiO_2	LOI*
OPC	20.8	4.6	4.8	65.6	1.2	1.7	1	0.07	-	-	2
FCC	47.76	49.26	0.6	0.11	0.17	0.02	0.02	0.1	0.01	1.22	0.5

To prepare the alkaline/activating solutions in order to produce alkali-activated binders, sodium hydroxide pellets were used. They were supplied by the company Panreac S.A. with a purity of 98%. The utilized waterglass (sodium silicate), composed of 28% SiO_2, 8% Na_2O and 64% H_2O, was supplied by Merck.

The 25-kilogram soil sample to be used was taken and homogenized by quartering. Then the fraction to be passed through the 4-mm opening sieve and dried in an oven at 60ºC was selected.

4.1.2.3. Method

We used a Harvard miniature mold to make the specimens, to obtain the optimum dry density and to know its compressive strength with no other stabilizers. A modified proctor test was run with soil without a stabilizer (Fig. 4.1-6) according to Standard UNE 103 501 [20]. Secondly (Fig. 4.1-7), a modified proctor was made to stabilize soil with OPC because it is the most widely used stabilizer. Finally, (Fig. 4.1-8), a modified proctor was performed to stabilize soil with AAC by taking FCC as the precursor and a sodium silicate-NaOH solution as the activator [18].

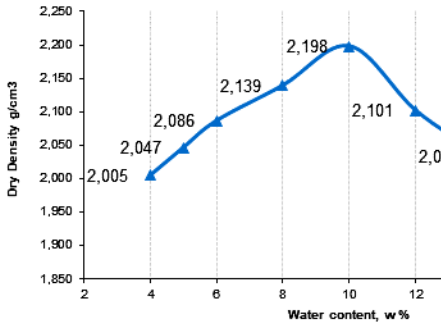

Fig. 4.1-6 Soil-modified proctor curve

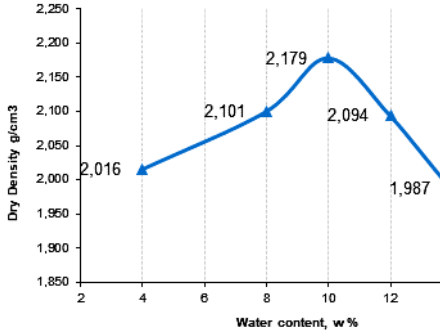

Fig. 4.1-7. Soil OPC-modified proctor curve

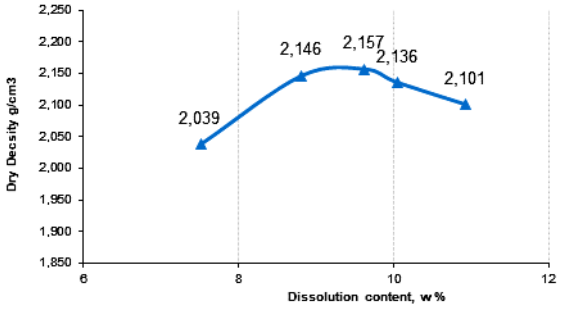

Fig. 4.1-8 Soil AAC-modified proctor curve

From the optimum dry density obtained by the modified proctor, soil mixtures were prepared with these stabilizers to compare their compressive strengths.

The mixture was made with the compacted soil with no stabilizer, the soil stabilized with 10% OPC, and the soil stabilized with AAC by adding 10% of FCC activated with the sodium silicate solution. The alkali solution consisted of 60.8% of Na_2SiO_3, 26% of H_2O and 13.22% of NaOH, was

prepared 30 minutes before and was used in an ambient temperature. The alkali solution/FCC ratio was 1.73 by mass.

To make the mixture with no stabilizer, we placed 1000g of soil in the mixer for 1 minute before adding water (97g) and finally mixing for another 2-minute period. The water/solid ratio content was 0.097.

To make the mixture with OPC, we placed 1000g of soil in the mixer for 1 minute before adding OPC and mixing for another 1-minute period, and finally adding water (110g) and mixing for 2 minutes. The water/solid content was 0.1.

To make the mixture with AAC, we placed 1000g of soil inside the mixer for 1 minute before adding the precursor (FCC, 100g) and mixing for another 1-minute period, and finally adding the activating solution (sodium silicate+NaOH+water, 107 g) and mixing for 2 minutes. The solution/solid ratio was 0.097 and the water/total solids ratio was 0.064.

To avoid the mixture from drying when making specimens, which can take a considerable time, all the mixture was placed inside a bag with an airtight seal. Then the amount of soil mixture, which corresponded to each layer to make up specimens, was placed inside smaller sealed bags. To prepare specimens, the process described in the “Experimental process” section was followed.

4.1.3. Results and Discussion

We compared the cylindrical and cubic specimens. As Figure 4.1-9 shows, the standard deviation was more pronounced in the AAC cylindrical specimens because its consistency was more plastic. Therefore, as shown in Figure 4.1-2, some cylindrical specimens hardly met the perpendicularity values of the different standards. However, the compressive strength data were fulfilled in both the cylindrical and cubic

specimens, with minimum values for using the soil for both road surfaces and CEB.

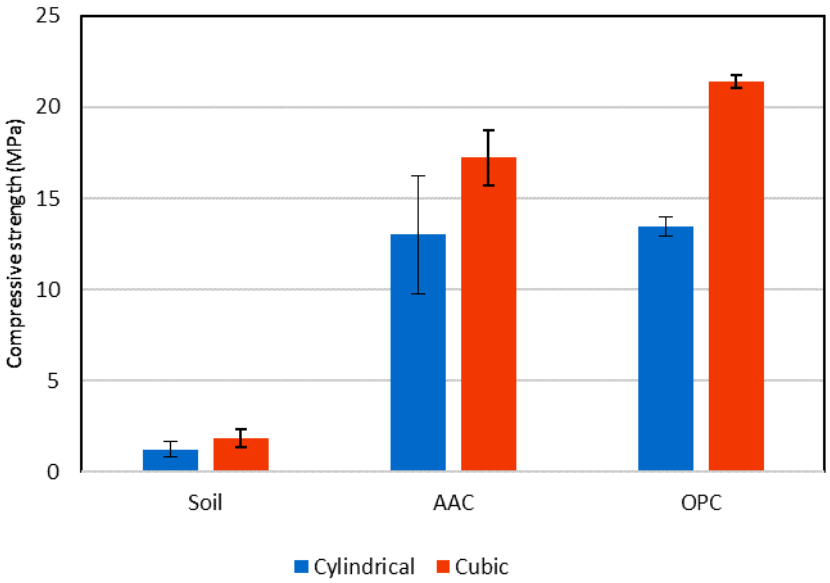

Fig. 4.1-9 Cubic and cylindrical specimens: soil without stabilizer, soil stabilized with OPC and soil stabilized with AAC at 7days.

We also compared the cubic specimens with no stabilizer and those with the different stabilizer types. Figure 4.1-10 shows how the compressive strength of the soil with no stabilizer was approximately 3MPa. When stabilizing with OPC, a better compressive strength was observed at earlier curing times. Approximately 24MPa was achieved with the soil stabilized with OPC. When stabilizing with AAC, the increase in compressive strength became more progressive, with lower compressive strength compared to OPC at earlier curing times, but with better compressive strength at 90 days compared to OPC, with

compressive strength coming close to 30MPa. This means that the development of the alkali-activated binding matrix is slower but much more effective than that for OPC.

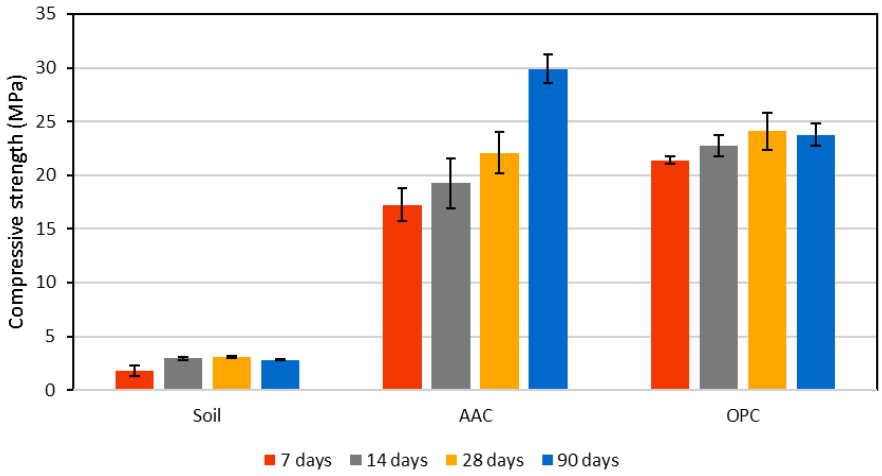

Fig. 4.1-10 Compressive strength at 7, 14, 28 and 90 days. Cubic specimens of soil with different stabilizations.

4.1.4. Conclusions

With a simple system, the method allows small-sized cubic specimens to be prepared to mitigate the problem of high standard deviation in the specimens stabilized with AAC, and the shape factors by the buckling and flatness of load faces. It improves ergonomics in handling by reducing weight. It also facilitates a large number of specimens being obtained with a small amount of sample, and allows many variables to be studied using only a little raw material to produce them, which cuts economic and environmental costs due to the reduction in the generated material and waste.

Thanks to its mechanical behavior, and compared to the soil without stabilizers, with both stabilizations by OPC and AAC, it proves effective and notably increases compressive strength. In the soil stabilization with AAC, the compressive strength progressively grows, with better values than that for OPC stabilized systems at 90 days.

References

1. UNE-EN 12390-1: (2013), Testing hardened concrete - Part 1: Shape, dimensions and other requirements for specimens and moulds

2. UNE-EN 41410: (2008), Compressed earth blocs for walls and partitions. Definitions, specifications and test methods.

3. ASTM, D-18C., ed., STP479-EB Special Procedures for Testing Soil and Rock for Engineering Purposes: Fifth Edition. West Conshohocken, PA: ASTM International, 1970. doi: 10.1520/STP479-EB

4. UNE-EN 196-1: (2005), Methods of testing cement - Part 1: Determination of strength

5. Auroville Earth Institute, Earthen architecture for sustainable habitat and compressed stabilised earth block technology, [consultation date: May 17, 2014], www.earth-auroville.com

6. NLT-310/90 Vibrating hammer compaction of treated granular materials

7. UNE-EN 13286-2: (2011), Unbound and hydraulically bound mixtures - Part 2: Test methods for laboratory reference density and water content - Proctor compaction

8. Khadka B., Shakya M. Comparative compressive strength of stabilized an un-stabilized rammed earth. Materials and Structures, vol 9, nº 49, pp 3945-3955, 2016.

9. Alrubaye A.J., Hassan M., Fattah M-Y. Stabilization of soft kaolin clay with silica fume and lime. International Journal of Geotechnical Engineering, vol 11, nº1, pp 90-96, 2017.

10. Rios S., Viana da Fonseca A., Baudet B. Effect of the porosity/cement ratio on the compression of cemented soil. Journal of Geotechnical and Geoenvironmental Engineering, vol 138, nº11, pp 1422-1426, 2012.

11. Zhang M., Guo H., El-Korchi T., Zhang G. Tao M. Experimental feasibility study of geopolymer as the next-generation soil stabilizer. Construction and Building Materials, vol 47, pp 1468-1478, 2013.

12. Rios S., Cristelo N., Viana da Fonseca A., Ferreira C. Stiffness behaviour of soil stabilized with alkali-activated fly ash from small to large strains. International Journal of Geomechanics, vol 17, noº 3, pp 1-12, 2017.

13. Zhang M., Zhao M.X., Zhang G.P., Nowak P., Coen A., Tao M.J. Calcium-free geopolymer as a stabilizer for sulfate-rich soils. Applied Clay Science, vol 108, pp 199-207, 2015.

14. Bouzón N., Payá J., Borrachero M.V., Soriano L., Tashima M.M., Monzó J. Refluxed rice husk ash/NaOH suspension for preparing alkali activated binders. Materials Letters, vol 115, pp 72–74, 2014.

15. Mejía J.M., Mejía de Gutiérrez R., Montes C. Rice husk ash and spent diatomaceous earth as a source of silica to fabricate a geopolymeric binary binder. Journal of Cleaner Production, vol 118, pp 133-139, 2016.

16. Puertas F., Torres-Carrasco M. Use of glass waste as an activator in the preparation of alkali-activated slag. Mechanical strength and paste characterization. Cement and Concrete Research, vol 57, pp 95-104, 2014.

17. Cosa J., Alamán M., Borrachero M.V., Payá J., Soriano L., Monzó J., Soil stabilization with alkali activated cements: A more sustainable solution for housing construction in developing countries. III International Congress of Development Studies. Zaragoza (Spain) from June 29th to July 1st, 2016, Proceedings pp 457-465.

18. Tashima M.M., Akasaki J.L., Castaldelli V.N., Soriano L., Monzó J., Borrachero M. V, Payá J. New geopolymeric binder base on fluid catalytic cracking catalyst residue (FCC). Materials Letters, vol 80, pp 50-52, 2012.

19. Mellado A., Catalán C., Bouzón N., Borrachero M. V., Monzó J.M., and J. Payá. Carbon footprint of geopolymeric mortar: study of the contribution of the alkaline activating solution and assessment of alternative route. RSC Adv. 2014, 4 (45), 23846-23852.

20. UNE-EN 103 501: (1994), Geotechnics. Compactation test. Modified proctor.

21. ASTM D1557-12e1 Standard Test Methods for Laboratory Compaction Characteristics of Soil Using Modified Effort (56,000 ft-lbf/ft3 (2,700 kN-m/m3)). West Conshohocken, PA; ASTM International, 2012. doi: https://doi.org/10.1520/D1557-12E01

22. UNE-EN 197-1: (2011), Cement - Part 1: Composition, specifications and conformity criteria for common cements

4.2. Comunicación oral presentada en el III Congreso Internacional de Estudios del Desarrollo en Zaragoza, con el título: Estabilización de suelos con cementos activados alcalinamente: Una solución más sostenible para la construcción de viviendas en países en desarrollo

Fecha del congreso anual	30/06/2016
Pág. Actas congreso	457-465
ISBN / ISSN	978-84-16723-36-2

Cosa, J , Alamán, M , Borrachero, MV , Payá, J , Soriano, L , Monzó, J

Resumen: En la agenda para 2030 de los objetivos de desarrollo sostenible (ODS), se expresa la necesidad de transformar la forma de construir y mejorar la sostenibilidad de las ciudades, garantizando acceso a la vivienda. También se pone de manifiesto la necesidad de una gestión eficiente de los recursos y desechos, reduciendo las emisiones de gases de efecto invernadero. En la estabilización de suelos, se pueden utilizar materiales considerados actualmente residuos, como es el caso del residuo de catalizador del craqueo catalítico, y la ceniza de cascara de arroz. El objeto de este estudio, es proporcionar una alternativa más sostenible a los materiales de construcción convencionales con elevado coste económico y medioambiental.

Abstract: On the agenda for 2030 of sustainable development goals (SDGs), It is expressed the need to make cities inclusive, safe, resilient and sustainable. Sustainable development cannot be achieved without significantly transforming the way we build and manage our urban spaces. Also highlights the need for efficient management of resources and waste. Stressing that action must be taken on emissions of greenhouse gases. Materials currently considered waste, such as the spent fluid catalyst cracking catalytic, and rice husk ash can be used in

soil stabilization. The purpose of this study is to provide a more sustainable alternative to conventional building materials with high economic and environmental cost.

Palabras clave: Materiales de construcción sostenibles, Reutilización de residuos, Cemento activado alcalinamente, Estabilización de suelos, Vivienda social

Keywords: Sustainable construction materials, Waste reuse, Alkali activated cement, Soil stabilization, Social housing

4.2.1 Introducción

Según Amnistía Internacional en el mundo existen cerca de 200.000 comunidades en asentamientos precarios. Con distintos nombres –favelas, villas miseria, ...–, son el hogar de más de 1.000 millones de personas; una cifra que podría llegar a multiplicarse por dos en 2030, según algunas previsiones (Amnistía Internacional 2015).

En septiembre de 2015, los estados miembros de la ONU aprobaron la agenda 2030 para el desarrollo sostenible, que incluye un conjunto de 17 Objetivos.

En su objetivo 11, se expresa la necesidad de transformar radicalmente la forma de construir y mejorar la sostenibilidad de las ciudades, garantizando el acceso a la vivienda.

En los países en desarrollo, los materiales de construcción pueden llegar a suponer el 100% del coste; ya que la autoconstrucción es la práctica habitual. Por tanto, utilizando materiales de bajo coste, como la tierra del

suelo donde se pretende levantar la vivienda, y diferentes residuos, se consigue proporcionar un método más accesible y sostenible (Salas 2010).

Si nos ceñimos a la dimensión “Durabilidad de la vivienda”, una vivienda se considera durable cuando se emplean materiales de construcción de calidad y estos se utilizan adecuadamente. La durabilidad no está relacionada con la modernidad del material, podemos tener materiales modernos poco durables y materiales tradicionales durables (Monzó 2012).

En el objetivo 9, se remarca la importancia de poner los avances tecnológicos al servicio de los desafíos económicos y ambientales. Ampliándose en el objetivo 12, a la necesidad de una gestión eficiente de los recursos y sus desechos.

En la técnica de estabilización de suelos mediante bloques de tierra comprimida, se pueden utilizar materiales considerados actualmente residuos, como es el caso del residuo de catalizador del craqueo catalítico (FCC), y la ceniza de cascara de arroz (CCA). Sólo la empresa estatal Colombiana Ecopetrol, que abarca el 35% de la producción nacional de crudo, generó en 2012 alrededor de 2000 toneladas de residuo de FCC, siendo mucho mayor esta cantidad si tenemos en cuenta la producción mundial. Por otra parte, la producción anual mundial de cascara de arroz es de en torno a 100 millones de toneladas. Esta cascarilla de arroz cuando es obtenida por proceso de pilado se convierte en un residuo que puede llegar a descomponerse produciendo focos de contaminación. Una parte de la cascarilla se incinera para obtener calor para el secado del grano en los molinos de arroz, generándose CCA que se convierte en un residuo.

Por otra parte, en explotaciones pequeñas en las zonas rurales, la cascarilla se incinera al aire libre para eliminar el residuo que se convierte en CCA, que podría ser utilizada como se propone.

En sus objetivos 7 y 13, se pone de manifiesto, la necesidad urgente de tomar medidas respecto al impacto producido por las emisiones de gases de efecto invernadero.

La Organización Meteorológica Mundial (OMM) alertó que por primera vez las concentraciones mensuales de dióxido de carbono en la atmósfera superaron el umbral de 400 partes por millón (ppm) en todo el hemisferio norte durante el mes de abril de 2014 (RPP noticias, ciencia y tecnología 2014).

En consecuencia, es necesario impulsar nuevas alternativas que permitan reducir estas altas tasas de emisiones de CO_2 a la atmósfera. Esto podría involucrar desde la industria química, hasta la industria de la construcción, que es la que nos atañe. Así, promoviendo el uso de nuevas tecnologías que fomenten, por ejemplo, el uso de materias primas reciclables, se podría lograr obtener materiales con un elevado rendimiento, bajos costos y un menor impacto ambiental. Estas iniciativas contribuirían a llevar a cabo una transición hacia el "desarrollo sostenible", entendido como forma de progreso que satisface las necesidades del presente, sin comprometer las necesidades de las futuras generaciones en todos los aspectos: social, humano y ambiental (ONU 1987).

Los materiales de construcción, al igual que la materia, experimentan un proceso inevitable de degradación. De tal manera que los recursos que hasta 1851 se creían inacabables como los combustibles, el agua y los materiales para la construcción, entre otros, se mostraron al mundo

susceptibles de ser finitos en un periodo corto para las expectativas de la población mundial (Acosta 2008).

4.2.2. Materiales y Métodos. Sección Experimental

4.2.2.1 Bloques de suelo estabilizado, prensa Cinva Ram

Hay vestigios de construcciones con tierra que datan de hace 8000 años, cuando surgieron civilizaciones en todos los continentes con nuevas maneras de emplear la tierra como material de construcción. La tecnología constructiva con tierra comprimida combina una fuerza de compactación sobre la tierra debidamente humedecida y mezclada con un agente estabilizante; el proceso de compactación se puede realizar por medios manuales o mediante una prensa. El producto realizado con tierra mediante una fuerza de compactación por medio de una prensa se conoce con el nombre de Bloque de Tierra Prensada o BTP. Su evolución fue impulsada por el desarrollo de máquinas prensadoras, entre las que se encuentran la prensa Cinva-Ram. La prensa Cinva-Ram, producto del programa de investigaciones del Centro Interamericano de Vivienda y Planeamiento (CINVA), en Colombia, fue concebida por el Ingeniero chileno Raúl Ramírez, se desarrolló con el objeto de proporcionar un elemento útil y económico para la autoconstrucción de pequeñas viviendas rurales. El proceso de producción de BTC se desarrolla mediante los siguientes pasos: conocimiento del material, estabilización, preparación mezcla tierra-cemento, prensado del material, fraguado y curado (González 2012).

4.2.2.2.Estabilizaciones convencionales (CP, Cal, Cal- Puzolana)

El uso de estabilizadores para la preparación de suelos deficientes o bloques de construcción está ampliamente establecido. Existen distintos tipos de estabilizadores, el más comúnmente utilizado es el cemento Portland (CP). Como alternativa a éste se utilizan diversas soluciones, entre ellas mezclas de Cal-Puzolana (Auroville Earth Institute 2014).

En las últimas décadas, la producción de cemento ha crecido considerablemente como consecuencia de un desarrollo económico y crecimiento demográfico. Sin embargo, la industria cementera está catalogada como un sector altamente contaminante y de gran impacto ambiental. La producción de una tonelada de CP requiere la explotación de un elevado volumen de materias primas (principalmente caliza y arcilla) y la emisión de aproximadamente una tonelada de CO_2 y otros gases contaminantes (NOx y SOx).

La producción de CP supone el 2% del consumo mundial de energía y el 5% de las emisiones mundiales de CO_2 (Noticias de la Ciencia y la Tecnología, 2016), lo que lo convierte en un material caro y contaminante; a pesar de ello, su producción mundial crece de forma espectacular. Hoy por hoy el CP es un material insustituible, pero en muchos casos este material se usa inadecuadamente (Vanderley 2002), especialmente en aplicaciones que requieren bajas resistencias mecánicas (Martirena 2004); en algunos casos se podría sustituir el CP por mezclas de cal y puzolanas (Day 1992). Una forma de reducir las emisiones totales en la producción de CP es sustituyendo parcialmente el clinker por otros subproductos o residuos sin merma de su calidad final (Gartner 2004).

Se propone como solución el uso de materiales conglomerantes sin CP. En este sentido, la sustitución total del cemento Portland se logra mediante el uso de los llamados cementos activados alcalinamente (CAA) y/o geopolímeros.

4.2.2.3.Estabilización no convencional (CAA y/o Geopolímeros)

Más recientemente se empiezan a usar para la estabilización de suelos con uso en ingeniería civil, cementos activados alcalinamente o geopolímeros (aluminosilicatos inorgánicos activados alcalinamente).

El término geopolímero ha sido aplicado desde los años setenta a una clase de materiales sintetizados a través de la activación alcalina de materiales cuya composición está formada fundamentalmente por sílice y alúmina. Los materiales geopoliméricos han sido aplicados en una gran variedad de sectores en la ingeniería, incluyendo su utilización como sustituto del CP para el encapsulamiento de desechos, paneles resistentes al fuego, cementos refractarios y en menor medida para la estabilización de suelos.

La exploración de geopolímeros como estabilizador de suelos de próxima generación tiene importantes implicaciones para las prácticas de la ingeniería civil. Los suelos estabilizados con geopolímeros necesitan menos tiempo para desarrollar una alta resistencia inicial frente a los estabilizados con CP. Gracias al aumento de la ductilidad de los suelos estabilizados con geopolímeros, se puede mitigar eficazmente el agrietamiento durante la construcción de pavimentos, mejorando también el proceso de curado. Adicionalmente, la menor contracción frente al CP puede reducir el daño causado por la fisuración debido a la retracción de los suelos.

En lo que a la estabilización de suelos con geopolímeros se refiere, el reto de hoy en día pasa por la obtención tanto de precursores como activadores de bajo coste económico y medioambiental, que haga competitivo su uso para la estabilización de bloques de suelo, ampliamente utilizados estos últimos en países en desarrollo.

4.2.2.4. Uso de residuos (CCA y FCC) en la preparación de Geopolímeros

Existe la posibilidad de utilizar residuos tanto en los precursores como en los activadores alcalinos, con el fin de reducir el coste económico y medioambiental, facilitando así el uso en países en desarrollo. Este es el caso de las escorias de alto horno, ceniza volante o el propio catalizador gastado de craqueo catalítico (FCC) que pueden ser utilizados como precursores (Tashima et al 2012).

Entre otros como activador alcalino se suele utilizar el silicato sódico, que tiene una elevada huella de carbono. El silicato sódico puede ser sintetizado a partir de mezclas de CCA e hidróxido sódico, reduciendo considerablemente de esta forma las emisiones de CO_2 (Mellado et al 2014).

Los activadores alcalinos para la síntesis de geopolímeros pueden ser preparados a partir de mezclas de CCA con NaOH sometidos a reflujo. La activación de FCC con CCA y NaOH, produce morteros con resistencias a compresión, en el rango de entre 31 y 41MPa, que es similar a la resistencia a la compresión de morteros de control preparados usando una mezcla de silicato sódico comercial y NaOH. Estos resultados pondrían de manifiesto, la posibilidad de utilizar dos materiales de desecho en los cementos alcalinamente activados de forma simultánea: CCA para el activador alcalino y FCC como el material precursor, reduciendo el coste económico y medioambiental en la producción de geopolímeros (Bouzón 2014).

El cemento activado alcalinamente obtenido mediante el uso de FCC como precursor y mezclas de CCA y NaOH como activador, se utiliza en

lugar del CP en la estabilización de suelos para bloques y su posterior uso en la construcción de viviendas.

4.2.3.Resultados

4.2.3.1. Influencia del tipo de estabilizador

En la Figura 4.2-1 se muestra la variación de la resistencia a compresión con el tiempo de curado para bloques de tierra comprimidos estabilizados con CP tipo CEM I 52,5R, bloques estabilizados con geopolímero y bloques sin estabilizar.

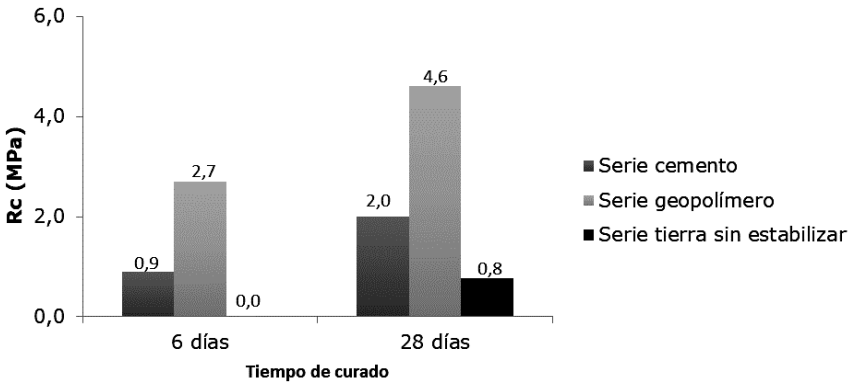

Fig. 4.2-1 Variación de la resistencia a compresión con el tipo de estabilizador y el tiempo de curado.

Los resultados ponen de manifiesto en primer lugar, que la resistencia a compresión es netamente superior, para todos los tiempos de curado, en los bloques estabilizados con geopolímero. Los porcentajes de incremento de la resistencia a compresión sobre los bloques estabilizados con CP para un mismo tiempo de curado oscilaron entre el 127% y el 264% dependiendo de éste. Este hecho pondría de manifiesto

el mejor comportamiento del geopolímero frente al CP para todos los tiempos de curado estudiados.

Para 28 días de curado, también se realizó una serie de bloques de tierra comprimida sin estabilizar. Los resultados que se muestran en la figura ponen de manifiesto, como cabía esperar, mucha menor resistencia para éstos frente a los bloques estabilizados con cemento Portland o geopolímero.

De esta forma para 28 días de curado, la resistencia a compresión de los bloques estabilizados con geopolímero fue 5,9 veces superior a la de los bloques sin estabilizar, y la resistencia a compresión de los bloques estabilizados con cemento Portland fue 2,6 veces superior a la de los bloques sin estabilizar.

Estos resultados pondrían de manifiesto las sustanciales mejoras que supone la estabilización del suelo.

4..2.3.2. Estudios preliminares de durabilidad

De acuerdo a la norma UNE 41410 y UNE-EN 772-1 los bloques se secaron en estufa a 105ºC hasta peso constante, posteriormente se dejaron enfriar y finalmente se ensayaron mecánicamente para obtener la resistencia compresión.

En la Figura 4.2-2 se representa la resistencia a compresión frente al tipo de estabilizante (cemento Portland, geopolímero y sin estabilizante), para los bloques secados en las condiciones indicadas anteriormente. La tendencia observada coincide con los resultados obtenidos en el apartado 3.1 para los 28 días de curado, en el que los bloques se secaron en ambiente de laboratorio. La resistencia a compresión de los

bloques estabilizados con CP y geopolímero fue 2,5 y 10,1 veces superior respectivamente respecto a la del suelo sin estabilizar. Se volvió a constatar que la resistencia a compresión de los bloques estabilizados con geopolímero fue muy superior a la de los bloques estabilizados con CP (en este caso cuatro veces superior).Para estudiar el comportamiento de los bloques de tierra estabilizados en climas húmedos, los bloques que previamente habían sido llevados hasta peso constante en estufa, se sumergieron en agua durante 2 horas siguiendo la normativa colombiana NTC 5324. Posteriormente se realizó el ensayo de resistencia a compresión, obteniendo la resistencia mecánica húmeda de los bloques. Los resultados obtenidos se muestran en la Figura 4.2-2, en la que se representa la resistencia a compresión frente al tiempo de inmersión en agua, para los bloques estabilizados con CP, con geopolímero y sin estabilizar.

Estos resultados ponen de manifiesto en primer lugar, que la inmersión en agua durante dos horas supone una reducción drástica de la resistencia a compresión para los tres tipos de bloques. Los bloques de tierra estabilizados con CP redujeron su resistencia a compresión en un 54,2%, los bloques de tierra estabilizada con geopolímero redujeron su resistencia a compresión en un 61,1%, y finalmente los bloques de suelo sin estabilizar se desintegraron en el agua perdiendo el 100% de su resistencia a compresión.

Se pone nuevamente de manifiesto que los bloques de tierra estabilizados con geopolímero dieron los valores de resistencia a compresión más altos. La resistencia a compresión de éstos fue 3,4 veces más alta que la de los bloques estabilizados con CP, si bien el porcentaje de reducción de la resistencia como consecuencia de la inmersión fue superior a la de los bloques estabilizados con cemento Portland (61,1% frente a 54,2%).

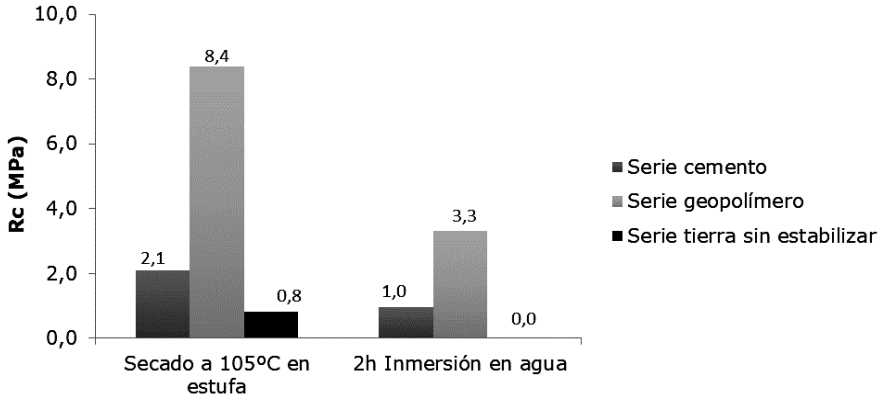

Fig. 4.2-2 Variación de la resistencia a compresión con la inmersión en agua durante 2h.

4.2.3.4. Coste económico

Para calcular el coste de producción, se considera nulo el coste del FCC, ya que se trata de un residuo y no tiene actualmente valor comercial. Así mismo, el coste de la CCA puede considerarse también nulo, ya que podrían ser los propios habitantes de zonas agrícolas quienes realizasen la labor de autoconstrucción, obteniendo por tanto ellos mismos la CCA a partir de la cascara de arroz. No obstante, si las zonas dónde se va realizar la construcción está alejada de los puntos de producción de los residuos deberían tenerse en cuenta los costes de transporte. La combustión podría realizarse de forma aislada o integrada en otros procesos en los que se aprovechase la cascara de arroz como combustible (cocina, calefacción, etc.). Para la fabricación de la solución activadora se utilizó un sistema que aislaba térmicamente y facilitaba la reacción de síntesis del silicato sódico. En la estimación de costes no consideramos la mano de obra, al tratarse de proyectos de cooperación al desarrollo basados en la premisa de autoconstrucción de las viviendas

por los propios beneficiarios. En este tipo de proyectos, habitualmente los beneficiarios aportan la mano de obra, y el gobierno local o la organización no gubernamental correspondiente el coste de los materiales y la parcela sobre la que se construirá la vivienda (Lizan 2013).

El volumen que ocupa un bloque una vez comprimido es 15cm x 30cm x10.5cm = 4725 cm^3, calculamos el número de bloques que serían necesarios emplear en 1 m^3, resultando un total de 211 bloques. Con este dato podemos calcular los Kg necesarios de material para ocupar un volumen de 1 m^3. En la siguiente tabla se muestran los costes unitarios aproximados y el coste total de los materiales empleados en la fabricación de 211 bloques de suelo estabilizado con geopolímero.

Tab. 4.2-1 Coste de producción de 1m^3 de suelo estabilizado con geopolímero

Material	Cantidad	Coste unitario	Costes Parciales
Tierra	1587,30 kg	0,00 €/kg	- €
FCC	158,70 kg	0,00 €/kg	- €
H_2O	0,23 m^3	0,80 €/m^3	0,18 €
CCA	66,70 kg	0,00 €/kg	- €
NaOH	68,60 kg	0,31 €/kg	21,30 €
Total			**21,48 €**

Se ha tomado como precio del cemento el coste de un saco de 50 Kg de cemento gris de la empresa colombiana Argos, que estaba en 19,69€, lo que equivaldría a un coste de 0,39€/Kg.

Tab. 4.2-2 Coste de producción de 1m^3 de suelo estabilizado con cemento Portland

Material	Cantidad	Coste unitario	Coste Parciales
Tierra	1587,30 kg	0,00 €/kg	- €
CP	158,70 kg	0,39 €/kg	61,89 €
H_2O	0,17 m3	0,80 €/m3	0,14 €
Total			**62,03 €**

Por tanto, en este caso el coste de un solo bloque sería aproximadamente de 0,3€, triplicando el coste de un bloque estabilizado con cemento activado alcalinamente (Alamán 2014).

4.2.4. Logros

4.2.4.1. Reducción de gases de efecto invernadero

Reducir el impacto ambiental por gases de efecto invernadero, concretamente las emisiones de CO_2 que conforma el 55% de estos gases. Para ello se sustituye el principal conglomerante utilizado en la actualidad, el CP causante de entre el 5 y el 7% del total de las emisiones de CO_2, por un cemento más amigable medioambientalmente, y por tanto con menor huella de carbono.

4.2.4.2. Uso de recursos sostenible

Uso más eficiente de los recursos, utilizando materiales considerados actualmente como residuos, como es el caso del FCC y la CCA con el consiguiente ahorro económico y medioambiental, consiguiendo además una mejora de las propiedades mecánicas y de durabilidad de los materiales obtenidos. Llegando a ser el coste de un BTC estabilizado con geopolímero, un tercio del coste de uno estabilizado con CP.

4.2.4.3. Nuevas oportunidades de negocio

Así mismo, también se presenta la posible creación y desarrollo de nuevos nichos de negocio para los países de implantación, como la fabricación de la disolución activadora, o la asesoría en el nuevo campo de los cementos más amigables medioambientalmente fabricados con residuos.

Además de otras fuentes de negocio indirectas como la posible industrialización de bloques prefabricados, o la distribución y venta de los hasta ahora considerados residuos (FCC y CCA).

4.2.4.4.Aplicación práctica

Tanto la falta de vivienda como la gestión de los residuos, son problemas muy acuciantes en los países en desarrollo. Se propone la posibilidad de utilizar materiales residuales en la preparación de cementos más amigables medioambientalmente para la construcción de viviendas sociales.

Retos fundamentales, por un lado, la conservación del medio ambiente, lo que implicaría una buena gestión de los residuos producidos entre los que se encuentran el residuo de catalizador del craqueo catalítico FCC y la ceniza de cáscara de arroz CCA. Por otro lado, la construcción de viviendas sociales, mediante el impulso de políticas para reducir el enorme déficit de viviendas sociales existente.

4.2.4.5. Innovación

El proyecto pretende el uso de precursores y activadores alcalinos obtenidos a partir de residuos, demostrándose más favorable desde el punto de vista económico y medioambiental.

Por otra parte, cabe resaltar el uso como precursor del FCC, obteniendo un comportamiento mecánico en bloques de suelo estabilizado superior al que presenta el CP.

Por un lado, la gestión adecuada de residuos para la obtención de cementos de activación alcalina y por otro, la elaboración de materiales prefabricados, a partir de estos cementos de activación alcalina para su uso en viviendas sociales.

4.2.5. Conclusiones

La utilización de un cemento activado alcalinamente y/o geopolímero, obtenido a partir de residuos, se considera una solución viable desde el punto de vista económico y medioambiental para la estabilización de bloques de suelo comprimido. Los residuos utilizados fueron catalizador de craqueo catalítico usado (FCC), como precursor y una mezcla de ceniza de cáscara de arroz (CCA) e hidróxido sódico como activador. La resistencia a compresión de los bloques estabilizados con el cemento activado alcalinamente fue netamente superior a la resistencia de los bloques estabilizados con cemento portland. En cuanto a los estudios preliminares de durabilidad, se observó también un mejor comportamiento de los bloques después de su inmersión de dos horas en agua. Finalmente indicar que tanto el coste económico como el coste medioambiental fueron inferiores para los bloques de suelo estabilizado con el cemento activado alcalinamente. Así pues podemos concluir que el estudio realizado abre la puerta a la posibilidad de utilizar los cementos activados alcalinamente obtenidos a partir de materiales residuales como FCC y CCA en la estabilización de bloques de suelo comprimido para uso en países en desarrollo.

4.2.6. Posibles direcciones de futura investigación

Entre algunas de las posibles líneas de investigación futura, se encuentran, el aprovechamiento de residuos industriales con alto contenido en NaOH para abaratar aún más el coste económico y medioambiental del activador, así como la optimización de los diferentes componentes de la dosificación.

Referencias

1. Acosta F, Alfonso F, Aguirre I, Barrenche S, Bene E (2008), Materiales alternativos: tierra/paja. Construccion III.

2. Alamán M (2014), Estudio para la estabilización de bloques de tierra mediante la utilización de geopolímeros a partir de residuos. aplicación para viviendas de bajo coste en barranquilla (Colombia). Proyecto Final de Carrera. Universidad Politecnica de Valencia.

3. Amnistía Internacional (2015). https://www.es.amnesty.org/temas/desc/vivienda/, fecha de consulta 10 Julio 2015.

4. Auroville Earth Institute, Earthen architecture for sustainable habitat and compressed stabilised earth block technology, [fecha de consulta: 17 de Mayo de 2014], www.earth-auroville.com

5. Bouzón N, Payá J, Borrachero MV, Soriano L, Tashima MM, Monzó J (2013), Refluxed rice husk ash/NaOH suspension for preparing alkali activated binders, Materials Letters, 115 (2014) 72–74.

6. Day RL (1992), Pozzolans for use in low-cost housing. A state of the art report. Research Report CE92-1, University of Calgary, Alberta, Canadá, pp. 87-95.

7. Gartner E (2004), Industrially interesting approaches to "low-CO_2" cements, Cement and Concrete Research. 34 (2004) 1489–1498.

8. González AM (2012), Técnica constructiva con tierra compactada, tecnología sostenible sin explorar. TRAZA N° 5, enero-junio 2012 / 100-107 / ISSN 2216-0647

9. Lizan J (2013), Utilización de residuos en hormigones geopoliméricos para uso en bloques de bajo coste económico y medioambiental. Proyecto Final de Carrera, Universidad Politécnica de Valencia.

10. Martirena JF (2004), Una alternativa ambientalmente compatible para disminuir el consumo de aglomerantes de clinker de cemento Portland: El aglomerante cal-puzolana

como adición mineral activa. Tesis Doctoral, Universidad Central Marta Abreu de las Villas (UCLV).

11. Mellado A, Catalán C, Bouzón N, Borrachero MV, Monzó J, Payá J (2014), Carbon footprint of geopolymeric mortar: study of the contribution of the alkaline activating solution and assessment of an alternative route, RSC Adv. 2014, 4, 23846.

12. Monzó J. (2012), Conferencia Cátedra Cemex-sostenibilidad, Materiales y tecnologías constructivas no convencionales: uso en países en vías de desarrollo, ICITECH.

13. Norma Técnica Colombiana NTC 5324, Bloques de suelo cemento para muros y divisiones, definiciones, especificaciones, métodos de ensayo y condiciones de entrega.

14. Noticias de la ciencia y la tecnología: http://noticiasdelaciencia.com/not/16258/nueva-tecnica-con-balance-neutro-de-emisiones-de-co2-para-fabricar-cemento/ (fecha de consulta 18 de mayo de 2016)

15. ONU (1987), Our common Future: Brundtland Report.

16. ONU, objetivos desarrollo sostenible, Agenda 2030 para el desarrollo sostenible: http://www.undp.org/content/undp/es/home/sdgoverview/post-2015-development-agenda.html, [fecha de consulta: 10 de Julio de 2015],

17. RPP noticias, ciencia y tecnología (2014), OMM: Concentración de CO_2 alcanza nivel récord en hemisferio norte.

18. Salas J (2010), Reflexiones sobre la enseñanza y la investigación tecnológica para la vivienda de las mayorías, pp.121-131, [fecha de consulta: 2 de Mayo de 2014], http://www. habitatysociedad.us.es

19. Tashima M.M, Akasaki J.L, Castaldelli V.N, Soriano L., Monzó J., Borrachero M.V, Payá J., (2012),New geopolymeric binder base on fluid catalytic cracking catalyst residue (FCC). Materials Letters 80, 50-52.

20. UNE-EN 41410: (2008), Bloques de tierra comprimida para muros y tabiques. Definiciones, especificaciones y métodos de ensayo.

21. UNE-EN 772-1 (2011), Métodos de ensayo de piezas para fábrica de albañilería. Parte 1: Determinación de la resistencia a compresión.

22. Vanderley MJ (2002), On the sustainability of the Concrete. Extended version of the paper commissioned by UNEP Journal Industry and Environment.

4.3 Comunicación oral presentada en la 10th International Conference on the Environmental and Technical Implications of Construction with Alternative Materials WASCON en Tampere (Finlandia), con el título: Soil stabilization using geopolymers obtained from wastes

Fecha del congreso anual	08/06/2018
Pág.	47-52
ISBN / ISSN	978-951-758-631-3 - 0356-9403

Juan Cosa, Lourdes Soriano, Mª Victoria Borrachero, Jorge Juan Payá. Poner la cita completa del congreso

Abstract: Soil stabilization is a technique based on the use of a binder, which is able to improve the bonding of soil particles, increasing the mechanical properties and durability. The binders usually used are lime, portland cement, and lime-pozzolan mixtures. All these binders, primarily portland cement, have a high carbon footprint. It is estimated that the production of one ton of portland cement generates approximately one ton of carbon dioxide. Research is currently being carried out into the development of binders whose production generates fewer greenhouse gases. This research it´s oriented towards the achievement of the Sustainable Development Goals, and would be fundamentally focused on the 11 goal (sustainable cities and communities), and the 13 goal (climate action). These binders are called alkali-activated cements, or geopolymers. These new binders consist of a precursor, which is a silicon-aluminous material and an activator, which is a high alkaline solution. The binding of precursor and activator favours the development of a range of chemical reactions whose products have cementing properties. More recently, research in the field of alkali-activated cements has focused on the use of waste materials in the composition of

precursors and / or activators. This would mean an even greater reduction in the production of greenhouse gases. In the research carried out, has been used as a precursor the spent catalytic cracking catalyst (FCC), which is a residue of the petroleum industry. Different residues such as rice husk ash (RHA), rice straw ash (RSA) and brew filtration material (BFW) have also been used in the composition of the alkali activator. Stabilized soil samples of 4cmx4cmx4cm were prepared and cured for 7 and 90 days at a temperature of 22ºC and relative humidity of 50%. The results of compressive strength showed the good mechanical behaviour of the stabilized soil. In none of the tested specimens were obtained mechanical strengths below 10 MPa. In the experiments in which FCC was used as a precursor, the highest compressive strengths were obtained using the composition of the activator RHA and BFW, where they exceeded 20 MPa. In these latter two cases, the mechanical strengths obtained were higher than the control specimens in which portland cement had been used as a binder. The results obtained allow us to hope for the use of geopolymers obtained from waste as a viable and more sustainable environmental option for soil stabilization.

Keywords: Sustainable Construction Materials, Waste Reuse, Alkali Activated Cement, Soil Stabilization.

4.3.1. Introduction

The soils stabilization consists of the incorporation of additives to the soil, so that they act physically or chemically on the properties of this. Although the mixture of two soils is also called stabilization, this process is called mechanical stabilization, in which the soil to be improved is mixed with another soil, which contributes to the properties of the former. For this case, we are interested in chemical stabilization, where the most used procedures are stabilization with lime, and more commonly with

portland cement [1-3]. Currently, the research focuses on the use of materials as an alternative to portland cement (OPC), in order to mitigate the environmental impact produced in its manufacture.

The geopolymers or alkaline activated cements (AAC) could respond to these needs, since they have been shown in various studies to be a good substitute for OPC [4-6]. The alkaline activation cements are based on the activation by alkaline solution of a precursor material of silicoaluminous nature. There are not much literature on soil stabilization with this type of binder, but existing studies give comparable results to OPC [7-9].

When a solution made from commercial sodium silicate (SIL) is used for the activation, there is an economic disadvantage of the AAC with respect to the OPC, however, if waste is used as a silica source to replace this commercial sodium silicate, it is markedly reduced the environmental and economic impact.

In this sense, there are several studies, in which waste is reused as a source of silica [10-12], the waste used must be rich in silicon oxide capable of reacting with sodium hydroxide, to achieve the formation of sodium silicate. Rice husk ash (RHA) has precedents of AAC with good results in soil stabilization [13].

The research work reuses residues such as the FCC in the stabilizer and BFW, RSA and RHA for alkaline activation. The compressive strength will be compared with soil without stabilizer, and it will be stabilized with OPC as control, whereas the FCC activates with SIL as control for AAC.

4.3.2. Method and materials

A sample of 25kg of soil is taken and a homogeneous intake is made by the technique of quartering in divisions of 1 kg for the different batching.

The selected soil is passed through # 4mm sieve and dried in an oven at 60ºC until constant weight. Mini proctor modified according to the UNE 103 501 standard, was made to soil with different stabilizers to know its optimum dry density.

To perform the kneading without stabilizer, 1000g of soil is first introduced into the mixer, where one minute is mixed, then the water is added gradually while kneading, and it is left to knead two more minutes.

To perform the kneading with OPC, 1000g of soil is first introduced into the mixer, where one minute is mixed, then the OPC is added, and another minute is allowed to mix, finally, the water is added gradually while kneading, and it is left to knead two more minutes.

To perform the kneading with AAC, 1000g of soil is first introduced into the mixer, where one minute is mixed, then the stabilizer is added, and another minute is allowed to mix, finally, the solution is added gradually, and knead two more minutes.

Cubic samples of 40x40x40mm are made, in 3 layers of filling with the same procedure used in the modified proctor, a mass of 1.5kg is dropped from 20 cm in height, with 19 blows for compaction. For curing, they are kept for 7 or 90 days in controlled temperature and humidity chamber at 22ºC and 50%H FCC was supplied by OMYA Clariana, OPC was supplied by LAFARGE. For the RSA, the straw was burned in a burner designed and built at the Universitat Politècnica de València (UPV), in order to obtain ashes of high reactivity. The BFW was supplied by Heineken, and the RHA was supplied by DACSA.

4.3.3 Characterization

4.3.3.1. Field emission scanning electron microscopy (FESEM)

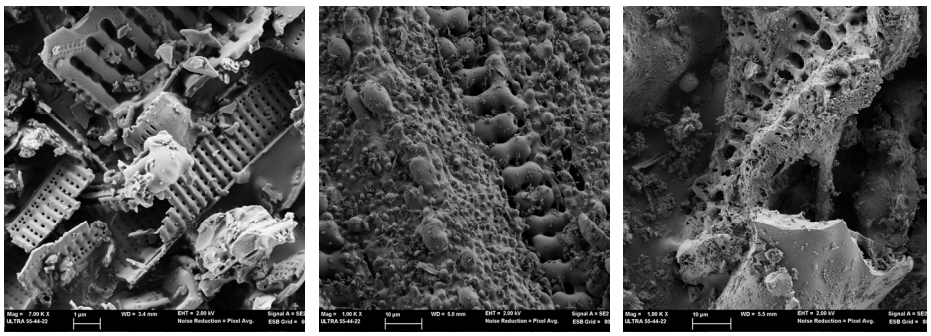

BFW RSA RHA

Fig. 4.3-1 Field emission scanning electron images of BFW, RSA and RHA. Higher magnification.

In BFW are appreciated the typical diatomaceous earth forms with flat parts in the form of grid with numerous micropores. In the RSA you can see phytoliths, in the shape of 8 that were also found in the RHA; where you can also see the inner part of the husk, constituted by a large quantity of ducts in the form of tunnels, which would suppose an increase of the specific surface of the material.

4.3.3.2. X-Ray fluorescence

Tab. 4.3-1 Composition in percentage of oxides of the materials used measured by x-ray fluorescence * loss on ignition, determined at 950ºC

	SiO_2	Al_2O_3	Fe_2O_3	CaO	MgO	SO_3	K_2O	Na_2O	P_2O_5	TiO_2	Cl^-	Others	LOI*
OPC	20,80	3,60	4,80	65,60	1,20	1,70	1,00	0,07	-	-	-	-	1,23
FCC	47,76	49,26	0,60	0,11	0,17	0,02	0,02	0,31	0,01	1,22	-	-	0,51
RSA	52,44	0,47	0,17	8,01	2,71	2,26	12,05	0,89	2,58	-	3,52	0,29	14,60
BFW	81.70	5.67	3.71	1.28	0.47	--	0.86	1.30	0.36	0.93	--	0.38	3.34
RHA	85,58	0,25	0,21	1,83	0,5	0,26	3,39	-	0,67	-	0,32	-	6,99

As can be seen in table 4.3-1, the activator silica content is, 52.44% for RSA, around 90% in the case of BFW and RHA. As will be seen later, these percentages will be related to the amount of sodium silicate that will be formed when reacted with sodium hydroxide, which will be the geopolymerization reaction activator. The amount activator present will have a direct relationship with the obtained mortars compressive strength.

4.3.3.3. Mineralogical composition (XRD spectra)

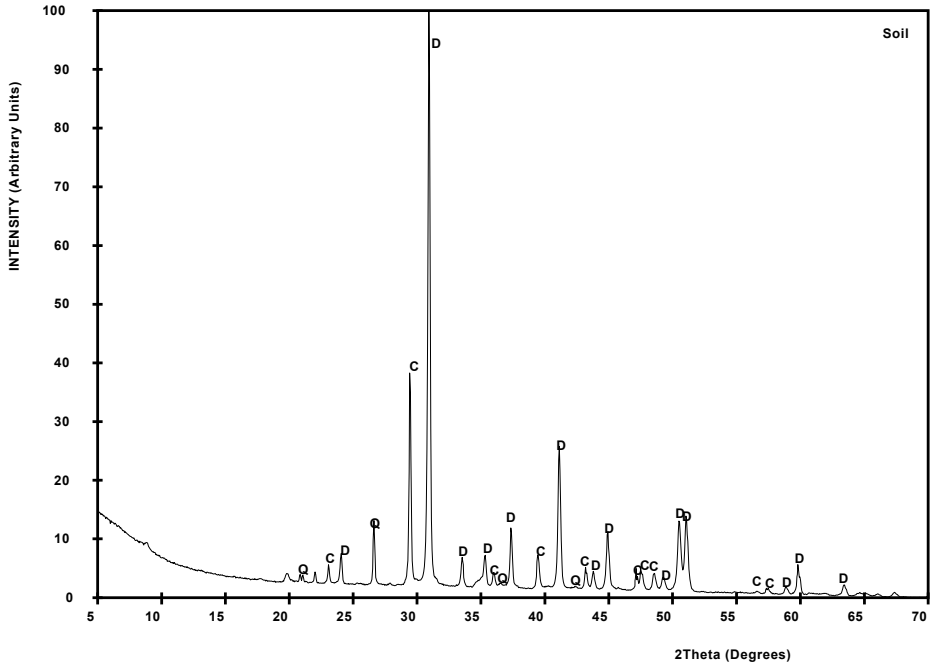

Fig. 4.3-2**.** Soil, Mineralogical composition. *D (Dolomite, $CaMg(CO_3)_2$), C (Calcite, $CaCO_3$), Q (Quartz, SiO_2)*

The soil used is mostly dolomitic, with calcite and quartz traces.

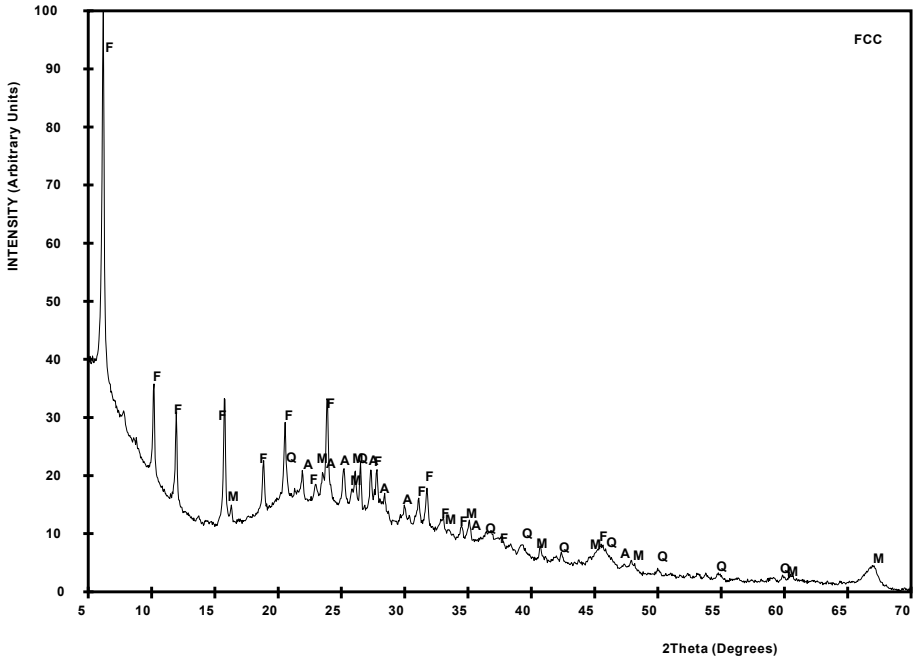

Fig. 4.3-3 Mineralogical composition FCC: *F (Faujasite, $Na_2Al_2Si_4O_{12}.8H_2O$), Q Quartz (), M (Mullite, $Al_6Si_2O_{13}$), A (Albite, $NaAlSi_3O_8$)*

The FCC used as a precursor has an amorphous character (deviation from the baseline) but also with peaks of crystalline materials, mainly a zeolite. Faujasite. As secondary components are silicates such as mullite, quartz and feldspars such as albite.

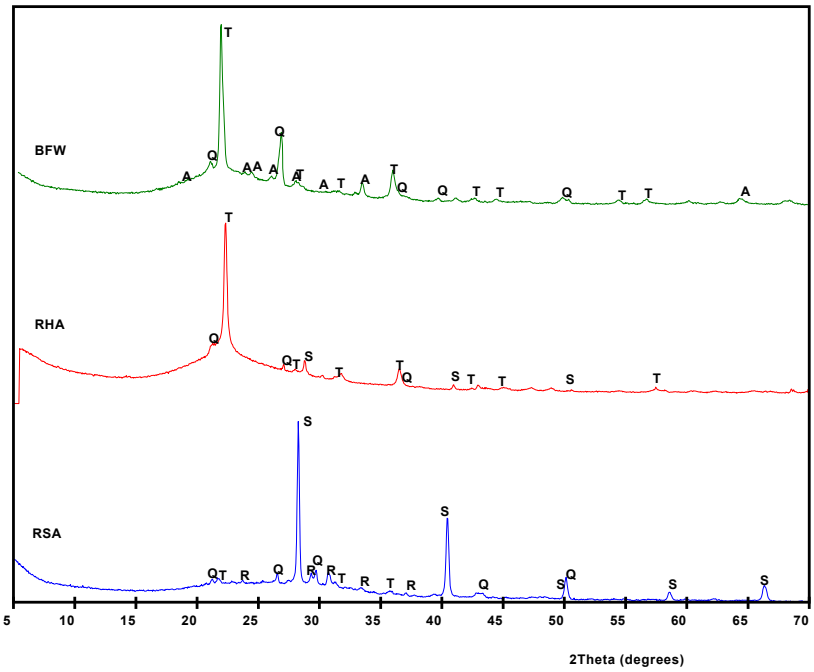

Fig. 4.3-4 Mineralogical composition.: *Q (Quarz, SiO_2), T (Cristobalite, SiO_2), S (Silvine, KCl), R (Arcanite, K_2SO_4), A (Anorthite, $CaAl_2Si_2O_8$)*

The activators used are BFW, RHA and RSA. RHA, with a very amorphous character, with small peaks of crystalline silica in cristobalite form. Presence of quartz is attributed to soil impurities between the husk. The alkalis present are in the form of KCl traces. On the other hand, the RSA also presents cristobalite, but its alkali content is important. It is detected as chlorides (KCl, silvina) and sulfates (K_2SO_4, arcanite). Finally, the BFW sample presents silica in cristobalite form and quartz form, with small anortite traces type feldspars.

4.3.4. RESULTS

4.3.4.1. Compressive strength (CS)

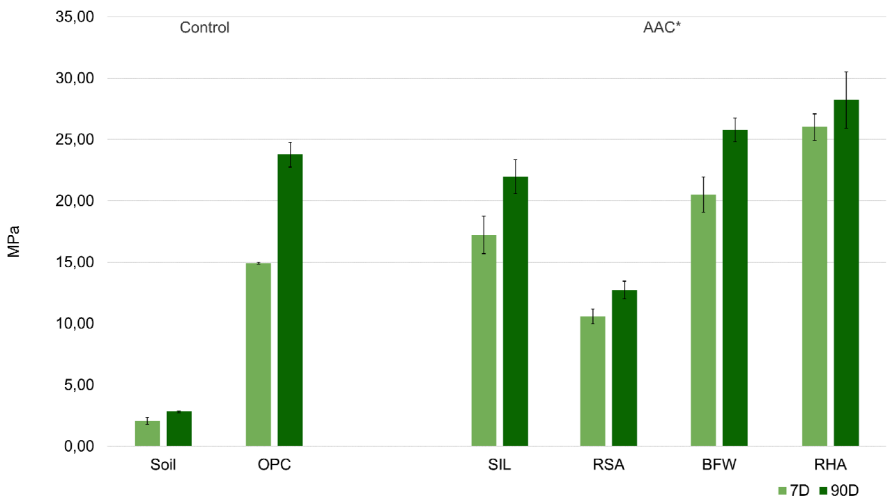

Fig. 4.3-5 Compressive strength results, to 7 and 90 days of soil without stabilizer (Soil), soil stabilized with OPC and soil stabilized with AAC, with FCC as precursor, and different activators, SIL, RSA, BFW and RHA.

As can be seen in figure 4.3-5, the soil without stabilizers offers an approximate 3 MPa CS, the soil stabilized with 10% OPC as a control stabilizer, reflects a result about 24 MPa. On the other hand, stabilized soils with 10% AAC offer values, between 13 MPa, up to 28 MPa for the same 90 days. From the above results, it is deduced that all the stabilizers based on FCC, improve the soil without stabilizer, as can be expected. Furthermore, in the stabilization by alkaline activation, it is possible to improve the CS results obtained with the OPC, for those activators whose silica content is equal to, or greater than 90%. In the

case of the use of rice straw ash, whose silicon oxide content is 52.4%, lower CS is obtained, but the soil strength without stabilizer is multiplied by 4, and would allow, for example, its use as stabilized soil in road paving.

4.3.5. Conclusions

The results obtained demonstrate the feasibility of the use of residues such as RSA, BWF and RHA in the activators preparation for the alkaline activation reaction. Likewise, the feasibility of using another residue, the FCC as a precursor in the alkaline activation reaction, is also confirmed. In this way, except for sodium hydroxide, the rest of the materials used in the preparation of the alkaline activated cement would be waste, thus reducing the carbon footprint of the binder used in the soil stabilization.

The results obtained show a correlation between the silica content of the activator (RSA, BFW and RHA) and the compressive strength of the stabilized soil. The compressive strength in all cases would be sufficient for use in road surfaces, demonstrating the possibility of using AAC instead of portland cement as a binder in soils stabilization.

References

1. Khadka B., Shakya M. Comparative compressive strength of stabilized an un-stabilized rammed earth. Materials and Structures, vol 9, nº 49, pp 3945-3955, 2016.

2. Alrubaye A.J., Hassan M., Fattah M-Y. Stabilization of soft kaolin clay with silica fume and lime. International Journal of Geotechnical Engineering, vol 11, nº1, pp 90-96, 2017.

3. Rios S., Viana da Fonseca A., Baudet B. Effect of the porosity/cement ratio on the compression of cemented soil. Journal of Geotechnical and Geoenvironmental Engineering, vol 138, nº11, pp 1422-1426, 2012.

4. Marinkovic S., Dragas J., Ignjatovic J., Tosic N. Environmental assessment of green concretes for structured use. Journal of Cleaner Production, vol 154, pp 633-649, 2017.

5. Tashima M.M., Akasaki J.L., Castaldelli V.N., Soriano L., Monzó J., Borrachero M. V, et.al. New geopolymeric binder base on fluid catalytic cracking catalyst residue (FCC). Materials Letters, vol 80, pp 50-52, 2012.

6. Huiskes DMA., Keulen A, Yu QL., Brouwers HJH. Design and performance evaluation of ultra-lightweight geopolymer concrete. Materials and Design, vol 89, pp 516-526, 2016.

7. Zhang M., Guo H., El-Korchi T., Zhang G. Tao M. Experimental feasibility study of geopolymer as the next-generation soil stabilizer. Construction and Building Materials, vol 47, pp 1468-1478, 2013.

8. Rios S., Cristelo N., Viana da Fonseca A., Ferreira C. Stiffness behaviour of soil stabilized with alkali-activated fly ash from small to large strains. International Journal of Geomechanics, vol 17, noº 3, pp 1-12, 2017.

9. Zhang M., Zhao M.X., Zhang G.P., Nowak P., Coen A., Tao M.J. Calcium-free geopolymer as a stabilizer for sulfate-rich soils. Applied Clay Science, vol 108, pp 199-207, 2015.

10. Bouzón N., Payá J., Borrachero M.V., Soriano L., Tashima M.M., Monzó J. Refluxed rice husk ash/NaOH suspension for preparing alkali activated binders. Materials Letters, vol 115, pp 72–74, 2014.

11. Mejía J.M., Mejía de Gutiérrez R., Montes C. Rice husk ash and spent diatomaceous earth as a source of silica to fabricate a geopolymeric binary binder. Journal of Cleaner Production, vol 118, pp 133-139, 2016.

12. Puertas F., Torres-Carrasco M. Use of glass waste as an activator in the preparation of alkali-activated slag. Mechanical strength and paste characterization. Cement and Concrete Research, vol 57, pp 95-104, 2014.

13. Alamán M. Estudio para la estabilización de bloques de tierra mediante la utilización de geopolímeros a partir de residuos. Aplicación para viviendas de bajo coste en Barranquilla (Colombia). Proyecto Final de Carrera. Universitat Politècnica de València, 2014.

4.4 Comunicación oral presentada en la 17th International Conference on Non-conventional Materials and Technologies NOCMAT en Mérida (México), con el título: Use of alkaline activated cements from residues for soil stabilization

Fecha del congreso anual	30/11/2017
Pág.	355-364

Juan Cosa Martínez, Lourdes Soriano Martínez, María Victoria Borrachero Rosado, Jorge Juan Payá Bernabeu, José María Monzó Balbuena

Keywords: Sustainable construction materials, Waste reuse, Alkali activated cement, Soil stabilization.

Abstract. In recent decades, Portland cement (OPC) production has grown significantly as a result of economic and population growth. However, the cement industry is classified as a highly polluting sector and of great environmental impact. The production of one tonne of OPC requires the exploitation of a high volume of raw materials (mainly limestone and clay) and the emission of one tonne of CO_2 and other polluting gases (NOx and SOx). The OPC is the most used binder in soil stabilization, one of the alternatives with less environmental impact, is the use of so-called alkaline activated cements (AAC) and / or geopolymers. In the research work, is used a fluid catalytic cracking catalyst (FCC) residue as a precursor and a mixture of rice straw ash (RSA) and sodium hydroxide as activator. Reducing the economic and environmental cost, making it viable in developing countries. To obtain the RSA, a burner has been designed and built in which the rice straw is transformed into RSA. During the burning process, the different burning zones and their temperatures were studied. The objective of these measurements is to

obtain the optimum quality RSA to synthesis of the alkaline activator in the geopolymerization reaction. The AAC was used for soil stabilization, the compressive strengths were obtained for ages between 7 and 90 days. Soils were stabilized with OPC and AAC, and the results were compared, being higher the results with OPC. However, the compressive strengths obtained with the AAC were sufficient for the stabilization of the soils.

4.4.1. Introduction

Is called stabilized soil to the homogeneous mixture of a soil with a binder and eventually water, which a suitably compacted to acquires sufficient strength and stiffness to support the load for which it has been designed. The commonly used binders are OPC and lime. There are several applications in civil engineering and also in architecture, such as road stabilization or building blocks for housing.

There are numerous studies about the use of cement or lime as soil stabilizers from the last century to the present [1-3], therefore, it is a field well studied and characterized. But in the last decades, researchers are focusing their efforts on using alternative building materials to Portland cement (OPC), to improve above all the environmental impact that involves the OPC manufacture.

Within this type of alternative materials, we can find so-called alkaline activated cements or geopolymers. These materials are based on the reaction of a silicoaluminous nature source with a solution of high alkalinity (activator). These materials have very good mechanical performance and in many fields can be an ideal substitute for OPC [4-6]. There are not many studies that use geopolymers as soil stabilizers, however, the studies that are emerging show very good results comparable to those obtained by OPC [7-9].In the field of soil stabilizers,

the use of geopolymers may has an economic disadvantage, since some times its use it requires an additional cost because the activator, this can make the final mixture more expensive. This problem can be solved by using as much waste as possible in the preparation of the geopolymer making it economically viable and environmentally friendly.

There are several research groups worldwide reusing residues to try to obtain a sodium silicate alternative to commercial [10-12]. For this, residues rich in silicon oxide are sought that are capable of reacting with the sodium hydroxide, forming sodium silicate. Among these studied residues is the rice husk ash (RHA), a residue that has obtained very positive results in studies with soils stabilized with geopolymers [13].

The present article wants to explore the possibility of using RSA in this type of mixtures based on the results of the RHA. The straw will be burned in a burner designed and built at the Universitat Politècnica de València (UPV), in order to obtain ashes of high reactivity.

4.4.2. Experimental

Materials. As is mentioned above, it is possible to stabilize soils with cement or geopolymer, using different materials that will be described briefly below. A OPC was used for cement stabilization, its oxides composition is shown in Table 4.4-1. In the geopolymer-stabilized soils the fluid catalytic cracking catalyst (FCC) residue is used as precursor material, its composition is shown in Table 4.4-1. To activate said material there are two preparation routes. The first route is the use of an activator solution formed by NaOH / Na_2SiO_3. The second one is the use of the RSA as a source of silica, which is reacted with NaOH for the formation of the sodium silicate.

The composition of the RSA is also shown in Table 4.4-1. It should be noted that the percentage of silica in the RSA exceeds 50%, a positive data for its use as a source of silica. This percentage is lower than the RHA (≅90%) which is the material previously studied in this type of mixtures, so its effectiveness is expected to be lower.

The FCC was supplied by the company OMYA Clariana and the RSA is obtained in the burner designed and located in the Universitat Politècnica de València (UPV). The FCC is factory milled having an average diameter of 18 microns while the RSA needs to be milled before use. For this, a Roller 1 jars mill is used where an average diameter of 40 microns is obtained. Subsequently, a ball mill model Nannetti Speedy1 is used where its average diameter is reduced to 13 microns.

Tab. 4.4-1 Composition in percentage of oxides of the materials used measured by x-ray fluorescence * loss on ignition.

	SiO_2	Al_2O_3	Fe_2O_3	CaO	MgO	SO_3	K_2O	Na_2O	P_2O_5	TiO_2	Cl^-	Others	LOI*
OPC	20,80	4,60	4,80	65,60	1,20	1,70	1,00	0,07	-	-	-	-	2,02
FCC	47,76	49,26	0,60	0,11	0,17	0,02	0,02	0,31	0,01	1,22	-	-	0,51
RSA	52,44	0,47	0,17	8,01	2,71	2,26	12,05	0,89	2,58	-	3,52	0,29	14,60

Methodology. An important part of investigation development about the use of RSA has been the design of the burner for RSA obtaining. The burner construction has been carried out in the facilities of the UPV, with an approximate capacity of $3m^3$ of biomass. The burner consists of concrete blocks forming a ring, with holes opening between blocks to supply oxygen to the combustion, a metal sheet cover composed of two parts is arranged in order to facilitate the fumes, preventing in turn, the output of particles from the combustion. At one meter in height, two metal

plates are placed, one to house the biomass and the other as a door, both perforated to allow the entrance of oxygen. Figure 4.4-1 shows the burner.

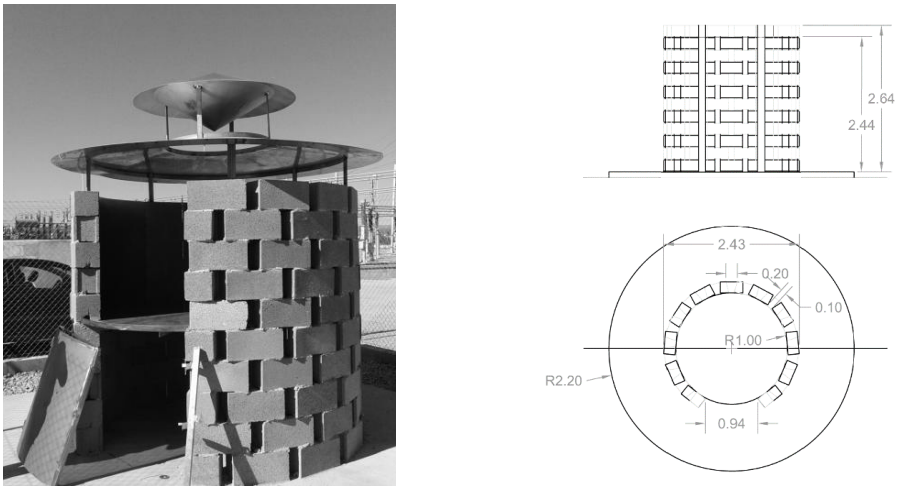

Fig. 4.4-1 Biomass Combustion Enclosure.

The temperature reached and the combustion time depend on the calorific value determined by the biomass, the amount of oxygen that exists between the biomass fibers, and the oxygen supplied by the different burner openings.

The RSA is a material obtained by own means, and it has been characterized by the techniques of X-ray diffraction, thermogravimetric analysis and scanning electron microscopy of field emission. Also, OPC, FCC and RSA have been characterized by X-ray fluorescence to determine their chemical composition.

The X-ray fluorescence kit is a Philips Magix Pro model, equipped with rhodium tube and beryllium window. The equipment used for the X-ray diffraction analysis is a Brucker AXS D8 Advance, the diffractogram being recorded for the interval 2Θ between 5º and 70º, with a pitch angle of 0.02 and an accumulation time of two seconds.

For the thermogravimetric analysis, was used a Mettler Toledo TGA 850 module, the sample was heated from 35 to 1000 ° C using an alumina crucible and heating at a rate of 20 ° C / min in an air atmosphere.

The equipment used for field emission scanning electron microscopy was a ULTRA 55-ZEISS equipment, and the samples were carbon coated for analysis.

As for the soil used, a sample of 25 kg has been taken and its homogenization is carried out by means of the quartet technique. After, we selecting the fraction that passes through the opening sieve 4mm and proceed to its drying at 60ºC. A thermogravimetry test was carried out on the soil used from 35 to 1000 ° C to determine the nature of the soil. Figure 4.4-2 shows the TG and DTG soil curves, observing a double peak in the DTG curve starting at 700ºC, indicating the presence of dolomite in the chosen soil.

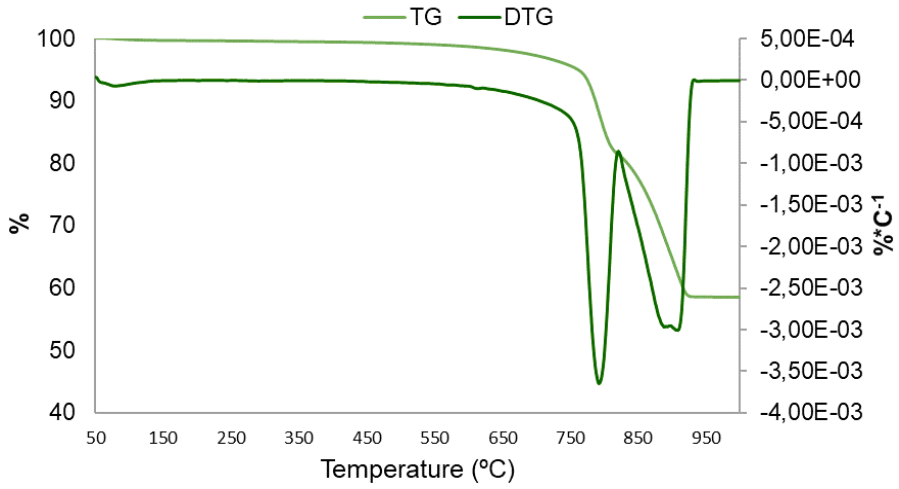

Fig. 4.4-2 TG and DTG curve (Soil).

From the optimum dry density obtained by mini harvard, soil kneading was done with different types of stabilizers, to make a comparison of their resistance to compression at ages between 7 and 90 days.

First, soil-water is compacted to know its compressive strength by its self, without other stabilizers, secondly, soil with OPC is stabilized as a pattern, because is the most used stabilizer. Subsequently, the program was marked for stabilization with alkaline activation cements, taking as precursor the FCC and the two types of activator previously indicated. The NaOH/ Na_2SiO_3 solution is composed of 60.8% Na_2SiO_3, 26% H2O and 13.22% NaOH. While the RSA activator solution contains 56.80% H2O, 17.04% NaOH and 26.16% RSA, to achieve the dissolution of the silica present in the RSA all the materials are mixed in a thermostated vessel and held for 24 hours.

Both in soil mixtures containing OPC and in the geopolymer-containing samples, these materials are used in 10% by weight with respect to the weight of soil, this percentage is within the usual percentages for soil stabilization (7-12%). The samples are kneaded together with the soil for one and a half minutes. After kneading, the entire kneading is pocketed to prevent the mixture from drying out, the mixture is divided into 24 plastic bags that are used to fill the mold designed to obtain cubic specimens of 40x40x40mm.

In the mold designed for this purpose, a dynamic compaction is applied, lowering a mass of 1.5 kg to 20 cm in height and performing 19 movements per layer (3 layers per cube). The specimens obtained are cured at an average temperature of 19 ° C. and a relative humidity of 65%.

To obtain the compressive strength of the specimens an Instron Model 270 press is used.

4.4.3. Results and discussion

Rice straw ash (RSA) characterization. The analysis of the characterization of the RSA is started by studying the obtained results by X-ray diffraction. As can be seen in Figure 4.4-3, the combustion of the RSA has produced an ash with a high amorphous character, such as Is observed with the deviation of the baseline between 15-35º. As crystalline phases the presence of Silvina (KCl), Calcite ($CaCO_3$), Arcanite (K_2SO_4) and Quartz (SiO_2) are observed. The presence of potassium compounds accounts for about 12% of K_2O obtained by X-ray fluorescence (Table 4.4-1). The presence of calcite may be due to soil contamination at the time of collection.

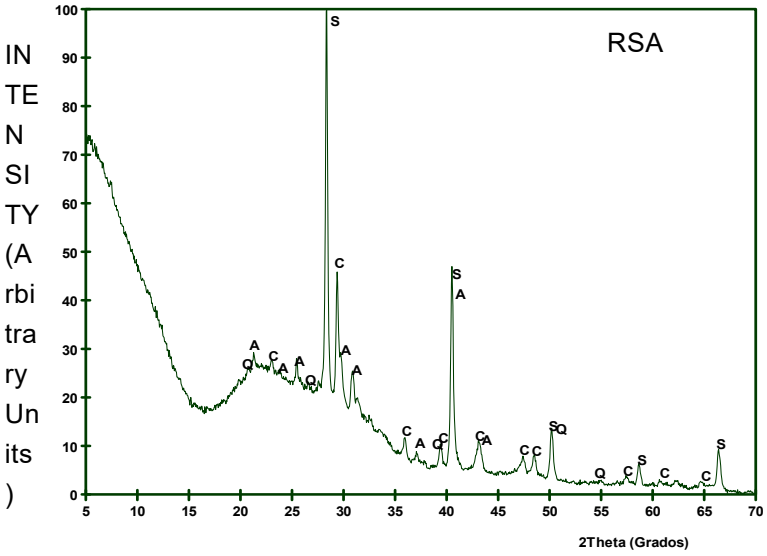

Fig. 4.4-3, Diffractogram corresponding to the RSA. S: Sylvite (KCl), C: Calcite ($CaCO_3$), A: Arcanite (K_2SO_4), Q: Quartz (SiO_2).

Figure 4.4-4 shows the TG and DTG curves obtained when heating the straw ash to 1000°C, as can be seen in the TG curve there is a continuous loss of mass throughout the interval, obtaining a percentage of mass loss around of 9%. The DTG curve shows us two major mass losses, one in the range of 450°C to 550°C due to incomplete straw burning, and another loss from the 850°C that may be due to the carbonates present in the sample probably due to soil contamination.

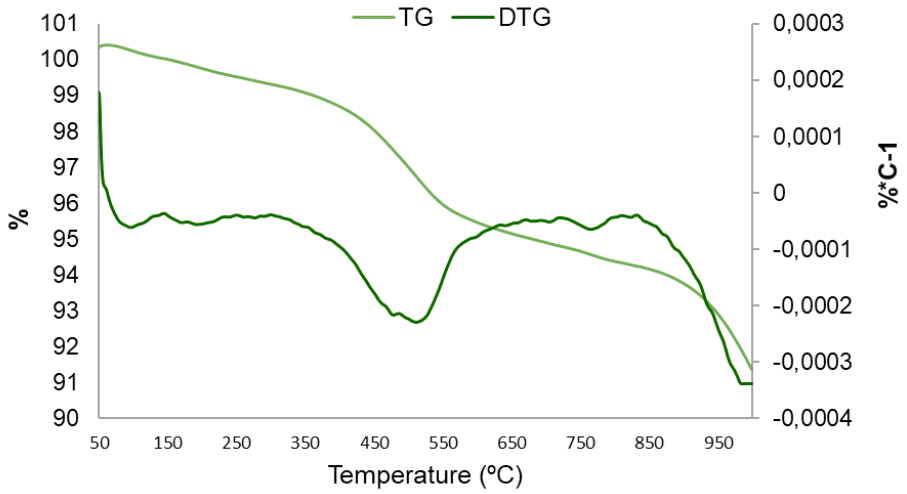

Fig. 4.4-4 TG and DTG curve (RSA).

Finally, on micrographs obtained by scanning electron microscopy of field emission, are shown a sample without milling to observe more clearly the structure of the straw after its combustion. In the micrographs the presence of phytoliths is observed, formations rich in silicon oxide that have conserved its structure in spite of the combustion of the same one.

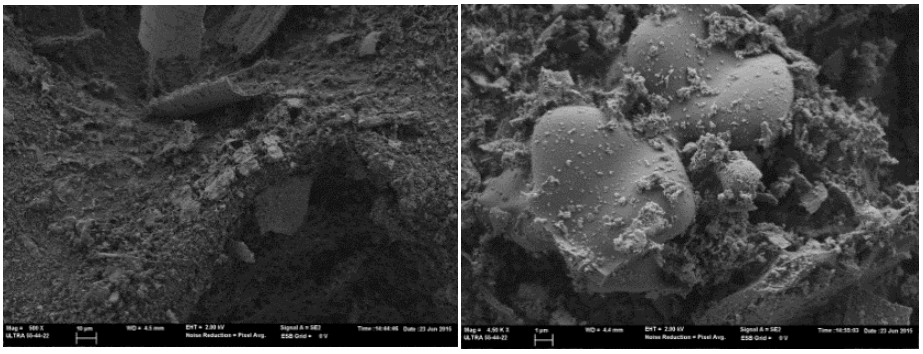

Fig. 4.4-5 Unmilled RSA Micrographs.

Compressive strengths (stabilized soils). The compressive strengths study was carried out to four curing ages to observe the evolution of the different soil stabilization systems. Results are plotted in figure 4.4-6.

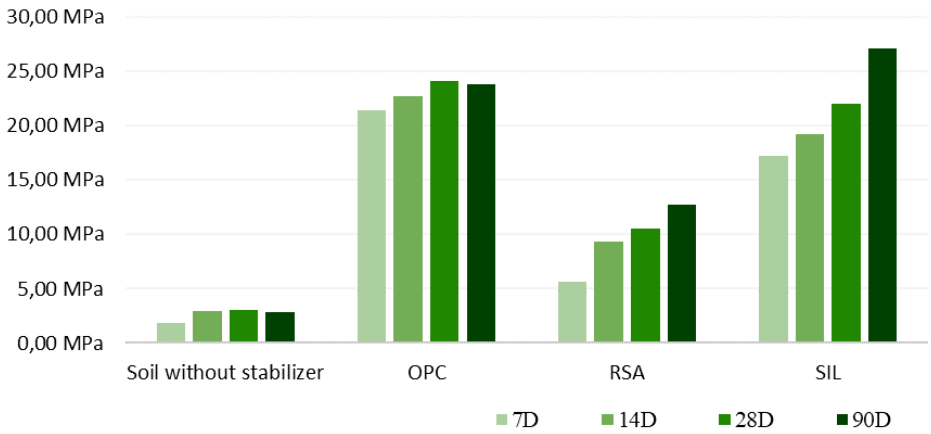

Fig. 4.4-6 Compressive Strengths in [Mpa] for Soils Stabilized at 7, 14, 28 and 90 Days of curing.

There are several behaviors in the different evaluated samples that distinguish between them. It can be observed that: In the case of soil without cementitious stabilizer, we obtain results of compressive strength in the range of approximately between 2 – 3 [MPa].

By adding 10% of OPC, we obtain a maximum of compressive strength of 24 [MPa], much higher than the soil without stabilizer.

In the case of stabilizing with a 10% FCC geopolymer activated with a NaOH/ Na_2SiO_3 mixture (SIL), a maximum compressive strength of 27.2[MPa] is obtained; these samples show a greater evolution of resistances with time from 7 to 90 days.

In the case of FCC geopolymer stabilizing, with RSA activator a compressive strength of 12.7[MPa] at 90 days of curing time is obtanined. It is lower than obtained by the cement samples and the NaOH/ Na_2SiO_3 mixture geopolymer, but much higher than the required for these kind of samples.

4.4.4. Conclusions

The present study has demonstrated the feasibility of using soil stabilization systems alternative to OPC using wastes. The use of geopolymers for soil stabilization using as a precursor the catalytic cracking catalyst residue gives lower results than the cement samples, but higher than not stabilized soils samples. The use of straw ash as a source of silica in the preparation of the activator reflect lower compressive strength results less than the use of the commercial silicate but is a very positive result, considering that the percentage of silicon oxide thereof is 52.4%. However, the compressive strengths achieved are sufficient for their application in stabilizing soils for their use in road pavements.

References

1.Khadka B., Shakya M. Comparative compressive strength of stabilized an un-stabilized rammed earth. Materials and Structures, vol 9, nº 49, pp 3945-3955, 2016.

2.Alrubaye A.J., Hassan M., Fattah M-Y. Stabilization of soft kaolin clay with silica fume and lime. International Journal of Geotechnical Engineering, vol 11, nº1, pp 90-96, 2017.

3.Rios S., Viana da Fonseca A., Baudet B. Effect of the porosity/cement ratio on the compression of cemented soil. Journal of Geotechnical and Geoenvironmental Engineering, vol 138, nº11, pp 1422-1426, 2012.

4.Marinkovic S., Dragas J., Ignjatovic J., Tosic N. Environmental assessment of green concretes for structured use. Journal of Cleaner Production, vol 154, pp 633-649, 2017.

5.Tashima M.M., Akasaki J.L., Castaldelli V.N., Soriano L., Monzó J., Borrachero M. V, Payá J. New geopolymeric binder base on fluid catalytic cracking catalyst residue (FCC). Materials Letters, vol 80, pp 50-52, 2012.

6.Huiskes DMA., Keulen A, Yu QL., Brouwers HJH. Design and performance evaluation of ultra-lightweight geopolymer concrete. Materials and Design, vol 89, pp 516-526, 2016.

7.Zhang M., Guo H., El-Korchi T., Zhang G. Tao M. Experimental feasibility study of geopolymer as the next-generation soil stabilizer. Construction and Building Materials, vol 47, pp 1468-1478, 2013.

8.Rios S., Cristelo N., Viana da Fonseca A., Ferreira C. Stiffness behaviour of soil stabilized with alkali-activated fly ash from small to large strains. International Journal of Geomechanics, vol 17, noº 3, pp 1-12, 2017.

9.Zhang M., Zhao M.X., Zhang G.P., Nowak P., Coen A., Tao M.J. Calcium-free geopolymer as a stabilizer for sulfate-rich soils. Applied Clay Science, vol 108, pp 199-207, 2015.

10.Bouzón N., Payá J., Borrachero M.V., Soriano L., Tashima M.M., Monzó J. Refluxed rice husk ash/NaOH suspension for preparing alkali activated binders. Materials Letters, vol 115, pp 72–74, 2014.

11.Mejía J.M., Mejía de Gutiérrez R., Montes C. Rice husk ash and spent diatomaceous earth as a source of silica to fabricate a geopolymeric binary binder. Journal of Cleaner Production, vol 118, pp 133-139, 2016.

12.Puertas F., Torres-Carrasco M. Use of glass waste as an activator in the preparation of alkali-activated slag. Mechanical strength and paste characterization. Cement and Concrete Research, vol 57, pp 95-104, 2014.

13.Alamán M. Estudio para la estabilización de bloques de tierra mediante la utilización de geopolímeros a partir de residuos. Aplicación para viviendas de bajo coste en Barranquilla (Colombia). Proyecto Final de Carrera. Universitat Politècnica de València, 2014.

4.5. Comunicación oral presentada en el 18º Seminario Iberoamericano de Arquitectura y Construcción con Tierra en La Antigua Guatemala (Guatemala), con el título: Uso de geopolímeros obtenidos a partir de residuos en la estabilización de suelos

Fecha del congreso anual	25/10/2018
Pág.	107-114
ISBN / ISSN	978-9929-778-74-0

Juan Cosa; María Victoria Borrachero; Jordi Payá; Lourdes Soriano; José María Monzó

Palabras clave: Cemento activación alcalina (CAA), Cerámica sanitaria (CS), catalizador de craqueo catalítico (FCC), Ceniza de cascara de arroz (CCA), Sostenibilidad.

Resumen: Habitualmente los suelos se estabilizan con cemento portland. El cemento Portland es un material con una elevada huella de carbono, ya que aproximadamente entre el 5 y el 7 por ciento de las emisiones de dióxido de carbono a nivel global son consecuencia de la producción de cemento Portland. Los geopolímeros son materiales que tienen poder conglomerante, pero tienen una huella de carbono mucho menor. El objetivo es la utlizacion de conglomerantes alternativos al cemento Porltand que presenten un menor coste económico y medioambiental, y que presenten similares o superiores prestaciones. Se prepararon probetas de suelo estabilizado de dimensiones reducidas utlizando un suelo de tipo dolomitico. El geolpolimero se preparó utilizando una mezcla de ceniza de cascarilla de arroz e hidróxido sódico como activador y como precursor residuo de catalizador de craqueo catalítico

(residuo producido en la industría del petróleo) y residuos de cerámica sanitaria. Los resultados ponen de manifiesto la viabilidad del uso de los geopolímeros obtenidos a partir de residuos como conglomerantes en la estabilizacion de suelos. Se realizaron mezclas de catalizador de craqueo catalítico (residuo producido en la industría del petróleo) y residuos de cerámica sanitaria obteniendo resistencias mecánicas de suelo estabilizado suficientes para una aplicación práctica.

4.5.1. Introducción:

El mundo se está viendo sometido a grandes cambios, debidos al crecimiento económico y demográfico, especialmente en algunos países en desarrollo, véase los denominados “BRICS” (Brasil, Rusia, India, China y Sudáfrica). Por ejemplo, en China, la producción de cemento ha aumentado un 3.000% desde 1980. Desde el año 2012, China fabricó más cemento que Estados Unidos desde 1900 (National geographic, 2017). Esto implica que tal como se aprecia en la figura 4.5-1, la producción mundial de cemento portland en 2017 según el US Geological Survey se sitúe en 4.100 millones de toneladas. Con la consiguiente repercusión en la emisión de CO_2, ya que la producción de una tonelada de cemento portland, implica la emisión de otra tonelada a la atmosfera de CO_2.

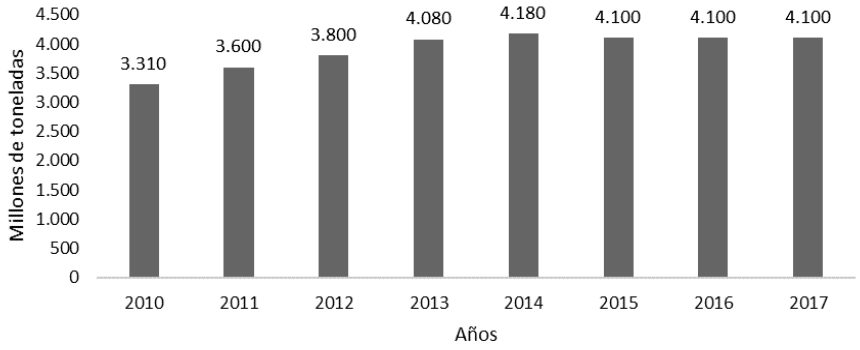

Fig. 4.5-1. Producción mundial de cemento portland de 2010 a 2017 (Fuente: US Geological Survey).

La Organización Meteorológica Mundial (OMM) alertó que por primera vez las concentraciones mensuales de dióxido de carbono en la atmósfera superaron el umbral de 400 partes por millón (ppm) en todo el hemisferio norte durante el mes de abril de 2014 (RPP noticias, ciencia y tecnología, 2014).

En este contexto derivado del desarrollo demográfico, en septiembre de 2015, los estados miembros de la Organización de Naciones Unidas (ONU) aprobaron la agenda 2030 para el desarrollo sostenible, que incluye un conjunto de 17 Objetivos (ONU, 2018). En su objetivo 11, se expresa la necesidad garantizar el acceso a la vivienda, así como de transformar la forma de construir mejorando la sostenibilidad de las ciudades. En el objetivo 9, explica que hay que aprovechar los avances tecnológicos para resolver problemas económicos y ambientales. Ampliándose en el objetivo 12, a la gestión eficiente de recursos y desechos. En sus objetivos 7 y 13, se manifiesta, la problemática que

supone el impacto producido por las emisiones de gases de efecto invernadero, y la necesidad urgente de tomar medidas.

Esta problemática surgida por el impacto ambiental derivado de la contaminación y del incremento constante del consumo energético, se ha transmitido a la sociedad civil, empresas y organizaciones que la componen, viéndose reflejado en la edificación a través de la creación de estándares y certificaciones. Así vemos el estándar Passivhaus basado en el ahorro y eficiencia energética del Passive House Institute de Alemania, donde se cuidan minuciosamente los acabados en encuentros de elementos constructivos con el fin de evitar cualquier filtración en los aislamientos térmicos que suelen poseer unas características y dimensionamiento muy superiores a las edificaciones tradicionales, no Passivhaus con reducciones respecto a las mismas de hasta el 90% del consumo energético (Passive House Institute, 2018).

Pero la edificación bioclimática va más allá del ahorro energético derivado de habitar en un edificio, implica cubrir muchos más aspectos de la edificación, siguiendo la misma línea han ido apareciendo diferentes certificaciones, como son, BREEAM del Building Research Establishment, institución creada en 1921 en Reino Unido (Breeam, 2018), LEED desarrollada por el US Green Building Council, institución creada en 1993 (Leed, 2018) o VERDE desarrollado por el Green Building Council España, institución creada en 2002 (GBCe, 2018).

Así, BREEAM, explica en su web que se “evalúan impactos en 10 categorías (Gestión, Salud y Bienestar, Energía, Transporte, Agua, Materiales, Residuos, Uso ecológico del suelo, Contaminación, Innovación)” (Breeam, 2018).

Podemos ver que tanto entidades de certificación como la propia ONU señalan la necesidad de reducir el impacto ambiental de nuestras

edificaciones, haciéndolas más sostenibles y en la medida de lo posible más accesibles. En algunos países en desarrollo, donde es común la autoconstrucción de la vivienda, el 100% del coste son los materiales de construcción utilizados. Utilizando materiales de bajo coste, como la propia tierra que podemos encontrar en el lugar de edificación de la vivienda, y diferentes residuos, se podría hacer de una manera más sostenible y accesible (Salas. J, 2010).

Cuando la ejecución de la vivienda se realiza mediante bloques de tierra comprimida (BTC), se puede optar por estabilizar el suelo, lo que permite mejorar las propiedades del BTC. Habitualmente se utiliza el cemento portland para estabilizar el suelo. Se puede sustituir el cemento portland, cuya industria está catalogada como de alto impacto ambiental por otro tipo de cemento con menor huella de carbono. Esto permite reutilizar residuos como parte de sus componentes, con ello, se consigue un tratamiento más adecuado de los residuos. Se reduce la contaminación, el gasto energético y económico (respecto a los BTC estabilizados con cemento portland), y con todo ello el impacto ambiental.

Estos cementos, son los cementos de activación alcalina (CAA), también conocido como geopolímeros. Estos cementos se componen por un precursor de naturaleza silicoaluminosa y un activador altamente alcalino. Al combinarlos, se produce una reacción química derivada del ataque alcalino del activador al precursor, que da lugar a una reacción de geopolimerización (Glukhovsky V.D., 1959, 1965, 1978, y 1981).

Se ha venido utilizando para la obtención de los CAA, Metacaolín, Escoria de alto horno, o Cenizas volantes (Marin, C et al., 2009; Khan, M.Z.N. et al., 2016; Nath, P et al. 2014). En menor medida residuo de catalizador del craqueo catalítico (FCC), o cerámica sanitaria (CS) para

el precursor (Trochez, J.J. et al., 2015; Tashima, M.M. et al., 2012 y 2013; Rodriguez, E.D et al., 2013; García de Lomas, M. et al., 2007; Cosa, J. et al., 2018). Como activador, lo más común es una disolución de hidróxidos con silicatos de sodio o potasio. Estudios más recientes muestran la posibilidad de utilizar residuos para la obtención del activador, como es la ceniza de cascara de arroz (CCA) (Bouzón, N. et al., 2014).

Los suelos estabilizados con CAA necesitan menos tiempo que los estabilizados con cemento portland para desarrollar altas resistencias a compresión, además mejoran la ductilidad y con ello el agrietamiento por retracción en los diferentes paramentos, mejorando por un lado el acabado estético, y por otro dificultando el anidamiento de insectos, tanto por la reducción de grietas, como por aumentar la alcalinidad del material. Algunos de estos insectos, son un verdadero peligro para el ser humano, como es el caso de la Vinchuca en países como Bolivia o Chile. Se estima que la Vinchuca infecta a 10 millones de personas en el mundo, y provoca 10.000 muertos al año derivado del mal de Chagas que transmiten (El Pais, 2013).

Los CAA se presentan por tanto como un sustituto al cemento portland. Este estudio se centra en la aplicación de los CAA en la estabilización de suelos cuya aplicación más extendida en la construcción arquitectónica, es el BTC, y en menor medida el tapial. Sin embargo, los CAA también pueden utilizarse como morteros u hormigones en aquellos elementos constructivos donde el uso de suelos estabilizados podría verse comprometido (figura 4.5-2), como es el caso de cimentaciones, determinados elementos estructurales, o revestimientos que pudieran verse afectados por los agentes atmosféricos. Así mismo, también cabe la posibilidad de su uso en refuerzo de cimentaciones deficientes de edificaciones ejecutadas, con aplicación de CAA, por ejemplo, mediante jet-grouting (figura 4.5-3).

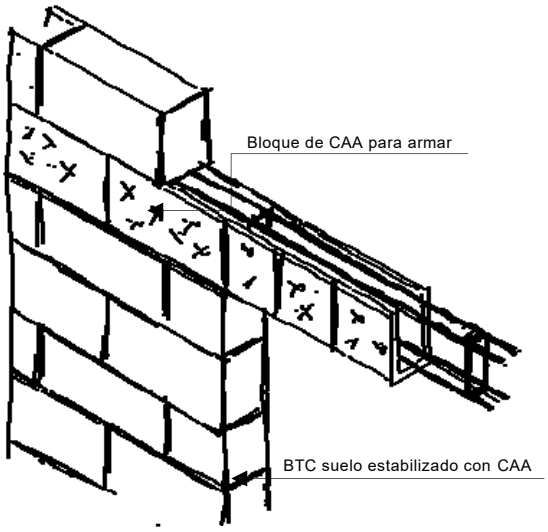

Fig. 4.5-2 Muro de cerramiento ejecutado con BTC de suelo estabilizado con CAA. Dintel de bloque prefabricado de hormigón de CAA para armado.

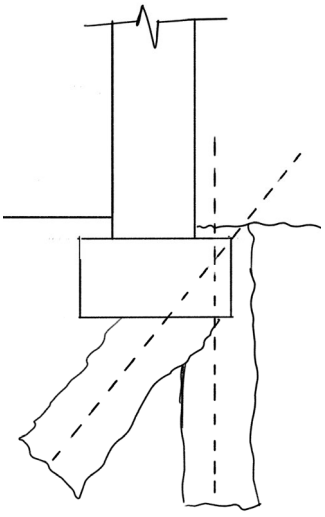

Fig. 4.5-3 Estabilización de zapa de cimentación, inyectando lechada de CAA ediante jet-grouting

4.5.2. Materiales y Métodos

En este estudio se utiliza un suelo de naturaleza dolomítica suministrado por PAVASAL, S.A., se ensayó a compresión el suelo compactado estabilizado con CAA y sin estabilizador, siempre con densidad seca optima de proctor, para conocer la diferencia que existe con estabilizador y sin el mismo. La muestra de suelo se homogeneiza mediante la técnica de cuarteo, y posteriormente se pasa por tamiz de 4mm y se sustrae la humedad en estufa a 60ºC, hasta conseguir peso constante.

Para el precursor del estabilizador, se ha optado por el uso de FCC, bien al 100%, o con sustituciones de FCC por CS, donde se ha optado por una relación 70%CS – 30% FCC, ya que en su uso en estudios anteriores en morteros parece una relación óptima si no en máxima resistencia a compresión, si la que más reduce el impacto económico y ambiental, aprovechando mejor la reutilización de residuos con una resistencia a compresión aceptable (Cosa, J. et al., 2018).

Para la disolución activadora se han utilizado tres opciones como fuente de sílice, silicato sódico comercial de Merck, con una composición de 28% SiO_2, 8% Na_2O, y 64% H_2O; un residuo de tierras diatomeas usado como filtrante en la industria cervecera (DH) y CCA, ambas con SiO_2 en su composición superior al 80%. En todas ellas se utiliza NaOH de Panreac S.A., el agua procede de la red de abastecimiento de la Universitat Politècnica de València.

La disolución activadora con silicato sódico comercial, se realiza con 60,8% de Na_2SiO_3, 24% de H_2O, y 13,22% de NaOH. Se utiliza a temperatura ambiente, por lo que se deja reposar 30 minutos para que pierda el calor producido por la reacción química. En el caso de las

disoluciones de residuos (DH y CCA), se utiliza un recipiente termostatizado para aprovechar la reacción exotérmica, se añade en primer lugar, el hidróxido sódico 19%, en segundo lugar, el residuo 18% (DH o CCA según el caso), por último, se añade el agua 63%. Se agita hasta que se obtiene una mezcla homogénea, despresurizando de vez en cuando, tras varias agitaciones. Se deja reposar 24 horas antes de su uso.

La amasada de suelo estabilizado, se realiza mezclando 1000g de suelo en la amasadora un minuto, a continuación, se añade 100g de precursor y se mezcla durante 1 minuto más, por último, se añaden 174g de la disolución activadora y se deja mezclar dos minutos más. La densidad seca óptima (figura 4.5-4), es la concreta para el suelo utilizado, obtenida a partir del ensayo de proctor modificado con mini Harvard.

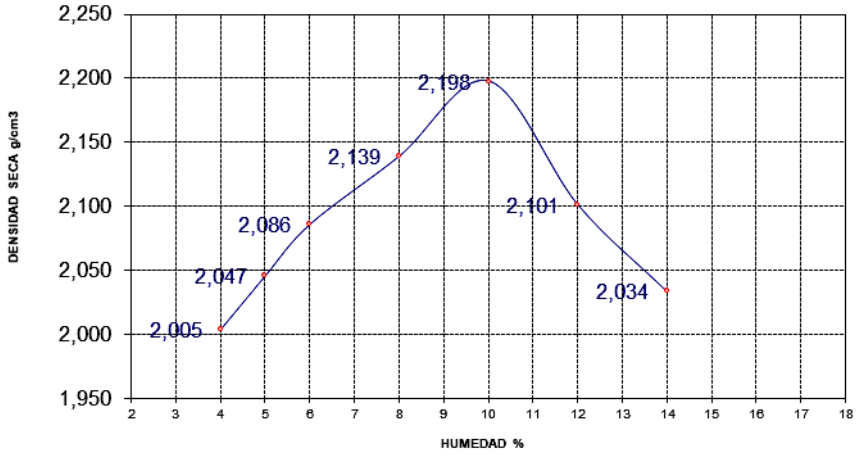

Fig. 4.5-4 Representación de la curva de proctor modificado mediante mini harvard.

Las probetas utilizadas para el estudio son de 40x40x40 mm, realizadas con un molde de diseño propio (ver figuras 4.5-5 y 4.5-6), siguiendo el procedimiento habitual para el proctor modificado. Se rellena el molde en tres capas dejando caer una masa de 1,5kg desde 20cm de altura, con 19 golpes por capa. El proceso de curado se realiza en una cámara controlada a 22ºC y 50% de humedad relativa. Al utilizar probetas de reducidas dimensiones, se reduce el coste de los recursos materiales, personales, y ambientales, permitiendo obtener resultados preliminares, antes de un estudio en detalle con BTC estabilizados con CAA o incluso de la ejecución de una vivienda con suelo estabilizado, bien sea con BTC o por tapial, que se realizará más adelante.

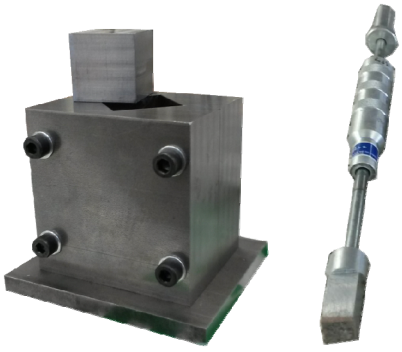

Fig. 4.5-5 Molde para probetas cúbicas.

Fig. 4.5-6 Probetas cúbicas de 40x40x40mm

4.5.3. Resultados

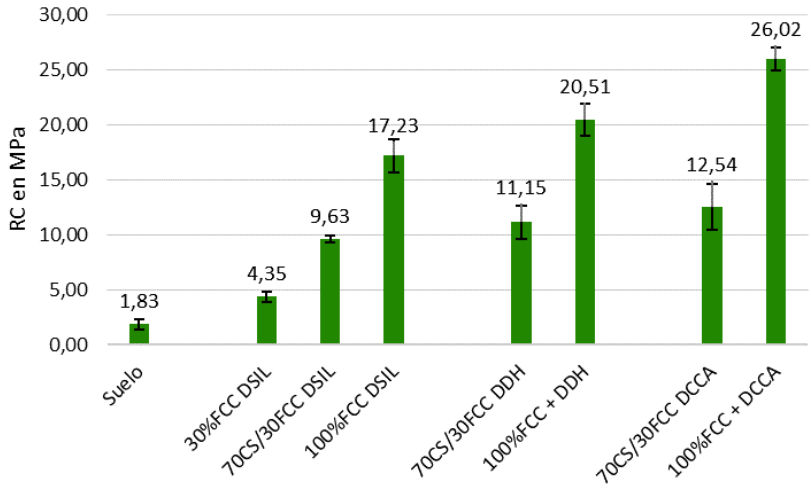

Fig. 4.5-7 Resultados en MPa de resistencia a compresión a 7 días. Suelo sin estabilizar, y suelo estabilizado con CAA, con diferentes disoluciones activadoras, disolución de silicato sódico (DSIL), de residuo de diatomeas (DDH) y de ceniza de cascara de arroz (DCCA).

En los resultados de la figura 4.5-7, se observa la resistencia del suelo sin estabilizador que se encuentra entorno a los 2MPa, por otra parte, se representa el suelo estabilizado con CAA, donde se ha hecho una división en función del tipo de disolución activadora.

Con un 30% de FCC se obtienen 4,35MPa a 7 días, con lo que los BTC realizados entrarían en 7 días dentro de las categorías propuestas por la norma UNE (UNE 41410, 2008), BTC 1 y 3, y cercano en sólo 7 días a BTC 5. Si se añade CS se observa un incremento considerable de la resistencia a compresión, llegando a 9,63MPa. Con 100% de FCC se obtienen 17,23MPa.

Si al estabilizar suelo, en lugar de silicato sódico comercial en la disolución activadora, se utiliza una disolución a partir de residuos como la DDH y DCCA, se obtienen para la relación 70%CS-30%FCC, 11,15MPa y 12,54MPa respectivamente. Siendo para el 100%FCC de 20,51MPa y 26,02MPa.

4.5.4. Conclusiones

Las resistencias a compresión obtenidas son muy superiores a las indicadas por las normas tanto para BTC, como si se pretende estabilizar suelo para caminos o firmes de carretera. De ello se desprende que con un pequeño aporte de residuos es posible mejorar notablemente las propiedades físicas del suelo estabilizado, independientemente de su uso en BTC, tapial, etc.

En el caso del sistema CS-FCC, se consigue incrementar notablemente las propiedades del suelo tras la estabilización, reduciendo la cantidad de FCC aportado, reutilizando un residuo que por sí mismo no tendría ningún valor, como es la cerámica sanitaria. En general, se demuestra por tanto que es viable el uso de residuos tanto en precursor como en el activador, de hecho, se observa que las disoluciones con residuo funcionan incluso mejor que las preparadas con silicato sódico comercial.

Es posible el uso de CAA como alternativa más sostenible al cemento portland en estabilización de suelos, con menor impacto económico y medioambiental. Mejorando por otra parte el acceso a la vivienda en países en desarrollo. Con un amplio abanico de aplicaciones. En construcción de viviendas de nueva planta, rehabilitaciones de edificios. En forma de BTC, tapial, solados, etc.

Referencias

1.China bate el récord en producción de cemento, 27 febrero (2017). Disponible en: http://www.nationalgeographic.com.es/mundo-ng/actualidad/china-bate-record-produccion-cemento_11123

2.RPP noticias, ciencia y tecnología, (2014). http://rpp.pe/tecnologia/mas-tecnologia/omm-concentracion-de-co2-alcanza-nivel-record-en-hemisferio-norte-noticia-695134

3.Objetivos de desarrollo sostenible, acceso 23 mayo (2018). Disponible en: https://www.un.org/sustainabledevelopment/es/objetivos-de-desarrollo-sostenible/

4.Passive House Institute, acceso 23 Mayo (2018). Disponible en : http://passivehouse.com/02_informations/01_whatisapassivehouse/01_whatisapassivehouse.htm

5.BREEAM, acceso 23 mayo (2018). Dispponible en: http://www.breeam.es/

6.LEED, acceso 23 mayo (2018). Dispponible en: https://new.usgbc.org/

7.GBCe, green building council España, acceso 23 mayo (2018). Dispponible en: http://www.gbce.es/

8.Salas J (2010). Reflexiones sobre la enseñanza y la investigación tecnológica para la vivienda de las mayorías, pp.121-131, acceso 2 mayo (2014), http://www. habitatysociedad.us.es

9.Glukhovsky V.D. Slag Alkaline Fine Aggregate Concretes. (1981) Kiev, USSR

10.Glukhovsky V.D. Soil silicates, Gosstroyizdat Publishers. (1959) Kiev

11.Glukhovsky V.D. Soil silicates, Their Properties, Technology and Manufacturing and Fields of Application, Doct Tech Sc. Degreee thesis. Civil Engineering Institute. (1965) Kiev

12.Glukhovsky V.D., Pakhomov V.A., Slag-Alkaline Cements and Concretes, Budivelnik Publishers. (1978) Kiev

13.Marin, C.; Araiza, J.L.R.; Manzano, A.; Avalos, J.C.R.; Perez, J.J.; Muniz, M.S.; Ventura, E.; Vorobiev, Y. Synthesis and characterization of a concrete based on metakaolingeopolymer. Inor. Mat. (2009), 45 (12), 1429-1432.

14.Khan, M.Z.N.; Shaikh, F.A.; Hao, Y.; Hao, H. Synthesis of high strength ambient cured geopolymer composite by using low calcium fly ash. Constr. Build. Mat. (2016), 125, 809-820.

15.Nath, P.; Sarker, P.K. Effect of GGBFS on setting, workability and early strength properties of fly ash geopolymer concrete cured in ambient condition. Constr. Build. Mat. (2014), 66, 163- 171.

16.Trochez, J.J.; Mejía de Gutiérrez, R.; Rivera, J.; Bernal, S.A. Synthesis of geopolymer from spent FCC: Effect of SiO2/Al2O3 and Na2O/SiO2 molar ratios. Mat. Constr. (2015), 65 (3), http://dx.doi.org/10.3989/mc.2015.00814.

17.Tashima, M.M.; Akasaki, J.L.; Castaldelli, V.N.; Soriano, L.; Monzó, J.; Payá, J.; Borrachero, M.V. New geopolymeric binder based on fluid catalytic cracking catalyst residue (FCC). Mat. Lett. (2012), 80, 50-52.

18.Tashima, M.M.; Akasaki, J.L.; Melges, J.L.P.; Soriano, L.; Monzó, J.; Payá, J.; Borrachero, M.V. Alkali activated materials based on fluid catalytic cracking catalyst residue (FCC): Influence of SiO2/Na2O and H2O/FCC ratio on mechanical strength and microstructure. Fuel. (2013), 108, 833-839.

19.Rodriguez, E.D.; Bernal, S.A.; Provis, J.L., Gehman, J.D.; Monzó, J.; Payá, J. Geopolymers based on spent catalyst residue from a fluid catalytic cracking (FCC) process. Fuel. (2013), 109, 493-502. http://dx.doi.org/10.1016/j.fuel.2013.02.053.

20.García de Lomas, M.; Sánchez de Rojas, M.I.; Frías, M. Pozzolanic reaction of a spent fluid catalytic craking catalyst in FCC-cement mortars. J. Therm. Anal. Calorim. (2007), 90 (2), 443-447.

21.Juan Cosa, Lourdes Soriano, María Victoria Borrachero, Lucía Reig, Jordi Payá and José María Monzó. Influence of Addition of Fluid Catalytic Cracking Residue (FCC) and the SiO2

Concentration in Alkali-Activated Ceramic Sanitary-Ware (CSW) Binders. Minerals (2018), 8(4), 123; https://doi.org/10.3390/min8040123

22.Bouzón N, Payá J, Borrachero MV, Soriano L, Tashima MM, Monzó J (2013), Refluxed rice husk ash/NaOH suspension for preparing alkali activated binders, Materials Letters, 115 (2014) 72–74.

23.UNE-EN 41410: (2008), Bloques de tierra comprimida para muros y tabiques. Definiciones, especificaciones y métodos de ensayo.

24.El Pais, El latigazo del Chagas (2013), Disponible en: https://elpais.com/elpais/2013/02/25/eps/1361790800_865167.html

4.6 Comunicación oral presentada en el 19º Seminario Iberoamericano de Arquitectura y Construcción con Tierra en Oaxaca de Juaárez (México), con el título: Propiedades de suelos estabilizados con Geopolímeros fabricados con residuos

Fecha del congreso anual	18/10/2019
Pág.	150-161
ISBN / ISSN	978-99923-880-6-8

Juan Cosa, José Monzó, Jordi Payá, Lourdes Soriano, Mª Victoria Borrachero

Palabras clave: activación alcalina, estabilización de suelo, resistencia a compresión

Resumen:La estabilización del suelo es una técnica basada en el uso de un aglutinante, que puede mejorar la unión de las partículas del suelo, aumentando las propiedades mecánicas y la durabilidad El aglutinante principal usado es el cemento portland, que presenta una gran huella de carbono El objetivo de este trabajo es estudiar la estabilización de un suelo dolomítico a partir de geopolímero preparado con reactivos químicos y usando un 85% de materiales residuales. Se ha estudiado por diversas técnicas la microestructura de estos suelos estabilizados. Los resultados demuestran que se pueden conseguir estabilizaciones similares a las conseguidas usando cemento portland, por lo que se considera la opción del uso de geopolímeros como una opción más viable y sostenible desde un punto de vista medioambiental.

4.6.1 Introducción

El lecho del suelo debe soportar todas las tensiones generadas transmitidas por las estructuras o capas que soporta. A menudo es débil y no tiene suficiente estabilidad en cargas pesadas. El diseño principal de muchos análisis geotécnicos en condiciones de servicio a largo plazo conlleva un análisis del refuerzo por la deformación y la tensión generada, así como la estabilidad de las estructuras del suelo. En los sistemas de edificios, cada desplazamiento puede generar tensiones internas que no se han previsto en el análisis y diseño de estructuras que deberían anticiparse (Ramaji, 2012).

Para la estabilización de suelos existen procedimientos con aditivos naturales o sintéticos para incrementar las propiedades de los suelos, que a veces son utilizados en conjunto. Las técnicas de estabilización de suelos pueden ser clasificadas desde distintos puntos de vista. Uno de ellos se muestra en la figura 4.6-1 (Hejazi et al., 2012).

Las prestaciones que se consiguen con la estabilización de suelos permiten una reducción del índice de plasticidad o de su expansión, y un incremento de la durabilidad y la resistencia.

Los métodos mecánicos como la compactación son ampliamente usados. En este método es importante conocer la relación entre el contenido óptimo de humedad y la densidad máxima en seco. Se han realizado muchos estudios en este sentido (Yan; Wu, 2009; Ferber et al. 2009). Se pueden destacar los estudios microestructurales, usando porosimetria de intrusión de mercurio (Wang et al., 2013; Cui, 2017).

Los aditivos químicos de tipo convencional tambien son ampliamente utilizados: Estos aditivos incluyen la cal, el cemento portland y las

cenizas volantes y todos ellos tienen en común que son a base de compuestos cálcicos. En presencia de agua, reaccionan químicamente bien con el suelo o por ellos mismos, mejorando la matriz del suelo, reduciendo la expansión, y mejorando la resistencia y durabilidad frente a los ciclos humectación-secado (Soltani et al., 2017a). Mecanismos como intercambio catiónico, floculación y sedimentación, reacción puzolánica y carbonatación son algunos de los procesos identificados en su uso como estabilizantes (Al-Swaidani; Hammoud; Meziab, 2016; Tashima et al, 2017). Otros aditivos usados son los betunes, aunque pueden tener un impacto negativo en el suelo, y su uso debe limitarse por su excesivo contenido en agua. Solo la introducción de betún espumado a la tecnología de construcción de carreteras permitió utilizar el aglomerante de betún para la estabilización del suelo (Hamzah et al., 2015).

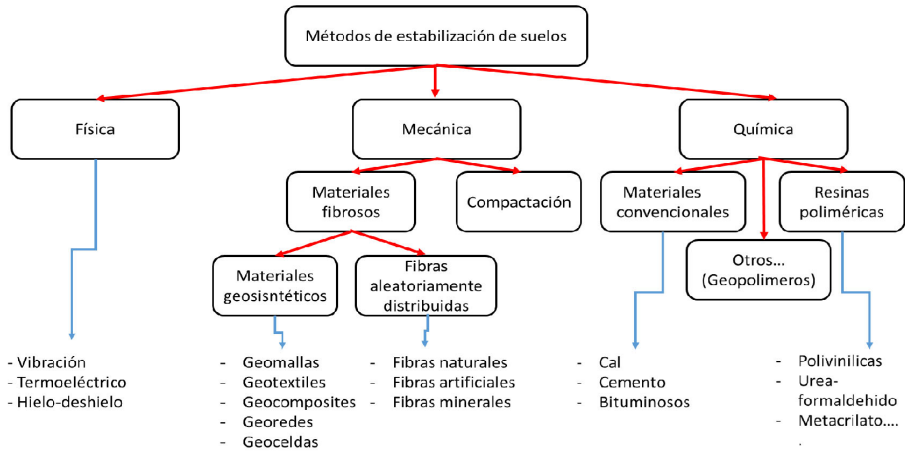

Fig. 4.6- 1 Clasificación de técnicas de estabilización de suelos (adaptada de Hejazi et al., 2012)

Existen otros aditivos que no son tan convencionales que tambien pueden reaccionar químicamente con el suelo y/u otros agentes que con la suficiente humedad pueden producir interacciones fisicoquímicas con la matriz del suelo. Estos productos pueden incluir aceites sulfonados (Soltani et al, 2017b), o resinas poliméricas (Onyejekwe; Ghataora, 2015)

Recientemente, las investigaciones realizadas sobre el desarrollo de materiales activados alcalinamente revelaron que este método tiene un enorme potencial para ser considerado como un nuevo tipo de conglomerante (Davidovits, 1998; Davidovits, 1994). La activación alcalina (o "geopolimerización") se ha descrito como una policondensación de estructuras de alúmina y sílice dispuestas alternativamente y tetraédricamente, interconectadas por átomos de oxígeno, que conlleva una etapa de destrucción donde se disuelven los enlaces de la materia prima para posteriormente producirse una reacción de coagulación seguida de una condensación y/o cristalización. El proceso de activación alcalina utiliza un material precursor (aluminosilicato) con una disolución fuertemente alcalina. Como precursor se han usado diversos tipos de fuentes de aluminosilicato, por ejemplo, cenizas volantes silicoaluminosas, escorias de alto horno granuladas molidas, las cenizas de combustible de aceite de palma, residuos de la industria petroquímica, etc. (Cristello et al., 2012; Pourakbar et al, 2015; Fasihnikoutalab et al., 2017; Paya et al., 2019). Varias publicaciones mostraron la efectividad del proceso geopolimérico para la estabilización del suelo (Habert et al., 2011, Sargent et al., 2013, Zhang et al., 2013, Cosa et al, 2017). Basadas generalmente en las pruebas microestructurales, estas investigaciones confirmaron que se desarrolla un gel polimerizado de aluminosilicato estructurado. Dentro de los huecos del suelo; este gel ayuda a formar microestructuras más

densas y, como resultado, mejora fundamentalmente, la resistencia a la compresión y la durabilidad.

4.6.2 Objetivo

El objetivo de este trabajo es estudiar la estabilización de un suelo dolomítico comparando la estabilización a base de cemento portland con la realizada a partir de geopolímero. Dichos geopolímeros son preparados a partir de reactivos químicos y usando un 85% de materiales residuales.

4.6.3 Materiales Y Métodos

El suelo que se ha utilizado para ser estabilizado es de naturaleza dolomítica (procedente de roca dolomítica machadada) y fue suministrado por la empresa Pavasal. Previo a su uso, la muestra de suelo se homogeneiza mediante un cuarteo y posteriormente se tamiza por 4mm, para retirar el material más grueso. El tamaño máximo fue de 4 mm y con la siguiente granulometría (% que pasa): 2mm = 73.6%: 1.15mm = 59.3%; 0.40mm = 39.3%; 0.16mm = 31.4%; 0.08mm = 26.9%. Posteriormente se seca en la estufa a 60ºC hasta peso constante, para eliminar la humedad.

El suelo ha sido estabilizado con cemento CEM I-42.5R (composición química en la tabla 4.6-1) y mediante un proceso de activación alcalina. Para el proceso de activación alcalina se requiere la mezcla de un precursor y de una disolución activadora fuertemente alcalina. En este trabajo, el precursor usado es un residuo de la industria petroquímica; el catalizador de craqueo catalítico (FCC) material residual de composición silicoaluminosa. Dicho precursor se adiciona en un 10% en peso respecto de la cantidad de suelo utilizado., y ha sido suministrado por la empresa Omnya Clariana, S.L.

La disolución activadora se prepara con una mezcla de NaOH comercial, suministrado por la empresa Panreac S.A., agua y una fuente de sílice. En este trabajo se usan dos opciones como fuente de sílice: una disolución de silicato sódico comercial de la empresa Merck, con una composición del 28% SiO_2, 8% Na_2O, y 64% H_2O; y una ceniza de cáscara de arroz (CCA) suministrada por la empresa Maicerías DACSA que es obtenida de un proceso de combustión con cogeneración de energía.

La disolución activadora con silicato sódico comercial se realiza con 60,8% de Na_2SiO_3, 24% de H_2O, y 13,22% de NaOH, a temperatura ambiente. Su preparación implica una liberación de calor, por lo que antes de utilizarla en la amasada se deja reposar al menos 30 minutos para que pierda el calor producido por la reacción química. En el caso de las disoluciones con CCA se utiliza un recipiente termostatizado para aprovechar la reacción exotérmica de la disolución del NaOH en la disolución de la sílice de la CCA; el procedimiento seguido es añadir en primer lugar, el hidróxido sódico, en segundo lugar, la ceniza de cáscara de arroz y finalmente el agua. Se agita hasta que se obtiene una mezcla homogénea, despresurizando de vez en cuando, tras varias agitaciones y se deja reposar 24 horas antes de su uso.

La amasada de suelo estabilizado, se realiza mezclando 1000 g de suelo en la amasadora un minuto, a continuación, se añade 100 g de precursor y se mezcla durante 1 minuto más, por último, se añaden 174 g de la disolución activadora y se deja mezclar dos minutos más. La densidad seca óptima (figura 4.6-2) es la concreta para el suelo utilizado, obtenida a partir del ensayo de Proctor modificado con mini Harvard según ASTM STP479. La energía de compactación usada fue de 2632 J/cm^3.

Las probetas utilizadas para el estudio son de 40x40x40 mm, realizadas con un molde de diseño propio (figuras 4.6-3 y 4.6-4), siguiendo el procedimiento habitual para el Proctor modificado. Se rellena el molde en tres capas dejando caer una masa de 1,5 kg desde 20 cm de altura, con 19 golpes por capa. El proceso de curado se realiza a temperatura ambiente en el laboratorio.

El ensayo a compresión se llevó a cabo en una máquina universal INSTRON modelo 3382, con una velocidad de desplazamiento de 1 mm/min.

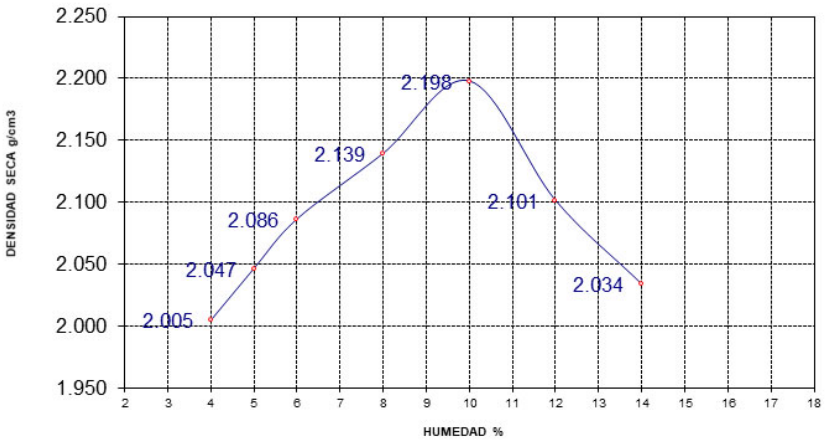

Fig. 4.6-2 Representación de la curva de Proctor modificado mediante mini harvard (tomada de Cosa et al., 2017)

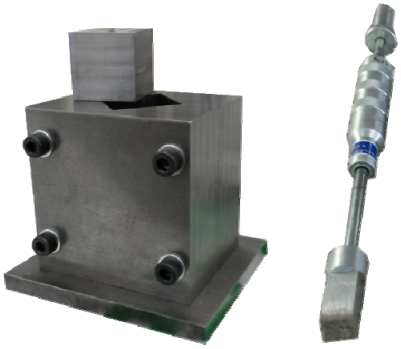

Fig. 4.6-3a. Molde de probetas cúbicas

Fig. 4.6-3b. Probetas cúbicas de 40 mm x 40 mm x 40 mm

Los estudios microestructurales han sido realizados mediante analisis termogravimétrico, y difracción de rayos X. Una porción de la muestra se machacó en un mortero y se tamizó por 125µm. La muestra resultante se secó a 60ºC durante 30 min y se guardó en un eppendorf, para ser sometida a los respectivos análisis.

Para la caracterización química del cemento, FCC y CCA se ha utilizado un equipo de fluorescencia de rayos X, Philips-MagixPro, equipado con tubo de rodio y ventana de berilio; Para el análisis por difracción de rayos X de los materiales de partida y de las mezclas de suelos estabilizados se han usado un difractómetro Bucker AXS-DS; el intervalo barrido de 2Θ ha sido desde 5-70º, con un ángulo de paso de 0.02º y un tiempo de acumulación de 2 s.

En el caso de las muestras analizadas por termogravimetria se ha usado un equipo Mettler Toledo-TGA 850 con un intervalo de calentamiento entre 35-1000^{0}C, a una velocidad de calentamiento de 20º/min, usando una atmosfera de aire seco de 70µL/min y en un crisol de alúmina.

4.6.4 Resultados y Discusión

4.6.4.1 Caracterización de los compuestos de partida

En la tabla 4.6-1 se muestra la composición química del cemento usado, del precursor geopolimérico FCC y de la CCA usada como fuente de sílice en la preparación de la disolución activadora. El FCC presenta en su composición SiO_2 y Al_2O_3 en proporciones en peso similares y la CCA tiene SiO_2 por encima de un 80%. Se utiliza una ceniza de cáscara de arroz original, con un tamaño de partícula de 62.3 µm (Bouzon et al., 2014).

Tab. 4.6-1 Composition in percentage of oxides of the materials used measured by x-ray fluorescence * loss on ignition.

	SiO_2	Al_2O_3	Fe_2O_3	CaO	MgO	SO_3	K_2O	Na_2O	P_2O_5	TiO_2	Cl^-	Others	LOI*
OPC	20,80	3,60	4,80	65,60	1,20	1,70	1,00	0,07	-	-	-	-	1,23
FCC	47,76	49,26	0,60	0,11	0,17	0,02	0,02	0,31	0,01	1,22	-	-	0,51
CCA	85,58	0,25	0,21	1,83	0,5	0,26	3,39	-	0,67	-	0,32	-	6,99

Respecto a la composición mineralógica de estos materiales se puede destacar que el DRX del FCC usado como precursor presenta como pico principal un aluminosilicato de naturaleza zeolitica (faujasita), acompañado de cuarzo, mullita y trazas de feldespatos tipo albita (Monzó et al, 2001). La ceniza de cáscara de arroz usada presenta una naturaleza fundamentalmente amorfa con picos de cristobalita (Cr) fundamentalmente y trazas de tridimita (T) y silvina (S). Los pequeños picos detectados de cuarzo (Q), se atribuyen a impurezas del suelo donde fue recogida la cáscara de arroz (figura 4.6-4a).

El suelo utilizado es de carácter dolomítico. Su difractograma de rayos X (figura 4.6-4b) muestra que es mayoritariamente dolomita (D) con calcita (C) y cuarzo (Q) como minerales secundarios y trazas de compuestos tipo filosilicatos como mica moscovita (M) (ver figura 4.6-4b). Así mismo, la curva DTG en su análisis termogravimetrico (Figura 4.6-4c) muestra un doble pico en el intervalo de temperaturas (600-800ºC), que indica una mezcla de dolomita y calcita (Cosa et al., 2017).

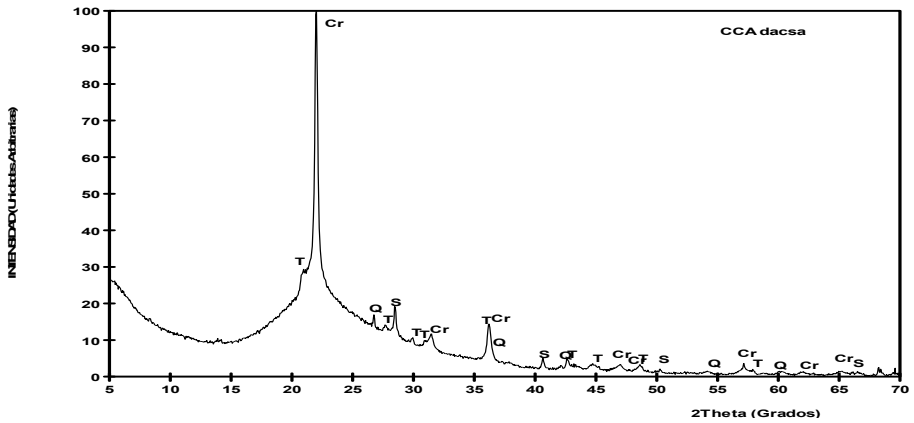

a)

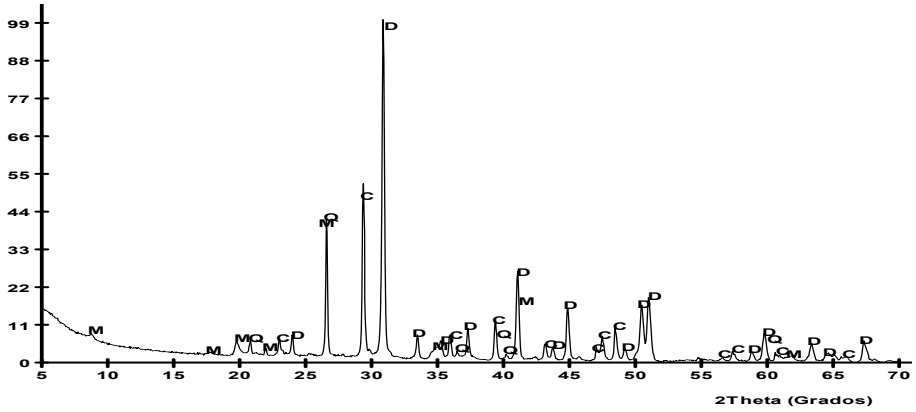

b)

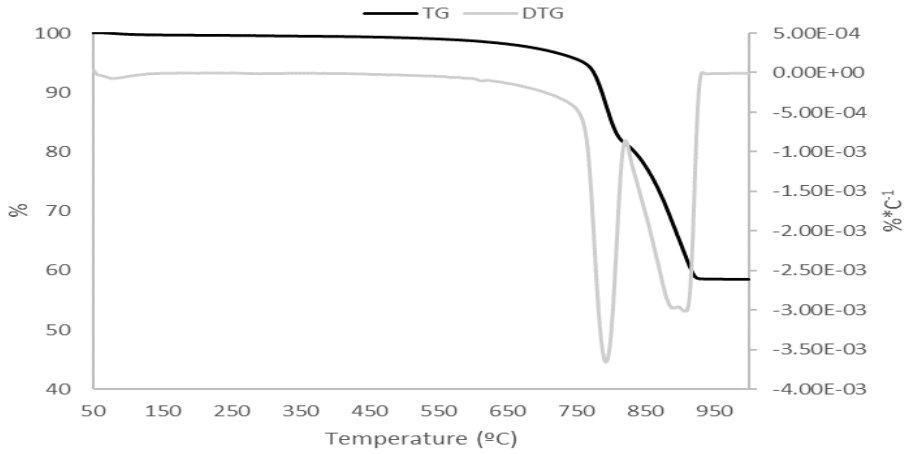

c)

Fig. 4.6-4a Difractograma de rayos X de la muestra de ceniza de cáscara de arroz; Fig. 4.6-4b Difractograma de rayos X de la muestra de suelo; Fig. 4.6-4c Curva TG y DTG de la muestra de suelo (Cosa et al., 2017)

4.6.4.2 Resistencias mecánicas a compresión

En la figura 4.6-5 se representan los valores de resistencia a compresión de las probetas de suelo sin estabilizar, solamente suelo + agua (denominadas "suelo") y las probetas de suelo estabilizado. Se puede observar que todas las muestras de suelo estabilizado cumplen con lo establecido en la norma UNE-EN 41410 (2008). Respecto a las probetas que contienen geopolímero las estabilizadas usando CCA son las que mayor resistencia a compresión presentan, por encima de las que contienen el silicato de sodio comercial o las que contienen cemento. Este mejor comportamiento del sistema con CCA constituye una doble mejora, se consiguen tanto beneficios en prestaciones mecánicas como mejoras para el medio ambiente. Este tipo de activaciones alternativas han demostrado que consiguen una reducción de la huella de carbono de hasta un 63% comparado con el cemento portland (Bouzon et al., 2014; Mellado et al., 2014)

Analizando los datos, se puede observar una doble mejora. Respecto del suelo estabilizado con cemento, la muestra con CCA muestra una ganancia de resistencia del 74% a 7 días, lo que indica una mayor velocidad de estabilización respecto al cemento. Por otra parte, el valor de resistencia a compresión del suelo con CCA se incrementa entre un 50-55% a 7 y 28 días, respecto a la estabilizada con geopolímero fabricado con silicato sódico.

4.6.4.3 Estudio de la microestructura de los suelos estabilizados: Termogravimetría.

Se han estudiado por termogravimetría las muestras de suelo estabilizado con cemento y con geopolimero activado de las dos maneras. En la figura 4.6-6a, se recogen las curvas DTG de las muestras de suelo con agua (suelo), estabilizado con cemento (OPC),

estabilizado con geopolimero (FCC + NaOH + $NaSiO_3$) (Sil) y estabilizado con geopolimero alternativo (FCC + NaOH + CCA) (CCA), todas ellas, a 28 días de curado. Se puede observar dos zonas diferenciadas por tramos de temperatura en estas curvas que son mostradas de forma ampliada en las figuras 4.6-6b y 4.6-6c

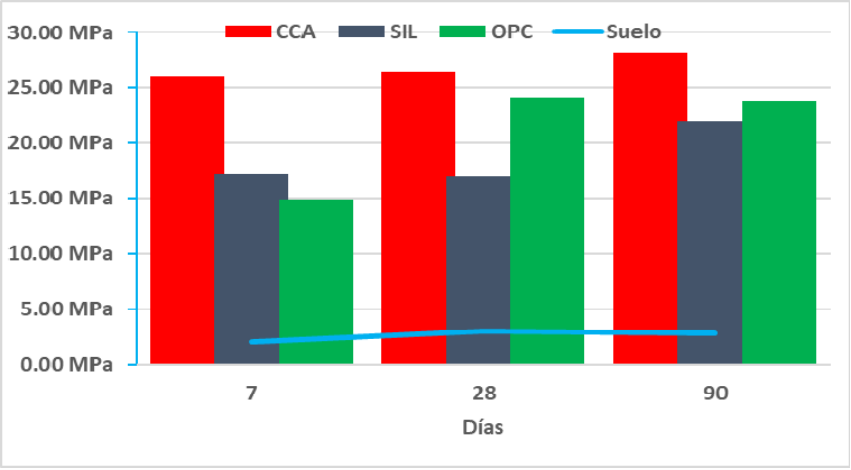

Fig. 4.6-5 Resistencias a compresión de probetas de suelo sin estabilizar (línea azul) y suelo establilizado con cemento (OPC), con FCC y mezcla de silicato sódico + NaOH (SIL) y estabilizado con FCC y mezcla de NaOH + CCA (CCA).

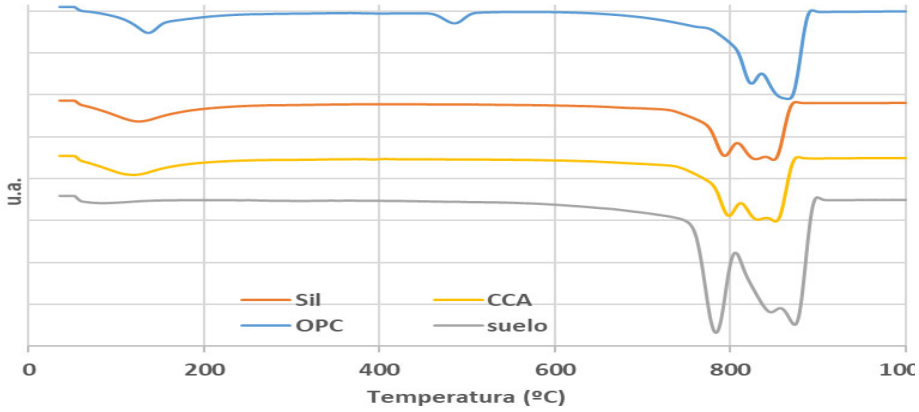

Fig. 4.6-6a Curvas DTG de las muestras de suelo curadas a 28 dias (Suelo: suelo+ agua; OPC: estabilizada con cemento portland; Sil: estabilizada con geopolímero a partir de FCC, Na_2SiO_3 y NaOH; CCA: estabilizada con geopolímero a partir de FCC, CCA y NaOH)

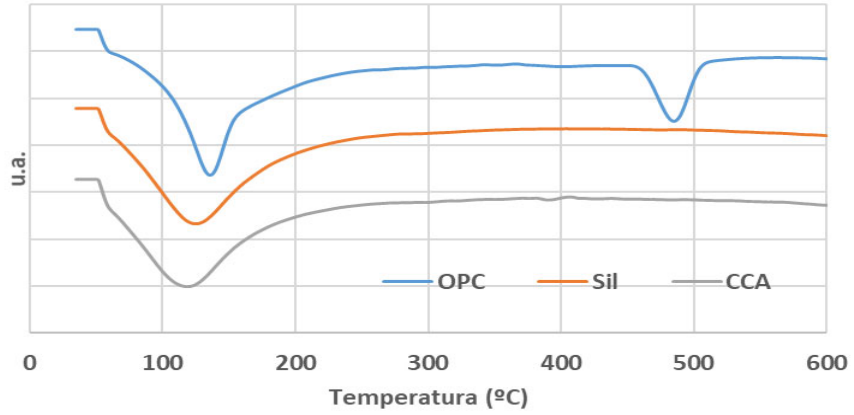

Fig. 4.6-6b Curvas DTG de las muestras de suelo estabilizadas a 28 días de curado. Zona

ampliada en el intervalo de temperaturas 35-600ºC

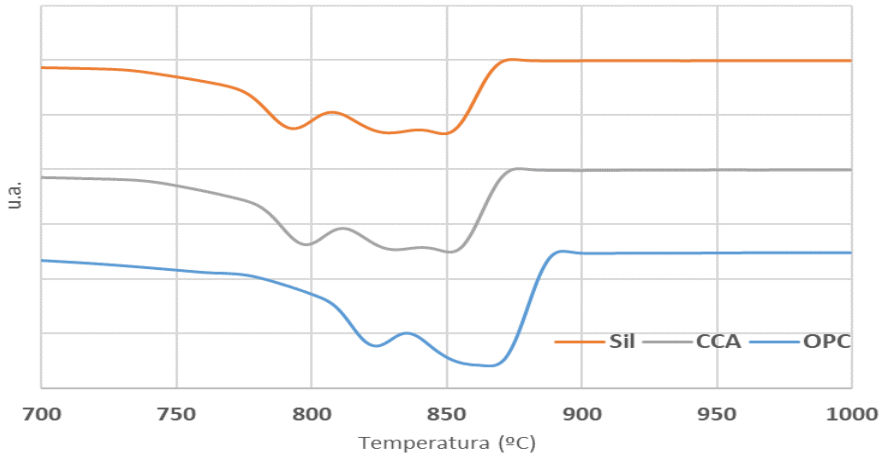

Fig. 4.6-6c Curvas DTG de las muestras de suelo estabilizadas a 28 días de curado. Zona ampliada en el intervalo de temperaturas 700-1000ºC

En la figura 4.6-6b se observan las curvas DTG de las muestras de suelo estabilizadas en el intervalo de temperaturas 35-600ºC. Entre 100-250ºC, se observa en la curva DTG en los suelos estabilizados un pico. En el caso de la muestra estabilizada con cemento, es debido a la formación de hidratos cementantes propios de la hidratación del cemento, (C-S-H fundamentalmente) mientras que en las muestras estabilizadas con geopolímero es debido a la formación de geles geopoliméricos tipo NASH (Tashima et al., 2012). Además, en la muestra estabilizada con cemento, se puede observar otro pico entre 450-550ºC, debido a la presencia de portlandita en la muestra, que también se ha formado por la hidratación del cemento portland.

Por otra parte, al observar el intervalo de temperaturas entre 750-900ºC, (Figura 4.6-6c) podemos destacar diferencias entre los picos debidos a la descomposición de los carbonatos. En la muestra de cemento se observan fundamentalmente dos picos solapados uno centrado a 824ªC y el segundo centrado a 868ºC.

En el caso de las muestras con geopolímero, se identifica una banda ancha con tres picos solapados (798ºC, 830 y 850ªC). Este hecho, es más visible en las muestras con CCA que las realizadas con el silicato comercial. Esto podría ser debido a una cierta interacción de los carbonatos del suelo con la reacción de geopolimerización. Este hecho ya ha sido detectado en otras investigaciones (Payá et al., 2012)

En la tabla 4.6-2, se recogen las pérdidas de masa obtenidas por termogravimetria con el tiempo de curado de las muestras de suelo analizadas.

Tab. 4.6-2. Datos termogravimétricos de las muestras de suelo analizadas.

Muestra	Tiempo de curado (días)	Pérdidas de masa (Pi %)			
		50-1000ºC	50-300ºC	450-550ºCº	700-950ºC
Suelo	7	37,65	--	--	34-84
	28	36,32	--	--	33,72
OPC	7	36,30	3,58	0,47	31,97
	28	35,36	3,89	0,70	30,47
Sil	7	33,07	2,68	--	25,49
	28	33,01	4,37	--	27,63
CCA	7	31,51	2,32	--	26,09
	28	33,97	3,83	--	28,36

Se puede observar que en general las pérdidas de masa totales (50-1000ºC) son elevadas. En las muestras estabilizadas con OPC, se detecta una pérdida de masa entre 50-300ºC, debido a la presencia de silicatos y aluminatos cálcicos hidratados y una pérdida en el intervalo entre 450-550ºC debido a la presencia de portlandita que va incrementándose con la edad de curado al hidratarse el cemento (1.93%, 2.88% de porcentaje de portlandita presente, calculado a partir de la perdida de massa entre 450-550ºC). En el caso de las muestras estabilizadas con geopolímero, no se observan diferencias significativas entre los dos tipos de muestras estabilizadas con geopolímeros. Entre 50-300ºC se detecta una pérdida de masa por la presencia de geles

NASH que también aumenta con la edad de curado, lo que indica que la reacción avanza al aumentar el tiempo de reacción. También se observa una ligera disminución de la pérdida de masa debida a la presencia de carbonatos respecto a los encontrados en las muestras estabilizadas por cemento, lo que corrobora la teoría de que parte del suelo puede reaccionar en el proceso de geopolimerización.

4.6.4.4 Estudio de la microestructura de los suelos estabilizados: difracción de rayos X

En la figura 4.6-a, b y c se muestran los difractogramas de las muestras de suelo estabilizadas. Cabe destacar que, para observar bien los picos debidos a los productos de estabilización, el ensayo de difracción se ha realizado en muestras con un 50% de estabilizante.

En todas las muestras estabilizadas se detectan como picos mayoritarios los compuestos mineralógicos presentes en el suelo (dolomita (D), pdfcard 360426; calcita (C) pdfcard 050586 y cuarzo (Q) pdfcard 331161. En la muestra de cemento se detectan como compuestos mineralógicos minoritarios la portlandita (P) pdfcard 040733 y trazas de etringita €, pdfcard 411451, magnesita (M) pdfcard 080479 y filosilicato tipo halloysita (H), pdfcard 291487.

En las muestras estabilizadas con geopolímero se observa una diferencia con la muestra anterior ya que se detecta una desviación de la linea base entre 15-35º 2θ, que es atribuible a la presencia de geles geopoliméricos tipo NASH (Tashima et al., 2012). Además, se detectan compuestos mineralógicos con sodio de la familia de las micas, como la Paragonita (P) pdfcard 120165. En el caso de la muestra activada con CCA tambien es detectada otra forma de sílice como la cristobalita (R) pdfcard 391425, que está presente en la CCA.

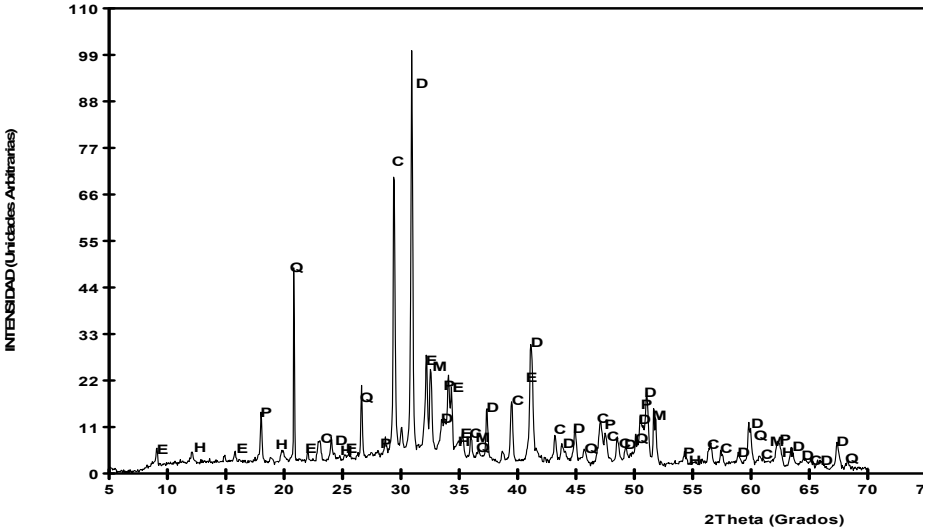

Fig. 4.6-7a Difractograma de rayos X de la muestra estabilizada con cemento Portland

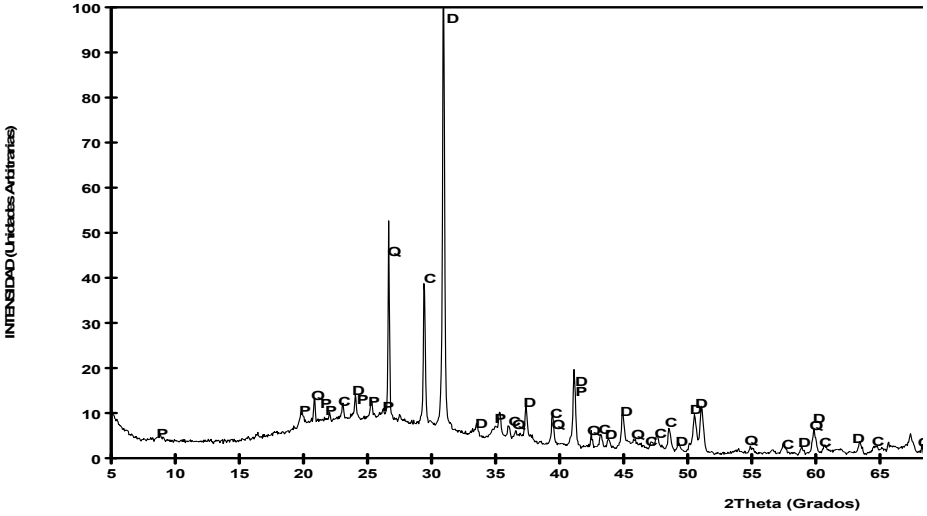

Fig. 4.6-7b Difractograma de rayos X de la muestra estabilizada con geopolimero a partir de FCC, Na_2SiO_3 y NaOH

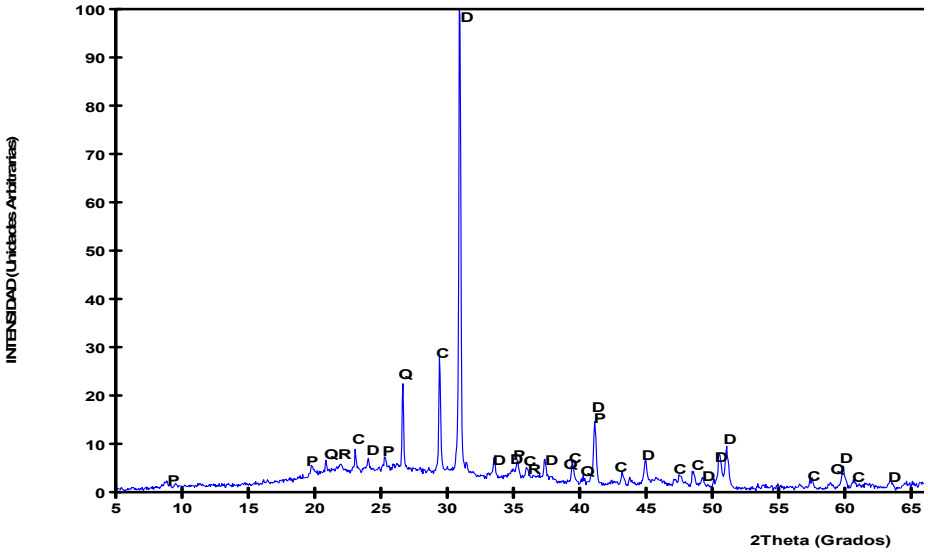

Fig. 4.6-7c Difractograma de rayos X de la muestra estabilizada con geopolimero a partir de FCC, CCA y NaOH

4.6.5 CONCLUSIONES

Se ha estudiado la estabilización de un suelo dolomítico mediante un proceso de geopolimerización usando para la fabricación de la disolución activadora una mezcla de hidróxido sódico con un reactivo comercial o un residuo de ceniza de cáscara de arroz como fuente de sílice. Las resistencias a compresión de estas últimas son en general las que mayor incremento presentan, tanto en comparación con suelo estabilizado con cemento como con en activación alcalina con el reactivo químico. La microestructura de las probetas de suelo se ha analizado mediante diversas técnicas comprobando que en las que contienen cemento se detectan compuestos de tipo cementante y portlandita, mientras que en

las activadas alcalinamente se detecta el gel geopolimérico tipo NASH. En DRX, se detecta en estos últimos la formación de material tipo filosilicato de la familia de las micas.

El uso de materiales residuales para fabricar geopolímeros y su posible utilización como estabilizador de suelos ha quedado demostrado que es una solución viable para sustituir al cemento como material estabilizador.

Referencias Bibliograficas

1.Al-Swaidani, A., Hammoud, I., Meziab ,A. (2016) Effect of adding natural pozzolana on geotechnical properties of lime-stabilized clayey soil. Journal of Rock Mechanics and Geotechnical Engineering, 8, 714-725. https://doi.org/10.1016/j.jrmge.2016.04.002

2.ASTM STP479 (1970). Special procedures for testing soil and rock for engineering purposes. USA: ASTM International

3.Bouzón, N, Payá, J, Borrachero, M. V., Soriano, L., Tashima, M. M., Monzó, J. (2013), Refluxed rice husk ash/NaOH suspension for preparing alkali activated binders, Materials Letters, 115 (2014) 72–74. https://doi.org/10.1016/j.matlet.2013.10.001

4.Cosa, J, Soriano, L., Borrachero, M. V., Payá, J., Monzó, J. (2017) Use of alkaline activated cements fromresidues for soil stabilization. In Proceedings of 17th International Conference on Non-Conventional Materials and Technologies (17thNOCMAT 2017) 357-365

5.Cristelo N, Glendinning S, Miranda T, Oliveira D, Silva R (2012) Soil stabilization using alkaline activation of fly ash for self-compacting rammed earth construction. Construction Building Materials 36, 727–735 https://doi.org/10.1016/j.conbuildmat.2012.06.037

6.Cui, Y. J. (2017) On the hydro-mechanical behaviour of MX80 bentonite-based materials. Journal of Rock Mechanics and Geotechnical Engineering 9, 565-574

7.Davidovits J. (1988) Geopolymer chemistry and properties In: Davidovits J., OrlinsEJ(eds) Proceedings of 1st European conference on soft mineralurgy (Geopolymer 88). The Geopolymer Institute, Compiegne, France, 25-48

8.Davidovits J. (1994) Properties of geopolymer cements. In: Procceding of first international conference on alkaline cements and concretes 1, 131-149

9.Fasihnikoutalab MH, Asadi A, Unluer C, Huat BK, Ball RJ, Pourakbar S (2017) Utilization of alkali-activated olivine in soil stabilization and the effect of carbonation on unconfined compressive strength and microstructure. Journal Materials in Civil Engineering 29, 601–613

10.Ferber V., Auriol J.C., Cui Y.J., Magnan, J.P. (2009) On the swelling potential of compacted high plasticity clays. Engineering Geology. 104, 200-210 https://doi.org/10.1016/j.enggeo.2008.10.008

11.Firoozi, A.A., Olgun C.G., Firoozi A.A., Baghini M.S. (2017) Fundamentals of soil stabilization. International Journal of Geo-Engineering, 8:26 https://doi.org/10.1186/s40703-017-0064-9

12.Habert G, d'Espinose de Lacaillerie JB, Roussel N (2011) An environmental evaluation of geopolymer based concrete production: reviewing current research trends. Journal Cleaner Production 19, 1229–1238 https://doi.org/10.1016/j.jclepro.2011.03.012

13.Hamzah H.N., Abdullah M.M., Yong H.C., Zainol M.R., Hussin K. (2015) Review of soil stabilization techniques: Geopolimerization method one of the new technique. Key engineering materials, 660, 298-304. Doi 10.4028/www.scientific.net/KEM.660.298

14.Hejazi, S.M., Sheikhzadeh, M., Abtahi, S.M., Zadhoush A. (2012) A simple review of soil reinforcement by using natural and synthetic fibers. Construction and Building Materials, 30, 100-116

15.Mellado, A.; Catalán C.; Bouzón, N.; Borrachero, M.V.; Monzó, J.M.; Payá, J. (2014). Carbon footprint of geopolymeric mortar: study of the contribution of the alkaline activating solution and assessment of an alternative route. RSC Advances, 4, 23846-23852. doi:10.1039/C4RA03375B

16.Monzó, J., Payá, J., Borrachero, M. V., Mora, E., Velázquez, S. (2001) Fluid Catalytic Cracking Residue (FC3R) as a New Pozzolanic Material: Thermal Analysis Monitoring of FC3R/Portland Cement Reactions, In: Seventh CANMET/ACI., International Conference on Fly Ash, Silica Fume, Slag and Natural Pozzolans in Concrete, Suplementary papers, 22-27.

17.Onyejekwe S., Ghataora G.S. (2015) Soil stabilization using proprietary liquid chemical stabilizers: sulphonated oil and a polymer Bulletin of Engineering Geology and the Environment 74, 651-665 https://doi.org/10.1007/s10064-014-0667-8

18.Payá J., Borrachero M.V., Monzó J., Soriano L., Tashima M.M. (2012) A new geopolymeric binder from hydrated-carbonated cement. Materials letters, 74, 223-225 doi:10.1016/j.matlet .2012.01.132

19.Payá J.; Agrela, F.; Rosales, J.; Martín Morales M.; Borrachero, M.V. (2019). Application of alkali-activated industrial waste. In: J. de Brito and F. Agrela. New Trends in Eco-efficient and Recycled Concrete.. Woodhead Publishing (Duxford, United Kingdom).

20.Pourakbar S, Asadi A, Huat B. B, Fasihnikoutalab, M. H (2015) Soil stabilization with alkali-activated agro-waste. Environmental Geotechnics 2, 359–370

21.Ramaji A. E. (2012) A review on the soil stabilization using low-cost methods. Journal of Applied Sciences Research, 8, 2193-2196

22.Sargent P, Hughes PN, Rouainia M, White ML (2013) The use of alkali-activated waste binders in enhancing the mechanical properties and durability of soft alluvial soils. Engineering Geology 152, 96–108 https://doi.org/10.1016/j.enggeo.2012.10.013

23.Soltani A., Taheri A., Khatibi M., Estabragh AR. (2017a) Swelling potential of a stabilised expansive soil: a comparative experimental study. Geotechnical and geological Engineering, 35, 1717-1744

24.Soltani A., Deng A.,Taheri A., Mirzababaei M. (2017b) A sulphonated oil for stabilisation of expansive soils. International Journal of Pavement Engineering https://doi.org/10.1080/10298436.2017.1408270

25.Tashima, M.M.; Akasaki, J.L.; Castaldelli, V.N.; Soriano, L.; Monzó, J.; Payá, J.; Borrachero, M.V. (2012) New geopolymeric binder based on fluid catalytic cracking catalyst residue (FCC). Materials Letters, 80, 50-52. https://doi.org/10.1016/j.matlet.2012.04.051

26.Wang, Y.X., Guo; P.P., Ren;W.X., Yuan B.X. (2017) Laboratory Investigation on Strength Characteristics of Expansive Soil Treated with Jute Fiber Reinforcement. International Journal of Geomechanics, 17

27.UNE-EN 41410 (2008). Bloques de tierra comprimida para muros y tabiques. Definiciones, especificaciones y métodos de ensayo. España: Asociación Española de Normalización y Certificación

28.Yan K., Wu. L. (2009) Swelling behaviour of compacted expansive soils. In GeoHunan international conference, ASCE 2009 https://doi.org/10.1061/41044(351)1

29.Zhang M, Guo H, El-Korchi T, Zhang G, Tao M (2013) Experimental feasibility study of geopolymer as the next-generation soil stabilizer. Construction Building Materials 47, 1468–1478 https://doi.org/10.1016/j.conbuildmat.2013.06.017

5 Discusion de resultados.

En este apartado se recoge una breve discusión sobre los resultados más importantes encontrados en los artículos indexados y congresos nacionales e internacionales que componen la tesis por compendio presentada. Para una mayor profundidad de discusión de resultados, se recomienda consultar las discusiones de resultados de los artículos y congresos por separado. Para una mayor compresión, hemos dividido esta discusión de resultados en dos subapartados: Aplicaciones a morteros y aplicaciones en suelos.

5.1 Aplicaciones a morteros

El objetivo de este apartado es estudiar morteros de activación alcalina donde parte del precursor utilizado son residuos cerámicos. Se han probado distintas mezclas: catalizador de craqueo catalitico (FCC), ceniza volante (FA) o escoria de alto horno (BFS) en mezclas con cerámica sanitaria (CSW) del 0-50%. En estos dos artículos los precursores tienen distinta composición química donde la principal diferencia es su composición en CaO, Se observa que la escoria presenta la mayor cantidad de calcio y el FCC y FA tienen una composición mucho menor. Es por ello y para activar la mezcla a temperatura ambiente que en el caso de las mezclas con FCC y FA se ha añadido un 4-4.5% de $Ca(OH)_2$.

En el caso de las mezclas con FCC (Cosa et al., Minerals, 2018. 123) para incrementar la sostenibilidad de la mezca se ha estudiado la influencia de la reducción de silice en las mezclas. Se encontró que existía un efecto sinérgico de la combinación CSW/FCC encontrándose los mayores valores al 50% de FCC. Con un menor contenido en FCC (20%) se han obtenido valores de resistencia a compresión cercanos a

40 MPa cuando son curados a 65ºC 7 dias, y para los que contenían 30% FCC a 28 días temperatura ambiente.

Las mezclas CSW/FCC presentaron unos valores muy variados de resistencia a compresión a 28 días de curado, en función del porcentaje de FCC y del contenido en sílice, aunque morteros con el 30% FCC mantenían resistencias a compresión de 40 MPa cuando la concentración de SiO2 se redujo de 7,28 a 4,37 mol kg^{-1}.

Los valores obtenidos de resistencia en estas mezclas con cantidades hasta el 50% de FCC y cantidades elevadas de silice (7.28 mol kg^{-1}) hacen pensar que podrían ser usadas en aplicaciones especiales para elementos de construcción que requieren tiempos cortos de curado y buenas resistencias mecánicas.

Podemos decir tambien que en la parte microestructural no se han detectado nuevas fases cristalinas en las mezclas CSW/FCC activadas alcalinamente, por lo que hay que concluir que el principal productos de reacción formado fue un gel N-A-S-H/(C,N)-A-S-H. Si se han detectado estructuras zeolíticas cuando la proporción de FCC es superior al 50%.

En el caso de las mezclas CSW/FA y CSW/BFS se comparan directamente precursores con distinta concentración de CaO. Es por ello que a las mezclas CSW/FA) se les añade un 4% de $Ca(OH)_2$. También se recoge en el articulo, (Cosa et al., Minerals, 2018, 337), un estudio de la influencia del contenido de hidróxido calcico en ambas mezclas, con FA y Con BFS. En estos sistemas, los que contienen escoria presentan mejores propiedades mecánicas que los sistemas con FA.

Podemos encontrar tambien las siguientes afirmaciones a modo de resumen:

Se puede concluir que la resistencia a la compresión de los morteros de activación alcalina con CSW al 100 % en peso mejoró con el contenido de BFS o FA, obteniéndose los mejores resultados en los sistemas combinados CSW/BFS con la adición de $Ca(OH)_2$, alcanzándose 55MPa a 90 días de curado y 20ºC o 7 dias 65ºC

Aunque el 4% en peso de $Ca(OH)_2$ fue consumido principalmente por BFS en los sistemas combinados CSW/BFS, las adiciones del 8% en peso mejoraron la reactividad de CSW

No se identificaron nuevas fases cristalinas significativas en los cementos combinados CSW, y $Ca(OH)_2$.

Aunque no se han podido identificar completamente podemos afirmar que Los geles N–A–S–H y N–(C)–A–S–H con bajo contenido de calcio probablemente se formaron en la mezcla de CSW/FA y una combinación de geles N–(C)–A–S–H/C–S–H/C–A–S–H se formaron en las mezclas CSW/BFS.

5.2 Aplicaciones a suelos

En esta tesis doctoral las aplicaciones a suelos son el resultado de un articulo indexado en el JCR y 6 congresos nacionales e internacionales.

Los resultados en el artículo de investigación constituyen el primer germen de estos resultados. En él se describe el diseño y construcción de un molde que permite hacer probetas cúbicas pequeñas (40 × 40 × 40 mm3). de suelo estabilizado con cemento portland (OPC) (10%). Además, alternativamente se prepararon probetas de activación alcalina basadas en FCC (10% también). Se muestran resultados a compresión de estas probetas. Además, se prepararon muestras cilíndricas con las mismas mezclas anteriores y se compararon los resultados de las resistencias en ambos casos.

Se encontraron mejor resultados en las muestras cubicas tanto en valores y ademas las desviaciones estándar de los valores obtenidos fueron mejores que en las probetas cilíndricas porque su consistencia es más plástica. El método de las muestras cúbicas permite preparar especímenes de pequeño tamaño, mejora la ergonomía, y facilita la obtención de un gran número de probetas con una menor cantidad de muestra.

Al comparar las muestras cúbicas sin estabilizador se obtiene que su resistencia a compresión fue, aproximadamente de 3 MPa. Al estabilizar con OPC, se detecta una mejor resistencia a la compresión a tiempos de curado más tempranos. Se lograron aproximadamente 24MPa con el suelo estabilizado con OPC a 90 días de curado. Al estabilizar con AAC, el aumento de la resistencia a compresión se hizo más progresiva, con menor resistencia a tiempos de curado tempranos, en comparación con OPC, pero con una mejor resistencia a la compresión a los 90 días en comparación con OPC, cercana a los 30MPa.

Esto significa que el desarrollo de la unión con mezclas de activación alcalina en la matriz es más lento, pero mucho más efectiva que la de OPC.

En los congresos recopilados en esta Tesis doctoral se explican diversos resultados tomando como base el uso de probetas cúbicas. En ellos se han usado distintos estabilizadores basados en reacciones de activación alcalina en aras de una mayor sostenibilidad.

Se han utilizado distintas mezclas precursoras como estabilizadores:

- OPC a modo de comparación

- Mezclas de activación alcalina como:

    - Precursor, FCC únicamente y mezclas de cerámica sanitaria FCC 30/70

    - Activadores: mezcla comercial de silicato sódico/NaOH y mezclas alternativas como ceniza de cáscara de aroz/NaOH, residuo de tierra de diatomeas de la industria cervecera/NaOH, y ceniza de paja de arroz/NaOH

De todos ellos se han obtenido buenos resultados, normalmente con resistencias a compresión superiores siempre a las indicadas por las normas, tanto para BTC como para estabilizar suelos para caminos o firmes de carretera. En el caso de sistemas con cerámica sanitaria se consiguen incrementar las propiedades físicas del suelo respecto de la estabilización con OPC y permite la reducción en la cantidad de FCC reutilizando un residuo importante como es la cerámica sanitaria.

En general, se demuestra por tanto que es viable el uso de residuos tanto en precursor como en el activador de hecho, se observa que las disoluciones con residuo funcionan a veces incluso mejor

que las preparadas con silicato sódico comercial.

En estabilización de suelos, es posible el uso de ceniza de cáscara de arroz y de residuos de diatomeas como alternativa más sostenible al cemento Portland, con menor impacto económico y medioambiental. Por otra parte, se mejora el acceso a la vivienda en países en desarrollo con un amplio abanico de aplicaciones en construcción de viviendas de nueva planta, rehabilitaciones de edificios en forma de BTC, tapial, solados, etc.

Tambien se ha estudiado pequeños aspectos de la durabilidad de estas mezclas. Concretamente se compara la estabilización de un suelo dolomítico con dos tipos de cementos activados alcalinamente. En los dos geopolímeros se utilizó como precursor el catalizador gastado de

craqueo catalítico (FCC) usando como activador una mezcla de hidróxido sódico y silicato sódico, ambos reactivos químicos comerciales y en el segundo geopolímero, una mezcla de ceniza de cascarilla de arroz e hidróxido sódico. Estos suelos estabilizados se compararon con el suelo estabilizado con cemento portland. Los resultados obtenidos mostraron mayores resistencias a compresión para los suelos estabilizados con geopolímero.

Las probetas fueron sumergidas en agua para estudiar su durabilidad en ambientes húmedos. Los resultados mostraron un mejor comportamiento, también, para los suelos estabilizados con geopolímero. Finalmente, se estudió la absorción de agua, siendo la menor aquella obtenida para las probetas estabilizadas con el geopolímero que utilizó una mezcla de hidróxido y silicato sódico como activador. Como conclusión, se ha demostrado la viabilidad del uso de este tipo de geopolímeros en la estabilización de suelos y la ventaja del uso de residuos que minimiza el impacto medioambiental final: menos cemento portland (por sustitución total con FCC) y menos reactivos químicos (con sustitución del silicato sódico por la ceniza de cascarilla de arroz).

Por ultimo, tambien se muestran resultados de bloques de suelo (BTC) fabricados con una máquina Cinvaram y estabilizados con cemento y con geopolímero, usando FCC como precursor y usando como activador una mezcla de ceniza de cáscara de arroz/NaOH.

De esta forma, para 28 días de curado, la resistencia a compresión de los bloques estabilizados con geopolímero fue 5,9 veces superior a la de los bloques sin estabilizar, y la resistencia a compresión de los bloques estabilizados con cemento Portland fue 2,6 veces superior a la de los bloques sin estabilizar.

Estos resultados pondrían de manifiesto las sustanciales mejoras que supone la estabilización del suelo con este tipo de geopolímero.

También estos bloques de BTC se secaron en estufa a 105ºC y luego se sumergieron en agua dos horas. Los resultados obtenidos muestran nuevamente, que los bloques de tierra estabilizados con geopolímero

dieron los valores de resistencia a compresión más altos. La resistencia a compresión de éstos fue 3,4 veces más alta que la de los bloques estabilizados con CP, si bien el porcentaje de reducción de la resistencia como consecuencia de la inmersión fue superior a la de los bloques estabilizados con cemento Portland (61,1 % frente a 54,2 %).

Podemos concluir en este apartado que estas mezclas de activación alcalina en estabilización de suelos suponen una innovación en este campo demostrándose su mejor capacidad desde un punto de vista económico y medioambiental y su posible uso en la fabricación de viviendas sociales en países en vías de desarrollo.

6. Conclusiones Generales

En lo que a la preparación de morteros se refiere la sustitución parcial de CSW por FCC mejoró significativamente el comportamiento de CSW como precursor en morteros de activación alcalina Las adiciones de FCC mejoraron las propiedades mecánicas del sistema y permitieron activar CSW a temperatura ambiente. Sin embargo, para confirmar y aceptar totalmente esta posibilidad de reutilización y valorización, se requieren más estudios sobre la durabilidad de los sistemas combinados CSW / FCC desarrollados.

Así mismo laa combinación de CSW con BFS o FA, amplía significativamente las posibilidades de reutilización y valorización de un residuo cerámico generado en grandes cantidades en todo el mundo, como precursor en cementos activados alcalinamente. Estos nuevos morteros desarrollados que son bajos en CO_2 constituyen una alternativa potencial al cemento Portland para ayudar a preservar el medio ambiente.

En lo que a estabilización de suelos se refiere se propone un sistema sencillo que permite preparar muestras cúbicas de pequeño tamaño para reducir el problema de la gran desviación estándar en las muestras estabilizadas con cementos de activación alcalina. Además, los problemas debidos al pandeo así como la falta de planeidad de las caras de los especímenes se consigue solucionar... También se facilita la obtención de un gran número de probetas con una pequeña cantidad de muestra, lo que reduce los costos económicos y ambientales por la menor producción de residuos Los resultados ponen de manifiesto que para 90 días de curado los suelos estabilizados con geopolímero presentaron resistencias a compresión superiores a los estabilizados con

cemento portland. En ambos casos se observo un incremento de la resistencia con el tiempo de curado

La utilización de un cemento activado alcalinamente, obtenido a partir de residuos, en la estabilización de bloques de suelo comprimidos produjo buenos resultados. Los residuos utilizados fueron catalizador de craqueo catalítico usado (FCC), como precursor y una mezcla de ceniza de cáscara de arroz (CCA) e hidróxido sódico como activador. La resistencia a compresión y la durabilidad de los bloques estabilizados con el cemento activado alcalinamente fueron superiores a las de los bloques estabilizados con cemento portland. Así mismo, el coste económico y medioambiental fue inferior, por lo que en determinadas condiciones podrían ser utilizados en países en desarrollo. Los resultados obtenidos también ponen de manifiesto el interés en el uso de residuos como son RSA, BWF y RHA en la preparación de activadores en los CAA y también del FCC como precursor en este mismo tipo de cementos. De esta forma tan sólo se utilizaría hidróxido sódico como reactivo químico en la preparación del CAA, el resto serían residuos. Los resultados obtenidos muestran una correlación directa entre el contenido de sílice del activador (RSA, BFW y RHA) y la resistencia a la compresión del suelo estabilizado. La resistencia a compresión en todos los casos sería suficiente para ser utilizado en suelos para firmes de carretera, lo que muestra la posibilidad de usar los CAA en lugar de cemento portland en la estabilización de suelos.

En el caso del sistema CS-FCC, se consigue incrementar notablemente las propiedades del suelo tras la estabilización, reduciendo la cantidad de FCC aportado e incrementando el contenido de CS, que es un residuo producido en grandes cantidades., Finalmente señalar que esposible el uso de CAA como alternativa más sostenible al cemento portland en la estabilización de suelos, con un menor impacto económico y

medioambiental, contribuyendo por otra parte a mejora de las viviendas e infraestructuras en países en desarrollo.

7. Desarrollo Futuro

Esta tesis tiene dos vertientes, por un lado, el de mitigar el impacto ambiental con la reutilización de deshechos en el desarrollo de cementos de activación alcalina como alternativa al cemento portland. Por otro lado, el social con la implementación práctica de estos morteros en países en vías de desarrollo. Por tanto, el desarrollo futuro debería encaminarse en estas líneas para optimizar los morteros reduciendo aún más el impacto ambiental, mejorar sus propiedades y reducir sus costes de producción. Ádemas se debe ahondar en la implementación de los CAA en los diferentes usos y tipos de suelos, así como su aplicación y desarrollo de estrategias para hacerlo viable para su uso real.

A fin de optimizar las proporciones de la mezcla en las soluciones de activación, dependiendo de la cantidad de BFS o FA en los sistemas combinados CSW, se podrían variar las concentraciones de Si y Al disponibles durante la sintesis.

Estudios del uso de CSW tanto como precursor y como árido en este tipo de sistemas.

Para abaratar aún más el coste económico y medioambiental del activador, se podría investigar el aprovechamiento de residuos industriales con alto contenido en NaOH.

Estudios de durabilidad de este tipo de suelos y determinación de otros parámetros geotécnicos

Aplicación de estos sistemas de estabilización en otros tipos de suelos arcillosos y con otras mineralogías distintas al suelo dolomítico utilizado en esta tesis doctoral.

Realizacion de pruebas piloto a escala real en estabilización de suelos o en bloques de tierra estabilizados.

Agradecimientos a empresas e instituciones

Agradecer al ministerio de ciencia e innovación por el soporte a mi investigación, mediante los fondos del proyecto APLIGEO BIA2015-70107-R y los fondos FEDER. También a las empresas: Ideal Standard por suministrar residuos de cerámica sanitaria, Omya Clariana S.A. por suministrar catalizador gastado del craqueo catalítico, a Balalva S.L. por suministrar cenizas volantes, a Cementval por suministrar escorias de alto horno, a Heineken España S.A. por el suministro de residuo del filtrado de cerveza (tierras diatomeas), a DACSA GROUP por la ceniza de cáscara de arroz, y a PAVASAL por suministrar suelo de tipo dolomítico. Támbien al servicio de Microscopía electrónica y al Instituto de Ciencia y Técnología del Hormigón de la Universitat Politècnica de València.

Índice de Figuras

Índice de Tablas